

Alameda Creek Restoration: Effect on Local Groundwater Supply



Alameda Creek Restoration: Effect on Local Groundwater Supply

Author(s)

Toine Vergroesen - Stichting Deltares Netherlands

Kees Nederhoff - Deltares USA

Betsy Romero Verastegui - Stichting Deltares Netherlands

Alameda Creek Restoration: Effect on Local Groundwater Supply

Client	Alameda County Flood Control District
Contact	Mr. Moses Tsang

Document control

Version	1.0
Date	22-02-2024
Project nr.	11209125-003
Document ID	11209125-003-BGS-0002
Pages	67
Classification	
Status	final

Author(s)

	Toine Vergroesen - Stichting Deltares Netherlands	
	Kees Nederhoff - Deltares USA	
	Betsy Romero Verastegui - Stichting Deltares Netherlands	

Contents

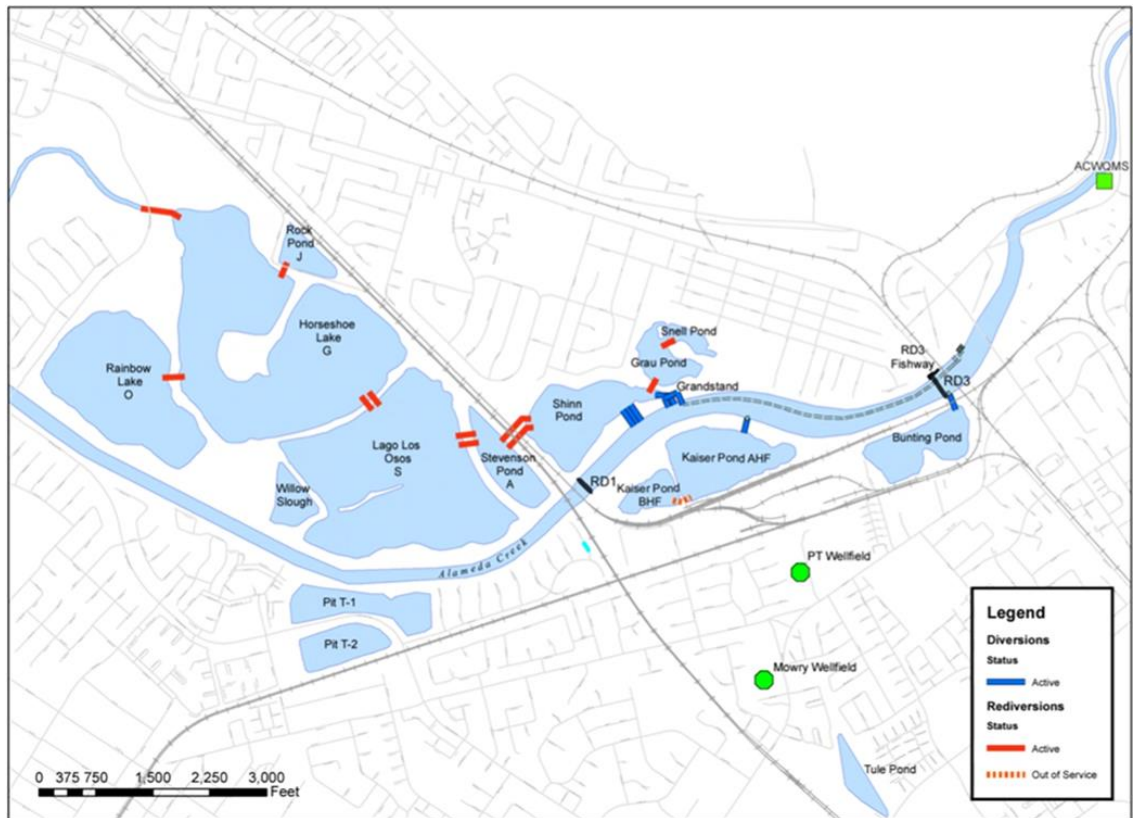
1	Introduction	6
2	Summary of Approach	8
3	Input Data, Model Setup, and Analysis	10
3.1	Introduction	10
3.2	Model concept and layering	10
3.2.1	Introduction	10
3.2.2	Exchange between groundwater and open water in Alameda Creek and Quarry Lakes	10
3.2.3	Layering concept based on NEBIM regional groundwater model	11
3.3	Model grid	14
3.4	Initial conditions	15
3.4.1	Bed level	15
3.4.2	Hydraulic conductivity	16
3.5	Forcing conditions	19
3.5.1	Rainfall and evaporation	19
3.5.2	Water levels in Creek and SF Bay	21
3.5.3	Abstraction wells	22
3.5.4	Model boundaries	23
3.6	Calibration and Validation data	23
3.6.1	Observed groundwater levels	24
3.6.2	Water balance of Quarry Lakes	26
3.7	Variations explored	28
3.7.1	Bed levels	28
3.7.2	Water levels	28
3.7.3	Analysis method	28
3.8	Analyzing the effect of Quarry Lakes Water Levels and Rainfall on Hydraulic Heads	29
4	Model Calibration and Validation	32
4.1	Introduction	32
4.2	Calibration	32
4.3	Validation	37
4.3.1	Introduction	37
4.3.2	Comparison to Observed Hydraulic Heads	37
4.3.3	Comparison with NEBIM Model Results	38
4.3.4	Comparison with Lake Infiltration	38
4.3.5	Validation figures	39
5	Model Application and Scenario Analysis	43
5.1	Introduction	43
5.2	Effect on Alameda Creek and Groundwater Exchange	43

5.3	Effect on Lake Infiltration	47
5.4	Effect on Hydraulic Heads in the Newark Aquifer	48
5.5	Effects on Phreatic Groundwater Level	50
5.6	Saline Intrusion	50
6	Conclusions and Recommendations	52
6.1	Conclusions	52
6.2	Evaluation and recommendations	52
	References	54
A	Sensitivity Analysis	55
A.1	Analysis of Bed Level Changes	55
A.2	Analysis of Hydraulic Heads and Flow Volumes in Aquifer	55
B	Additional figures	62
B.1	Differences in bed level between the proposed design and current situation	62
B.2	Hydraulic conductivity values applied	64
B.3	Bed levels for variations explored	65

1 Introduction

Alameda Creek is one of the larger streams in the San Francisco Bay Area. In 1970, Alameda Creek was channelized by the US Army Corps of Engineers (USACE) to protect the neighborhoods of Fremont, Union City, and Newark from extreme floods. Historically, the creek fed the tidal Baylands directly with sediment, nourishing this living infrastructure over time. The channel was not designed to move sediment, and as a result, sediment builds up in the channel, reducing flood storage capacity and creating a continual need for dredging. Alameda County Flood Control District (ACFCD) recognized this need and proposed a channel redesign.

Part of the proposed channel redesign lowers the bed level to increase sediment transport rates in Alameda Creek. However, this lowered bed level possibly increases the water exchange between the creek and the surrounding groundwater system. In particular, the potential increase in seepage from the Quarry Lakes Regional Recreation Area into Alameda Creek is one of the concerns of Alameda County Water District (ACWD). Figure 1 provides an overview of the situation.



ACWD Groundwater Recharge and Supply Facilities

Figure 1 Overview of area of interest with the upstream part of Alameda Creek and the Quarry Lakes to which creek water can be diverted by inflating rubber dams RD1 and RD3.

In January 2023, ACFCD and ACWD discussed the channel redesign. ACWD presented an initial approximation of the project effects using a generalized global model that was based on a regional Niles East Bay Integrated Model, NEBIM (Woodard & Curran, 2021). This steady-state model was applied to calculate the effects of the channel redesign on the local groundwater situation (ACWD, 2022). The results of these preliminary analysis indicated an

average annual upwelling of 2600 acre-feet (3.6 cfs) to Alameda Creek and ACWD recognized that additional investigations were warranted. In the commission of ACFDC, Deltares applied a steady-state local groundwater model with parameters that were based on the East Bay Plain Groundwater Model report to study the effects on the Quarry Lakes, referred to as Phase 1 (Deltares, 2023). The Phase 1 analysis revealed that the initial project effect calculations substantially overestimated the seepage by assuming constant lake levels at a 20-year high, an infrequent occurrence. By applying a more typical 20-year average lake level, the seepage estimates were significantly reduced. The analysis also noted that the regional NEBIM model has a grid resolution that is ~1000 coarser compared to the local Deltares model. The coarser resolution inflated the potential effects (see Figure 2). Preliminary findings from Deltares suggested that deepening the creek could only lead to an increase in upwelling of 65-225 acre-feet/year (0.09-0.31 cfs). Notably, the proposed creek deepening might actually decrease upwelling relative to the historical USACE design. Moreover, alterations to the creek bed downstream of Isherwood Bridge may have more effect on the groundwater system than modifications near Quarry Lakes.

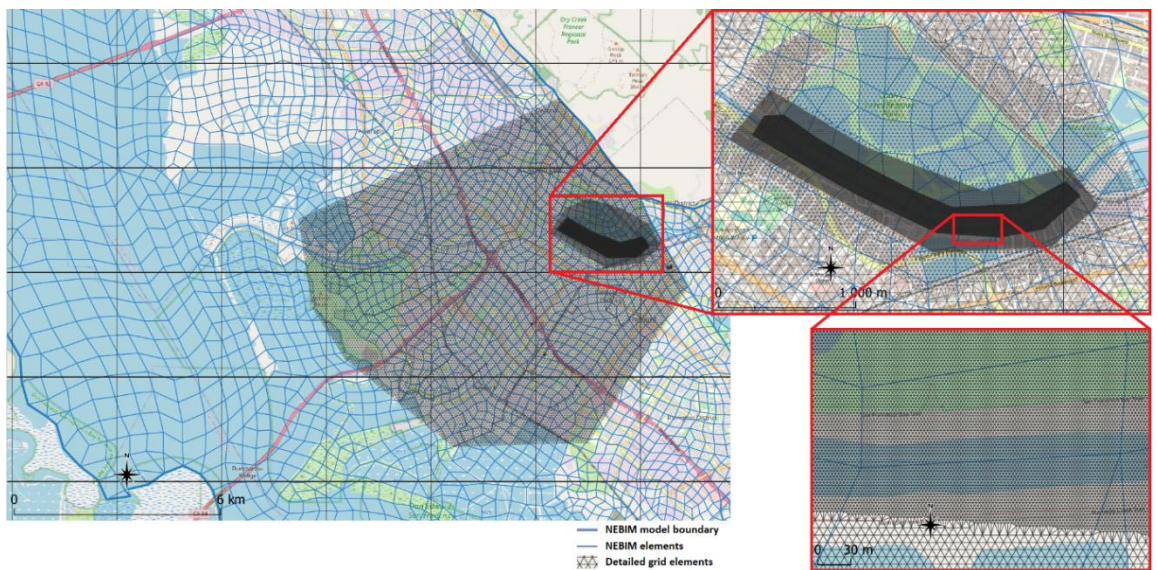


Figure 2 Impression of different element sizes of the NEBIM regional model (blue lines) and applied local model (black lines).

After the presentation of the Deltares modeling effort to ACWD and ACFCD it was decided to develop a high-resolution child model based on dynamic variations of the lake levels to address the critical concerns. It was decided that the child model will be calibrated using historic data collected by ACWD. The main reason for proceeding forward with a more detailed child model was to address the limitations encountered in Phase 1 due to time constraints and the unavailability of some hydrogeological data. Both ACWD and ACFCD teams felt that expanding the grid density for better resolution around Alameda Creek, integrating more comprehensive geohydrological data for enhanced model calibration, and employing the updated model to evaluate the impacts of channel deepening will enhance the model reliabilities and its findings.

This report provides the findings of the child model developed by Deltares and provides more accurate estimates of the potential effects of the Alameda Creek restoration on the local groundwater supply.

2 Summary of Approach

The main objective of this study is to determine the effect of locally deepening Alameda Creek on the surrounding groundwater levels and groundwater flow. Therefore, a local high-resolution groundwater model has been developed based on the regional NEBIM model. This local model is developed in MODFLOW6 and has been applied with an unstructured grid to ensure maximum flexibility in grid density. MODFLOW6 is a U.S. Geological Survey modular finite-difference flow model, which is a computer code that solves the groundwater flow equation. For more information, one is referred to Hughes et al., (2022).

The approach followed three steps (Figure 3). These steps are described in more detail in the outline below.

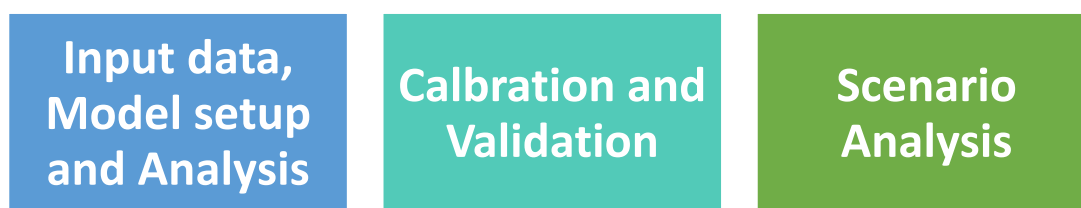


Figure 3 Overview of Approach (steps from left to right).

We developed a local high-resolution groundwater model, a child model of NEBIM, to study the effects of an adjustment of Alameda Creek on the groundwater system with a very dense grid at the part of the creek where bed level changes are proposed (see Figure 4 for the location of the developed child model). The grid gradually gets less dense as the distance from the creek increases. At some other locations, like the banks of the Quarry Lakes and several canals, the grid density is also locally increased. The grid density at the creek required to get reliable calculation results was extensively tested, see Section 3.3 and Appendix A.

As a starting point the NEBIM model and its layering was used. This is a well calibrated regional groundwater model maintained by ACWD. NEBIM contains four aquifers with aquitards on top of each aquifer. The four aquifers have been named the Newark, Centerville, Fremont, and Deep Aquifers, listed from shallowest to deepest. However, there is significant hydraulic connection between the Centerville and Fremont Aquifers within the Niles Cone Basin and thus previous efforts have locally classified these as one continuous aquifer (i.e., “The Centerville-Fremont Aquifer”). This also goes for the child model area. The Deep Aquifer has at the most only negligible effect on the hydrology of the creek. Therefore, it is excluded in the child model, leaving four model layers, two aquifers and two aquitards. The aquitard on top of the Newark Aquifer has been adjusted to the latest information from a recently developed texture model that describes for areas of 100 by 100 ft the percentage coarse material in the soil for 10 ft thick layers to a depth of 70 ft below MSL. In the child model, all four layers are given a horizontal and a vertical hydraulic conductivity (k_H and k_V). The horizontal conductivities of the Newark and Centerville-Fremont aquifers are applied from NEBIM. The vertical conductivities of these aquifers are applied through an anisotropy factor. The conductivities of the aquitards are derived through calibration. Initial conditions on layering and conductivities are elaborated on in Sections 3.2 and 3.4.

The boundaries of the child model are either fixed (east and west side) or so far from the creek (north and south side) that their influence on the calculation results at the creek is negligible. The west boundary of the child model is in the San Francisco Bay and is given a fixed head.

The east boundary is at Hayward Fault and is applied as a no-flow boundary. The north and south boundaries are approximately parallel to the groundwater flow direction and are also applied as no-flow boundaries. Moreover, we account for rainfall, precipitation, and abstraction. Lastly, water levels along Alameda Creek (as computed) and Quarry Lakes (as observed) are imposed. Forcings are described in detail in Section 3.5. Water levels in Alameda Creek are computed by a detailed hydrodynamic Delft3D model (Figure 4). From the calculation results of the Delft3D model, daily averages are produced for each creek element in the child model.

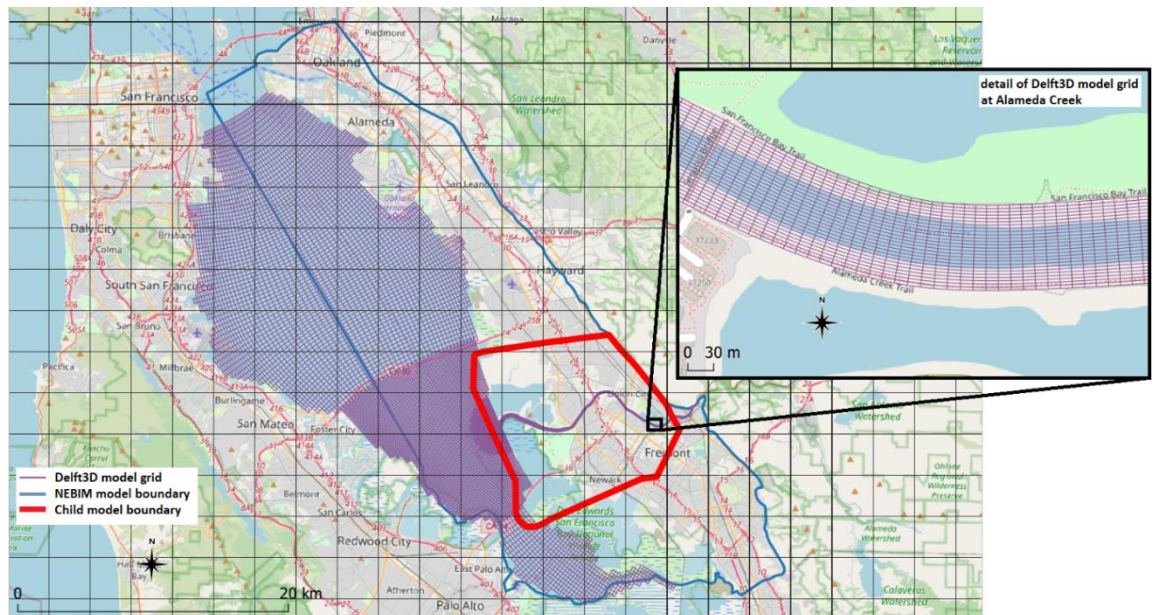


Figure 4 Overview of locations of NEBIM model, Delft3D model and the high-resolution local groundwater model developed in this study ("Child model").

The child model is calibrated on a period of 365 days, preceded by a similarly long period, in this report referred to as "warmup period", for model spin-up. The selected period for actual model calibration is from 15-02-2019 to 14-02-2020, in which the net rainfall is equal to the long-term average. The same goes for the preceding warmup period from 15-02-2018 to 14-02-2019. The time-dependent model calibration starts from a steady-state calculation for a long-term average period. The start of the warmup period coincides with a moment in time that the net rainfall of the previous 365 days equals the long-term average (see Figure 20 in Section 3.6). Prior to model calibration a steady-state parameter sensitivity analysis was conducted for all three scenarios and for two different grid densities (see Appendix A). The sensitivity analysis resulted in the selection of the minimum grid density of 16 ft and in a good impression of the effect of the different calibration parameters on the calibration results. The child model has been calibrated on timeseries of observation wells in the Newark and in the Centerville-Fremont aquifers. The model has been validated for a 13-year period, starting in 2010, in which both water levels in the Quarry Lakes and rainfall varied considerably more than during the calibration period. The model is also validated on derived infiltration volumes from the Quarry Lakes. Calibration and validation of the child model are described in Section 4.

After the model development and validation, the model has been applied to answer several practical questions about the redesign option of Alameda Creek and its implications on the groundwater system. Three bed level scenarios were considered: 1) USACE design, 2) current condition and 3) proposed situation. These inquiries encompassed a broad spectrum, including the average and maximum lowering of the groundwater table and the loss of groundwater volume in acre-feet per year (AF/year). Information on the variations explored and analysis method are discussed in Section 0. Model Application and Scenario Analysis are described in Section 5.

3 Input Data, Model Setup, and Analysis

3.1 Introduction

This chapter discusses the concept and schematization of the high-resolution local groundwater child model and the data that are applied for model input, for model calibration and validation and for the model scenarios.

3.2 Model concept and layering

3.2.1 Introduction

In this section, we explore the concept and layering of the developed local high-resolution groundwater model, focusing on the interaction between groundwater and the surface waters of Alameda Creek and Quarry Lakes. The model, building upon the NEBIM regional groundwater model, incorporates detailed data and analyses to accurately reflect the area's hydrological dynamics. Central to our model is the understanding of how daily water level variations in Alameda Creek and the Quarry Lakes' influence the surrounding groundwater in the model simulation. Our approach allows us to capture the complex interplay between surface water and groundwater, essential for realistic simulations. Subsequently, we discuss the layered structure of the groundwater model, which was carefully calibrated and informed by updated data and texture analyses. This structure is crucial in representing the geological and hydrological realities of the region, ensuring that our model provides an accurate and comprehensive understanding of the water system dynamics.

3.2.2 Exchange between groundwater and open water in Alameda Creek and Quarry Lakes

The local high-resolution groundwater model utilizes the daily average water levels of Alameda Creek, derived from the Delft3D model's calculations (Figure 4). This detailed hydraulic flow model incorporates various scenarios, including the specific bed levels of Alameda Creek. The Delft3D model determines Alameda Creek's water levels and depths by analyzing observed discharges, the operational status of rubber dams (either raised or lowered), and the tidal water levels in San Francisco Bay. For a range of bed level variations, the model produces daily average water levels for the designated time period. For more information on the Delft3D model, see Deltares (2024).

For each daily timestep, average water levels in the creek, calculated by the Delft3D model, were compared to bed levels for each MODFLOW6 model cell (see Figure 5). In cells where creek water levels exceed bed levels, water levels were set to the former. Here, water can either seep into the groundwater (if the creek level is above the groundwater level) or flow from the groundwater into the creek (if the groundwater level is higher). Conversely, in model cells where the creek bed exceeds creek water level, the water level was fixed to the bed level. In such cases, the element can only contribute to draining groundwater into the creek, provided the groundwater level is higher than the creek bed.

It is important to note the driving force for water infiltration varies based on the relative levels of groundwater and creek bed. If the groundwater level is above the creek bed, infiltration is driven by the difference between the creek water and groundwater levels. If the groundwater level falls below the creek bed, infiltration depends on the difference between the creek water level and the creek bed level, regardless of how deep the groundwater is beneath the creek bed.

This principle also applies to the interaction between the Quarry Lakes' water levels and the surrounding groundwater. A key distinction is that the lakes' water levels are typically higher than the nearby groundwater levels, making the drainage of groundwater into the lakes a rare occurrence.

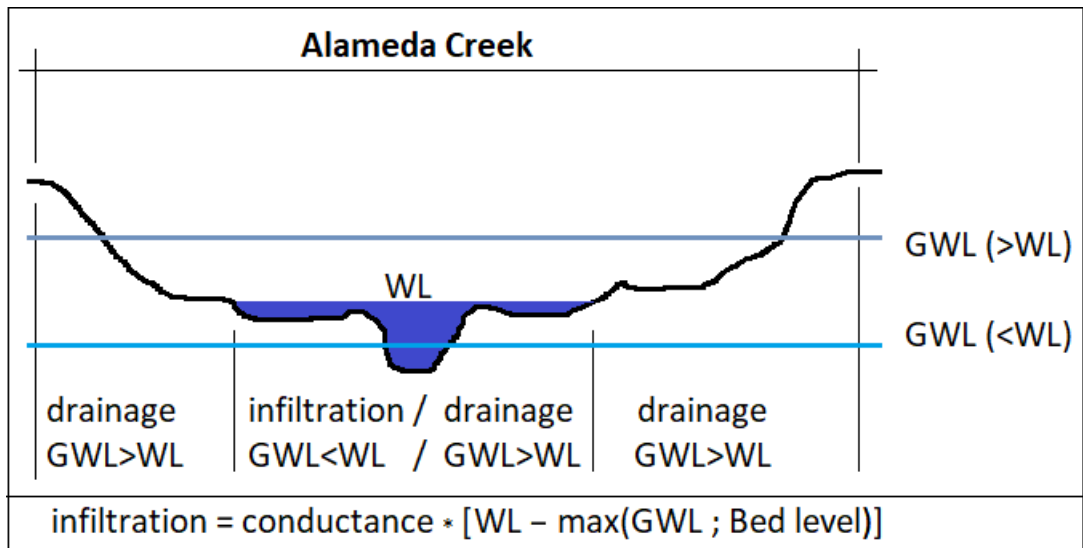


Figure 5 Principle of interaction between creek water level (WL) and groundwater level (GWL).

3.2.3 Layering concept based on NEBIM regional groundwater model

The layering in the NEBIM regional groundwater model forms the foundation for the local groundwater model's structure in this study's area. NEBIM features three aquifers, each capped with aquitards. These include, from top to bottom, the Newark Aquifer, the Centerville-Fremont Aquifer combination, and the Deep Aquifer. Previous steady-state groundwater model studies indicated that the Deep Aquifer has a minimal effect on the water exchange between Alameda Creek and the surrounding groundwater (Deltares, 2023). It is also separated from the Centerville-Fremont Aquifer by a thick, high-resistance aquitard. Consequently, to reduce calculation times, the Deep Aquifer is excluded from the local model used in this study.

The topmost section of the child model integrates the Newark Aquifer (layer 2 in the child model) and its overlying aquitard (layer 1), as defined in NEBIM. The level of separation between layer 1 and 2 has been updated with recent data and insights from a detailed texture model by Woodard & Curran (W&C) by personal communication on December 2, 2023. Figure 6 shows this for the section of Alameda Creek between BART Weir and Ardenwood Blvd Bridge. In this figure, the line between Proposed Layers 1 and 2 is the updated top of the Newark Aquifer (layer 2 in the child model).

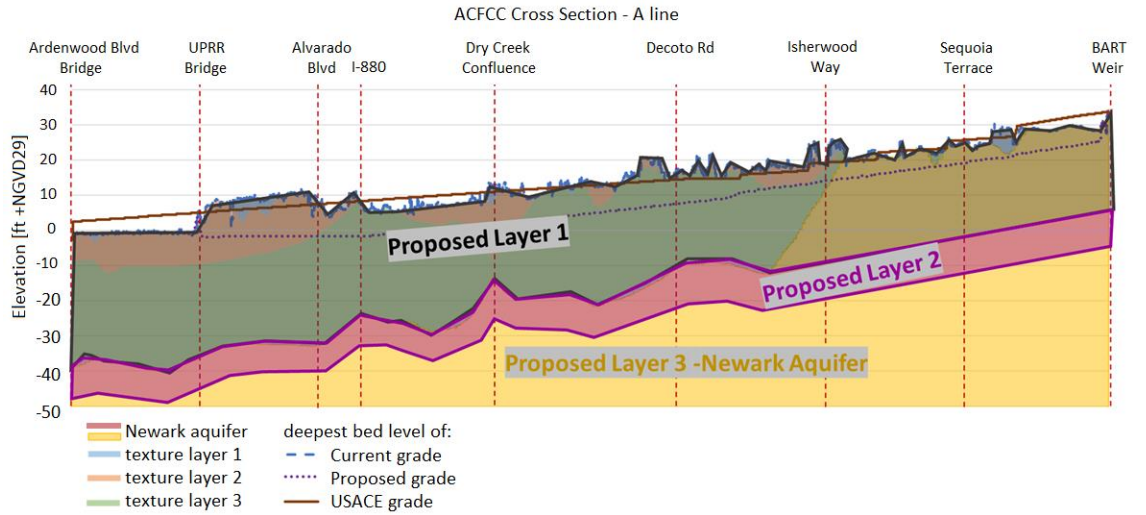


Figure 6 Schematization of top layers at Alameda Creek between Ardenwood Blvd Bridge and BART weir as derived by W&C. Proposed Layer 1 is the aquitard on top of the Newark Aquifer. Proposed Layer 2 is the top 10 ft of the Newark Aquifer and Proposed Layer 3 is the rest of the Newark Aquifer.

Texture model

This texture model offers layers every 10 ft from +70 ft to -70 ft (NGVD29), specifically regarding the proportion of coarse material in each layer. While all layers maintain a 10 ft thickness, the topmost layer varies. Data points are spaced every 100 ft in the area surrounding Alameda Creek. Figure 7 shows an example of the texture model for the 10 ft thick layer below the top layer, that can vary from near 0 ft to almost 10 ft.

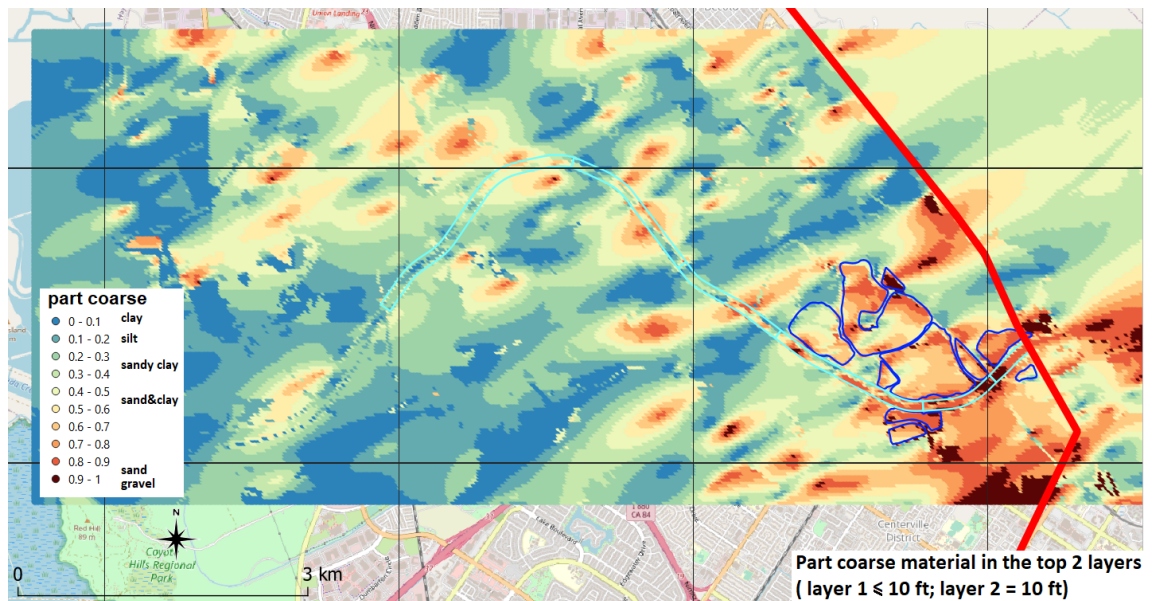


Figure 7 Part of coarse material in layer 2 of the top 2 layers of texture model. Layer 2 is always 10 ft thick. Layer 1 varies between 0.0001 and 10 ft.

W&C will derive the hydraulic conductivities for each layer from the coarse material content, applying a specific formula and adjusting for vertical hydraulic conductivity through an anisotropy factor.

$$K = [P_c \cdot K_c^p + (1 - P_c) \cdot K_f^p]^{1/p}$$

Where:

- K horizontal hydraulic conductivity [ft/d]
- K_c hydraulic conductivity [ft/d] of layer with 100% coarse material
- K_f hydraulic conductivity [ft/d] of layer with 0% coarse material
- p between -1 and 1

In this method K_c, K_f and p are determined during calibration and will remain unchanged in model scenarios that affect the thickness and composition of the layer. The corresponding vertical hydraulic conductivity will be determined along the process by applying an anisotropy factor.

Applied in child model

Layer 1 in the child model comprises three distinct texture layers with varying hydraulic conductivities, generally lower than those of the underlying Newark Aquifer (Layer 2 in the child model). Notably, between Isherwood Way and BART weir, the upper layers contain a higher proportion of coarse material, resulting in significantly greater hydraulic conductivity compared to areas downstream of Isherwood Way (illustrated in Figure 7). Except for this area with clearly coarser material, we applied a single value for the horizontal conductivity of layer 1, the top aquitard.

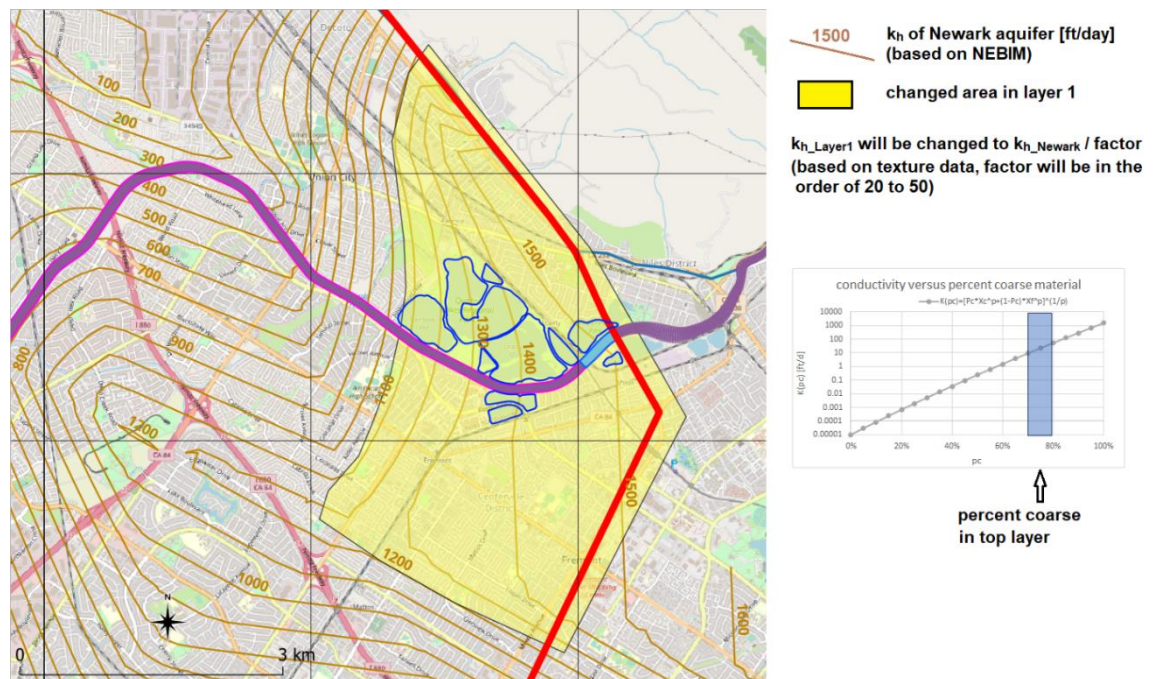


Figure 8 Applied area with larger hydraulic conductivities in top layer.

For the area with clearly coarser material in the top layers, the yellow marked area in Figure 8, we applied a different approach. For this area, for the horizontal hydraulic conductivity we applied the value of the Newark Aquifer divided by a factor. In this area the percentage coarse material in the top layer is roughly between 70 and 80%, indicating a soil composition between sand and clay (50%) and sand (90%). Based on that the horizontal hydraulic conductivity in the top layer is estimated to be a factor 20 to 50 lower than the horizontal hydraulic conductivity in the underlying Newark Aquifer.

In the child model, the Newark Aquifer is not divided into a top 10 ft layer and a remaining portion, like W&C proposed (Figure 6). We tested both configurations and found negligible differences in the resulting hydraulic heads, with variations at observation wells all within 0.01 ft. Considering runtime efficiency and memory space requirements, we opted for an undivided Newark aquifer in the local groundwater model.

3.3 Model grid

Given the reasons outlined in the preceding sections, we opted for an unstructured MODFLOW6 grid in our study. The initial step in creating this grid involves developing a triangular grid, which serves as the foundation for constructing a Voronoi grid, featuring elements surrounding the nodes of the triangles.

We developed two model grids with varying densities in the Alameda Creek bed area. The first, referred to as the 8ft-grid, has a minimum triangular node distance of 8 feet. The second, known as the 16ft-grid, features a minimum node distance of 16 feet. The 8 ft-grid, which spans the area between Ardenwood Blvd and BART weir, includes the horizontal segment of Alameda Creek as originally designed by the USACE. Figure 9 provides a comprehensive overview of the input elements used in grid generation.

The 8ft-grid contained 283,300 elements with a minimum size of 9 ft². The 16ft-grid contains 173,520 elements with a minimum size of 22 ft². That means that the 16ft-grid has almost 40% less elements. Sensitivity testing showed that the 16ft-grid resulted in similar outcomes and was therefore used in this study (Appendix A).

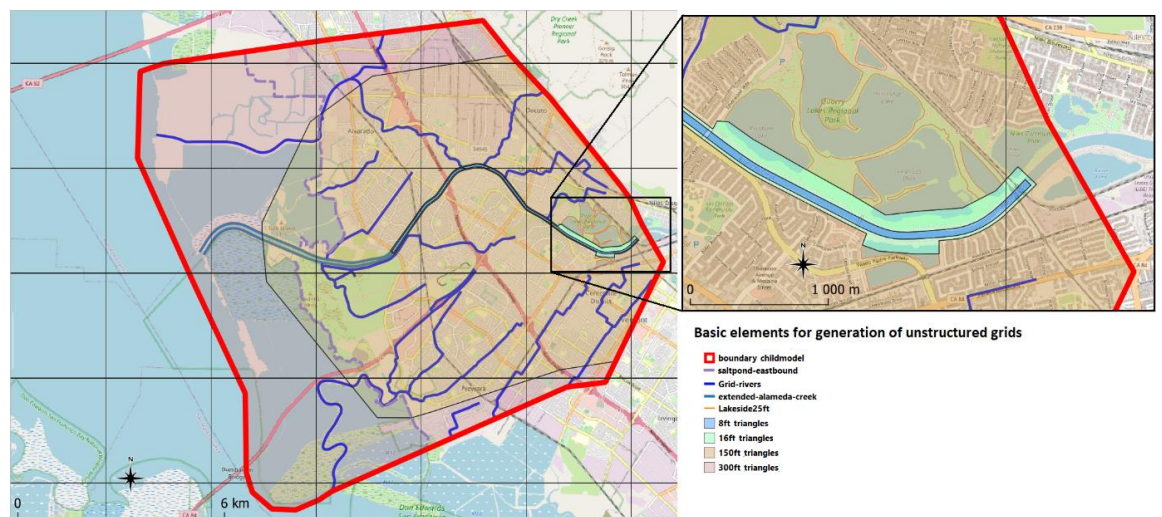


Figure 9 Applied input elements for the generation of the model grids.

The grids incorporate four varying density polygons: 8 ft, 16 ft, 150 ft, and 300 ft. In the 16ft-grid, the 8 ft density polygon is adapted to a 16 ft density polygon for consistency. The grid generator is programmed to seamlessly transition between these different densities. Additionally, to achieve localized higher densities, grid support lines are strategically placed along drainage canals, the eastern boundary of the salt ponds, and the banks of the lakes. For a visual interpretation of the grid, one is referred to Figure 10.

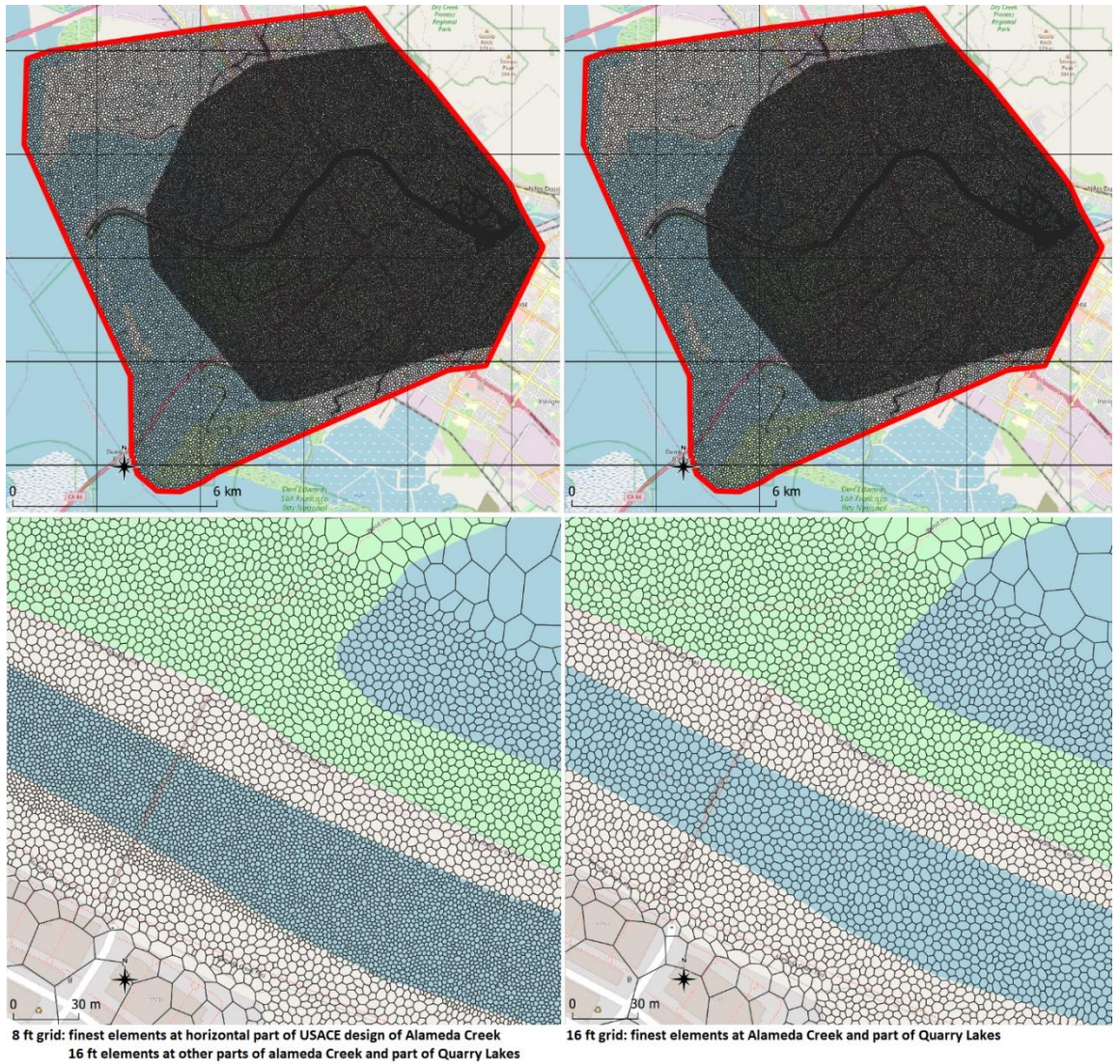


Figure 10 Resulting model grids with on the left side the 8ft-grid and on the right side the 16ft-grid. The top part shows the entire model grid. The bottom part shows an example of the difference in density between the two grids in the Alameda Creek area.

3.4 Initial conditions

3.4.1 Bed level

The model employed in this study is essentially a “child” derived from the well-calibrated NEBIM model. As such, the schematization of layers and parameter values from NEBIM serves as the foundational starting point for our high-resolution local groundwater model.

However, there are notable deviations from NEBIM:

- The surface elevation data is based on the 2019 LiDAR from ACFCD, which offers a detailed 3 x 3 ft raster.
- For the Alameda Creek area stretching from Ardenwood to the BART weir, we utilize a recent 1 x 1 ft topo-bathymetry raster dataset. This dataset reflects the current state and is adjusted for both the proposed scenario and the original USACE design.

Figure 11 offers a comprehensive overview of the surface elevation and bed level of Alameda Creek. It illustrates the water levels in the Quarry Lakes as observed on the specific date of study (approximately 20 ft +NGVD29). The figure also shows various other creeks and canals in proximity to Alameda Creek. Most of these are incorporated into the child model as rivers, characterized by a fixed drainage level and bed resistance that influence the exchange between groundwater and river water. The Quarry Lakes and Alameda Creek, while also modeled as 'rivers', are treated distinctively compared to other creeks and canals. The mechanism of water exchange between these bodies and the groundwater has been elaborated earlier in Section 3.2.2.

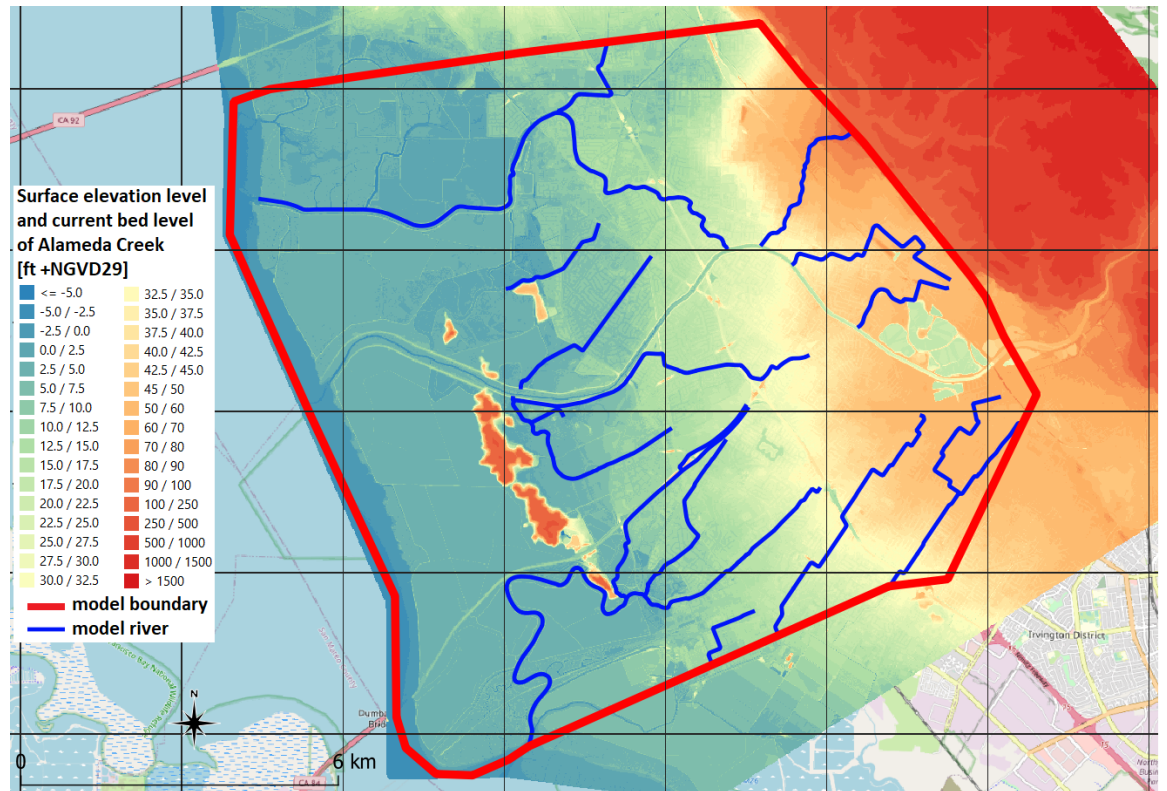


Figure 11 Applied surface elevation level in the child model. Based on 1 x 1 ft raster dataset for the current situation in Alameda Creek and 3 x 3 ft raster dataset (EdenLand DEM 2019-2021) for the rest of the model area.

3.4.2 Hydraulic conductivity

In the applied high-resolution local groundwater model, we have adopted the hydraulic conductivities of the Newark and Centerville-Fremont aquifers as determined in the NEBIM model. The horizontal hydraulic conductivities (k_H) for both aquifers are based on contours derived from NEBIM for the Newark Aquifer and the Centerville-Fremont Aquifer, respectively (see Appendix B.2 for figures).

We pragmatically determined the following values during model calibration and sensitivity analysis. The conductivity specifications for the child model's layers are as follows:

- **Layer 1. The aquitard on top of the Newark Aquifer:**
 - The horizontal hydraulic conductivity (k_H) of layer 1 is set at 0.5 ft/day, except for the yellow area in Figure 8, where it is set at the k_H of the Newark aquifer divided by 50.
 - The vertical hydraulic conductivity (k_V) of layer 1 is set at k_H divided by 10.
- **Layer 2. The Newark Aquifer:**
 - The horizontal hydraulic conductivity (k_H) of layer 2 is derived from contour lines based on NEBIM (shown in Appendix B.2 in Figure 62).
 - The vertical hydraulic conductivity (k_V) of layer 2 is set at k_H divided by 5.
- **Layer 3. The aquitard below the Newark Aquifer:**
 - The horizontal hydraulic conductivity (k_H) of layer 3 is set at 0.05 ft/day.
 - The vertical hydraulic conductivity (k_V) of layer 3 is set at 0.005 ft/day.
- **Layer 4. The Centerville-Fremont Aquifer:**
 - The horizontal hydraulic conductivity (k_H) of layer 4 is derived from contour lines based on NEBIM (shown in Appendix B.2 in Figure 63).
 - The vertical hydraulic conductivity (k_V) of layer 4 is set at k_H divided by 5.

Figure 12 shows the resulting horizontal transmissivities of the aquifers (layers 2 and 4) and the vertical hydraulic resistances of the aquitards (layers 1 and 3). The parameters from layer 1 down to layer 4 applied in the child are at the left side of this figure. The same parameters applied in NEBIM are at the right side. The black line in the NEBIM figures separates the NEBIM elements that lie inside the child model boundary from the elements that lie outside the child model boundary.

The transmissivities of the Newark Aquifer and the Centerville-Fremont Aquifer are based on NEBIM conductivities and layer thicknesses and hence only show minor differences to the transmissivities applied in NEBIM. The red colored area at the eastern child model boundary in NEBIM layer 2 is the Hayward Fault that has given a very low hydraulic conductivity in NEBIM. The red area in layer 4 in the eastern part of NEBIM indicates the absence of a second aquifer east of Hayward Fault.

The vertical hydraulic resistances of the top aquitard (layer 1) and the aquitard between the two aquifers (layer 3) clearly differ from NEBIM. Especially in layer 1 the differences in vertical hydraulic resistances between the child model and NEBIM are large and the resistances in the child model are generally much lower. In layer 3 the differences are also clear, but NEBIM has much lower resistances in the eastern half of the child model and higher resistances in the western part of the child model.

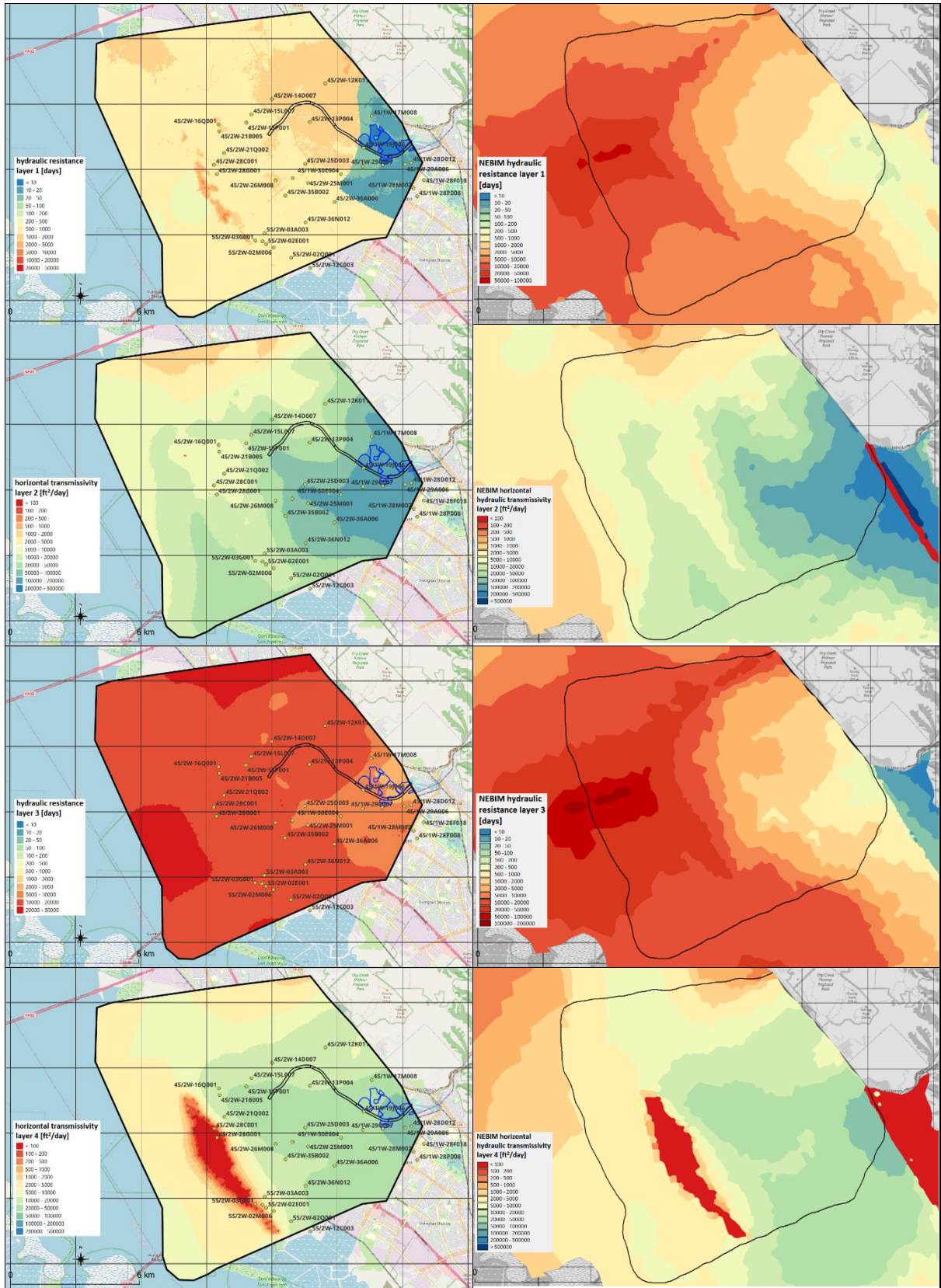


Figure 12 Model parameters per layer after calibration (left side) and in NEBIM (right side).

3.5 Forcing conditions

3.5.1 Rainfall and evaporation

The local groundwater model incorporates a recharge mechanism at its surface, representing the net flux of incoming rainfall and outgoing evapotranspiration. In this area, long-term potential evapotranspiration (plant evaporation) is nearly double the long-term rainfall. Evaporation of open water is more than twice as high as rainfall. However, daily rainfall variability is much higher than that of daily evaporation. The model area, predominantly urban, features a mix of houses and roads (paved areas) and gardens and public green spaces (unpaved areas). Rainfall runoff from paved surfaces often flows to unpaved areas, leading to soil infiltration. Excess water percolates to the underlying groundwater, typically beyond the reach of plant roots. Consequently, actual evapotranspiration likely occurs in unpaved areas only when soil moisture is sufficiently high, resulting in net groundwater recharge, despite evaporation exceeding rainfall by a factor of two.

NEBIM contains a module that calculates recharge based on rainfall, evapotranspiration, soil parameters and land use. The calculated recharge in NEBIM is always higher than zero across the entire model domain. W&C supplied us with daily NEBIM recharge data for the cells that lie in the child model area, up until 30-09-2020 (WY 2020).

We deviated from that by applying single recharge values for the entire child model (for each day). We applied the observed daily rainfall at PT wellfield and the observed daily pan evaporation at De Laveaga. The daily evaporation values were divided by 1.3 to generate daily open water evaporation values (Linacre, 1993). Daily rainfall and open water evaporation was only applied for water balance checks of the Quarry Lakes.

For the land part of the model, we applied rainfall and potential evapotranspiration by taking 80% of the open water evaporation. Actual evapotranspiration was determined as the maximum of the potential evapotranspiration and the observed rainfall. Thus, omitting negative values of daily net rainfall. To be compliant with the NEBIM recharge, total net rainfall of the child model area for the period of Januari 2010 to September 2020 was made equal to the total recharge of NEBIM for the same area and for the same period (Figure 13). To accomplish that, a factor of approx. 0.0048 was required. For each day the recharge of the child model was the result of multiplying the net rainfall of that day with this factor.

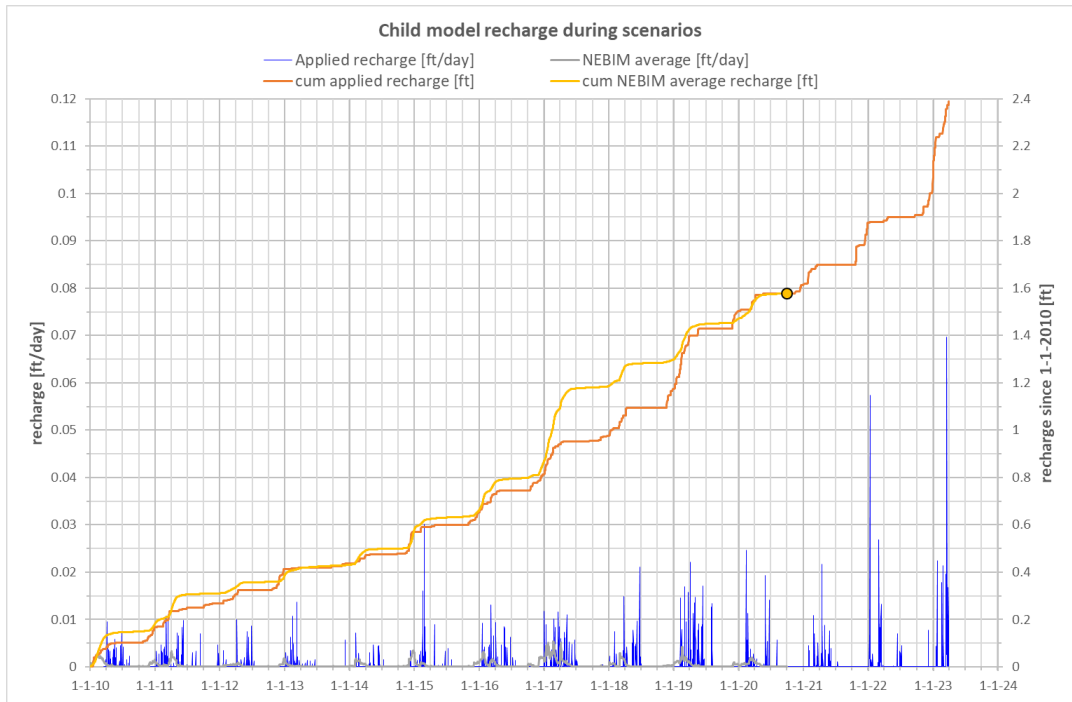


Figure 13 Applied daily recharge for scenario calculations (blue lines), compared to the average NEBIM recharge (grey lines). The dot at 30-09-2020 is the moment in time when the total applied recharge (orange line) since 01-01-2010 is equal to the total NEBIM recharge (yellow line).

Figure 14 shows the local differences of the recharge in NEBIM. The local minimum of the NEBIM recharge is always almost zero. Its local maximum varies more than the recharge we applied in our child model. Main reasons for this approach are that this way we are independent of other models, we are consistent for the period that NEBIM has not yet generated data (October 2020 – January 2023), but the total applied recharge is still in line with the calibrated NEBIM recharge.

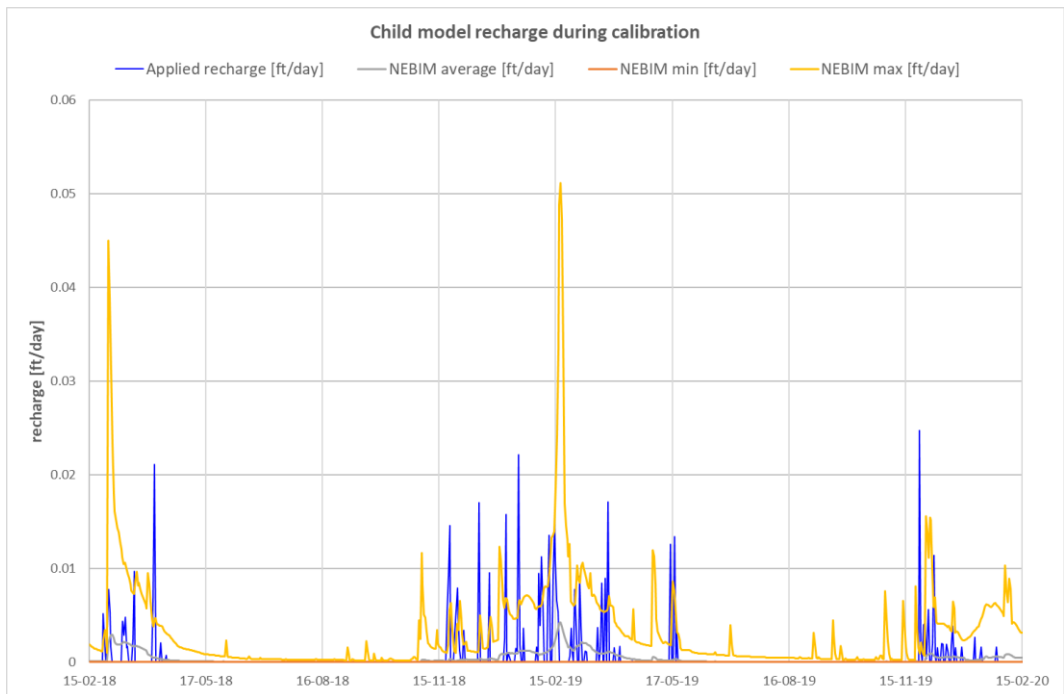


Figure 14 Applied daily recharge for warmup and calibration period (blue lines), compared to the average NEBIM recharge (grey lines), its local minimum (orange lines) and its local maximum (yellow lines).

3.5.2 Water levels in Creek and SF Bay

In this study, key water level inputs include those from San Francisco Bay, Quarry Lakes, and Alameda Creek. Due to the daily calculation timestep of the model, tidal water levels in San Francisco Bay are set at Mean Sea Level (MSL) in the San Francisco Bay. As detailed in Section 3.2.2, the water levels in Alameda Creek are based on daily averages calculated by the Delft3D model.

Quarry Lakes water levels are derived from daily observations, applied uniformly across Rainbow Pond, Horseshoe Lake, Lago Los Osos, Rock Pond, and Willow Slough, collectively referred to as 'Basic Lakes' in Figure 15. Horseshoe Lake boasts an almost complete record of daily observations over the selected 13-year scenario period, with only 26 days unrecorded, primarily in the initial six months. Shinn Pond also had a near-complete dataset, with only 80 days missing in the analyzed period. However, Stevenson Pond exhibited significant data gaps, with over 47% of days unrecorded in the scenario period and nearly 39% in the calibration period. Kaiser Pond BHF has less frequent, monthly recordings starting from March 2020.

For missing water level data, we employed interpolation for smaller gaps and comparative analysis with other lakes' water levels for larger gaps. Pit T-1 and Pit T-2, located south of Alameda Creek, have long been disconnected and no longer receive creek water. Essentially, their water levels can be viewed as visible groundwater. Notably, Pit T-1's water levels are well-monitored, with comprehensive data except for three extended periods. The calibration period, however, has no data gaps. In the child model, Pit T-2 is assigned the same water level as Pit T-1.

The consistently lower water levels observed in Pit T-1 compared to the Basic Lakes, even during dry periods, indicate that the Quarry Lakes are perpetually infiltrating to the groundwater.

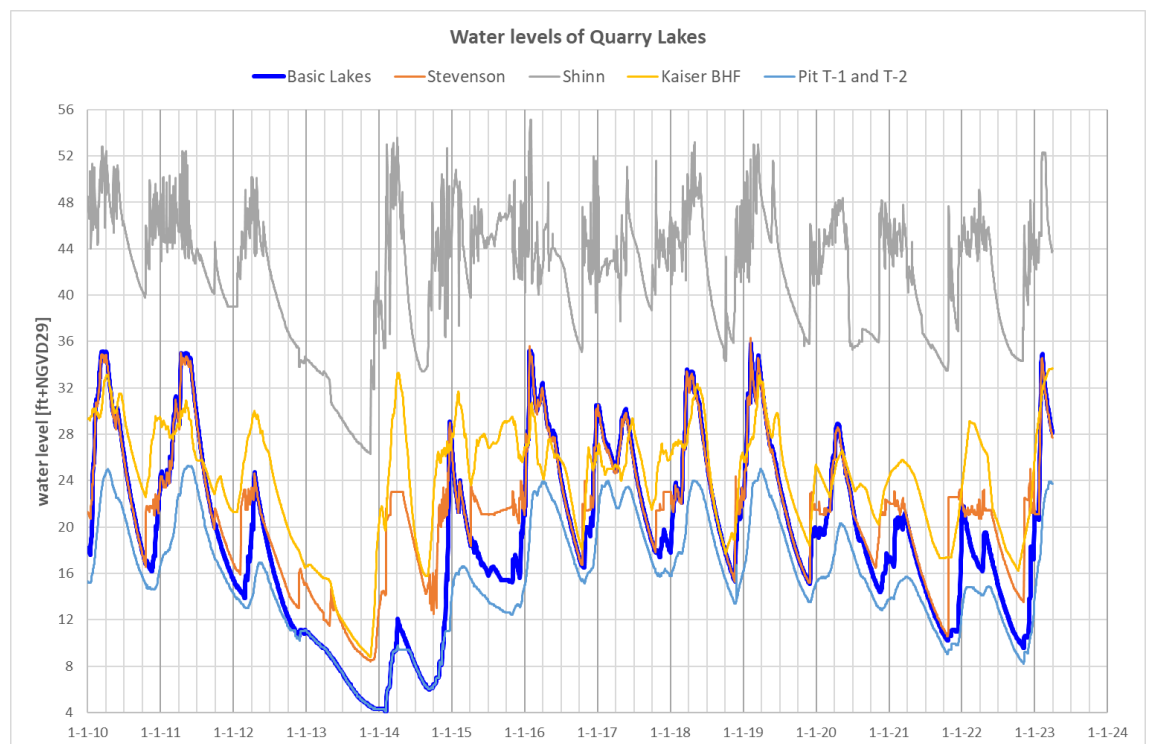


Figure 15 Applied daily water levels of the Quarry Lakes. For the basic lakes (blue line), Rainbow Pond, Horseshoe Lake, Lago Los Osos, Rock Pond, and Willow Slough, the same water level is applied in the child model (source ACWD).

3.5.3 Abstraction wells

In this study, all significant abstraction wells are included, as shown in Figure 16. Notably, the wells of the Mowry Wellfield are consolidated into a single well. The boundary of the local groundwater model has been drawn straight through the center of this single well. Likewise, the model boundary has been drawn through the Bellflower and Farwell Wells. The abstraction rates for these wells are adjusted based on the proportion of the well radius that lies within the model boundary, assuming radial flow towards the wells. Specifically, the abstraction rate is 50% for Mowry, 35% for Farwell, and 55% for Bellflower.

The abstraction rates for each well are recorded monthly. Figure 17 presents a comprehensive summary of these monthly totals for both the Newark Aquifer and the Centerville-Fremont Aquifer, spanning from January 2010 to March 2023. On average, over this period, the abstraction from the Centerville-Fremont aquifer is approximately four times that from the Newark Aquifer.



Figure 16 Abstraction wells, as applied in the child model, in the Newark Aquifer (red) and in the Centerville-Fremont Aquifer (green).

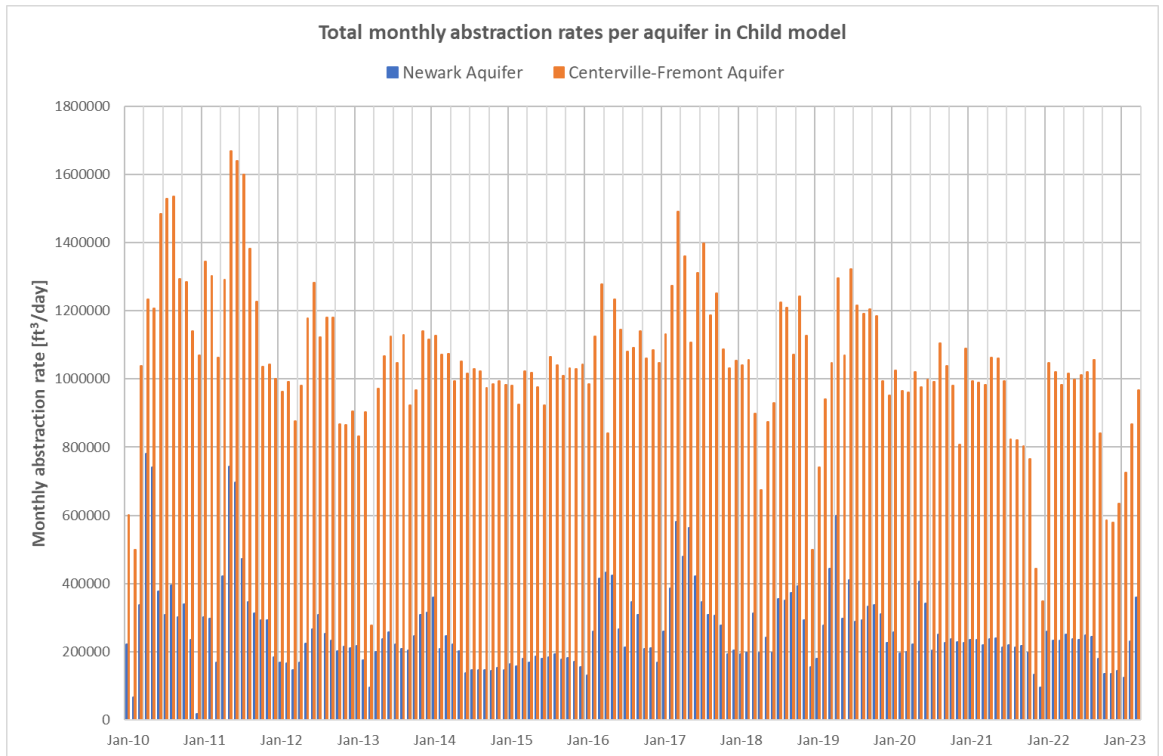


Figure 17 Monthly abstraction rates. Totals per aquifer, as applied in the child model.

3.5.4 Model boundaries

The boundary of the local groundwater model is presented by the thick red line visible in aerial overview figures, see for example Figure 3 or Figure 16. Along the portion of the boundary that intersects with San Francisco Bay, layer 1 is assigned a fixed level at MSL (0.27 ft+NGVD29). This specific level is based on the long-term daily average water level calculated by the Delft3D model.

For the remainder of the model boundaries, encompassing all four layers of the child model, we implement zero flow boundaries. This means no groundwater flow across these boundaries is assumed. Notably, the eastern boundary of the child model aligns with the Hayward Vault, an area where groundwater flow is considered negligible. The northern and southern boundaries are aligned approximately parallel to the regional groundwater flow. This orientation is particularly relevant in the southeastern part of the model, where regional flow is influenced by the abstraction wells situated along the boundary.

3.6 Calibration and Validation data

The calibration and validation of the child model are crucial steps to ensure its accuracy and reliability. For calibration purposes, we utilize hydraulic head observations from wells within both the Newark Aquifer and the Centerville-Fremont Aquifer. These observed hydraulic heads provide a benchmark to compare and adjust against the model's calculations.

The validation process involves a water balance approach. In this phase, we incorporate not only the observed hydraulic heads but also daily rainfall and evaporation data. Additionally, observed water levels in the Quarry Lakes and recorded diversions from Alameda Creek are factored into the validation. This multi-faceted approach allows for a thorough examination of the model's performance, independent of the calibration data, ensuring that the calculated results closely align with real-world observations.

3.6.1 Observed groundwater levels

In the local groundwater model, the monitoring of groundwater levels is conducted through a network of observation wells. Specifically, we have 31 observation wells in the Newark Aquifer and 30 observation wells in the Centerville-Fremont Aquifer, as depicted in Figure 18 and Figure 19, respectively. These wells have provided observation data spanning from January 2010 to March 2023, although the duration of data collection varies for each well. Observation frequencies range from biannual to weekly. We applied a calibration period of February 15, 2019, to February 14, 2020, in which the net rainfall is equal to the long-term average (Figure 20). The calibration period is preceded by a similarly long warmup period in which the net rainfall also is equal to the long-term average.

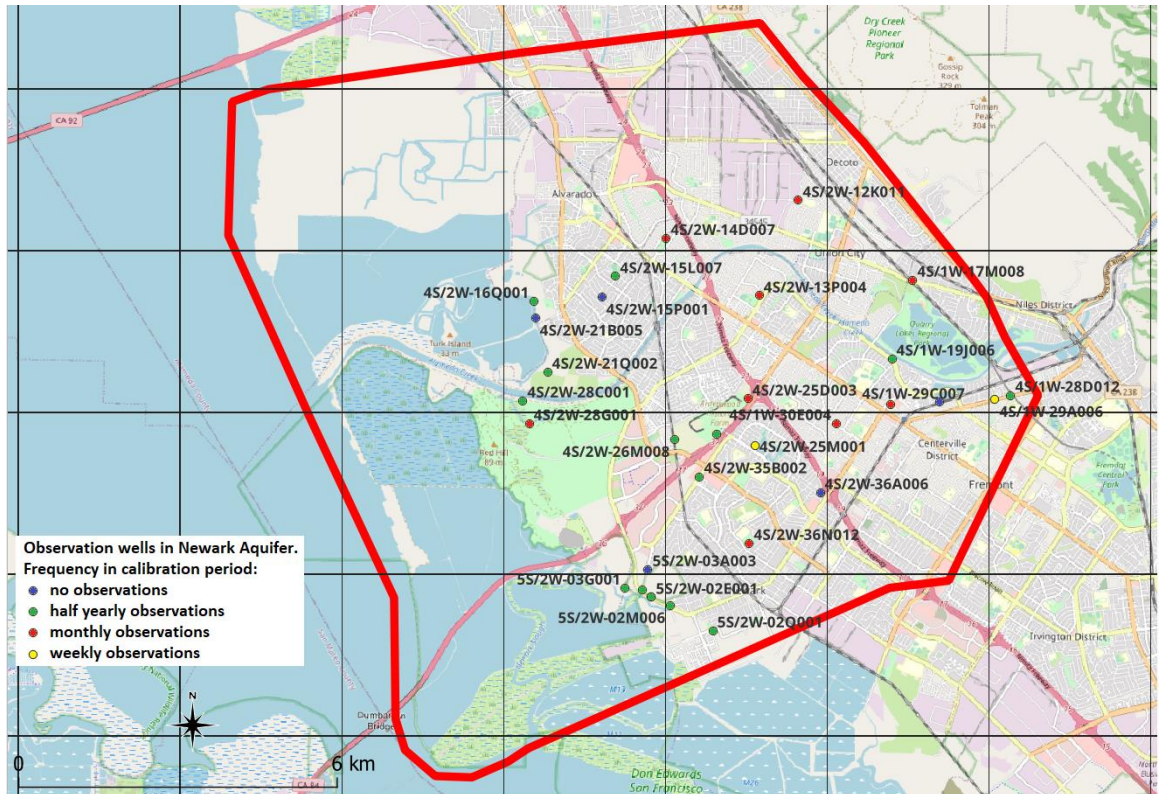


Figure 18 Observation wells in the Newark Aquifer, as applied in the child model.



Figure 19 Observation wells in the Centerville-Fremont Aquifer, as applied in the child model.

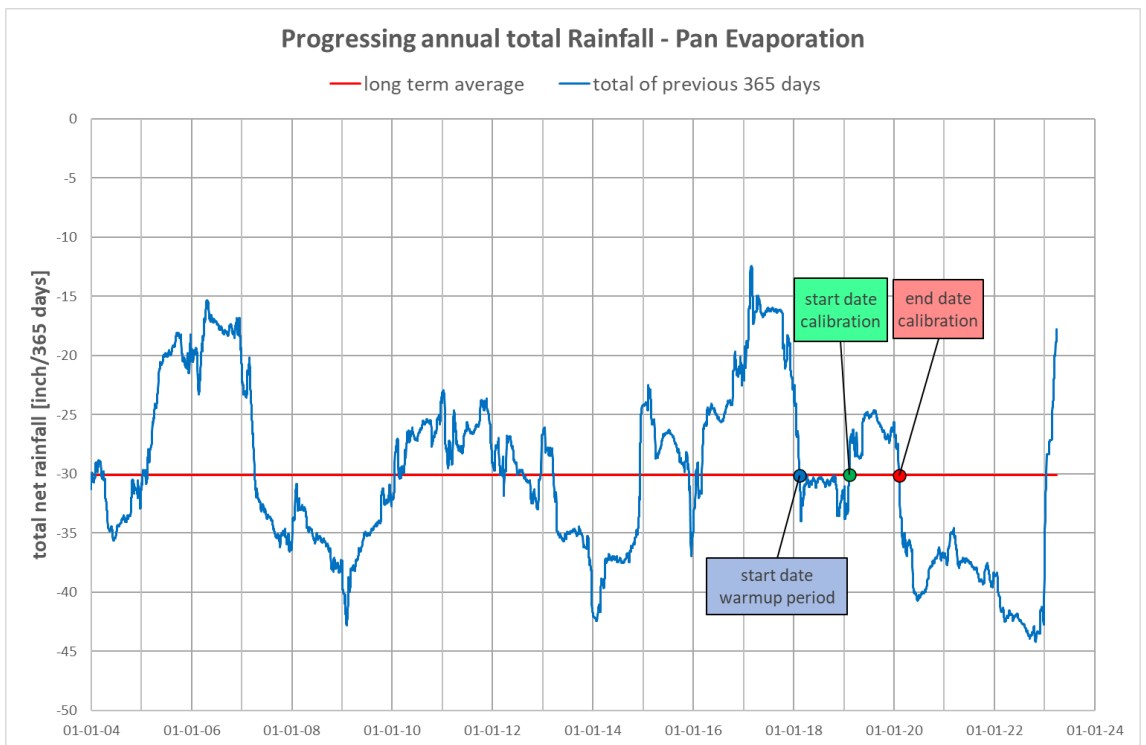


Figure 20 Selection of warmup period and calibration period.

3.6.2 Water balance of Quarry Lakes

ACWD provided valuable daily data on Alameda Creek water diversions into Shinn Pond (as shown in Figure 22) and daily lake water levels (Figure 15). Utilizing Google Earth satellite images of the Quarry Lakes at different water levels (Figure 21) and the high-resolution topobathymetry from 2019-2021, we established a relationship between the water level and surface area of the lakes. A daily water balance was constructed using this relationship, along with rainfall and evaporation data. The primary output of this balance is the lake infiltration rate into the groundwater, which we then compare with the infiltration rate calculated by the child model for validation purposes.

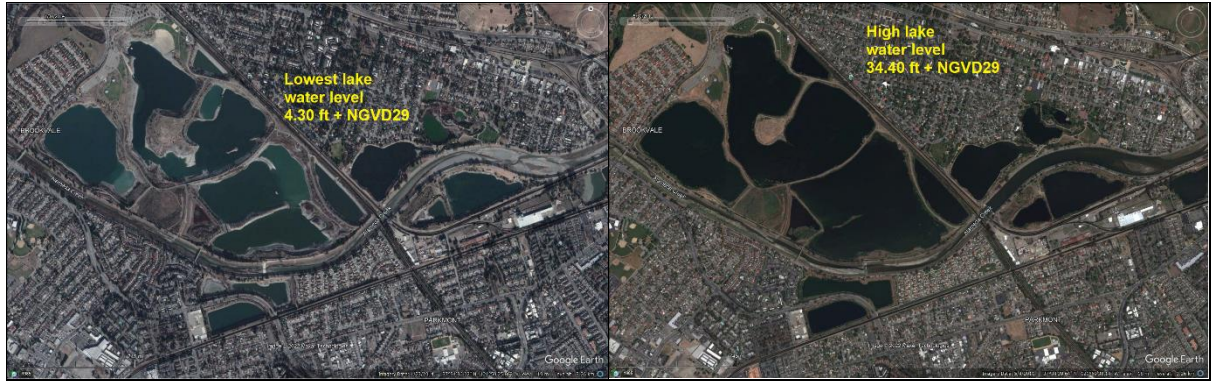


Figure 21 Google Earth satellite images of the Quarry lakes at different dates. Left: January 2014. Right: May 2011.

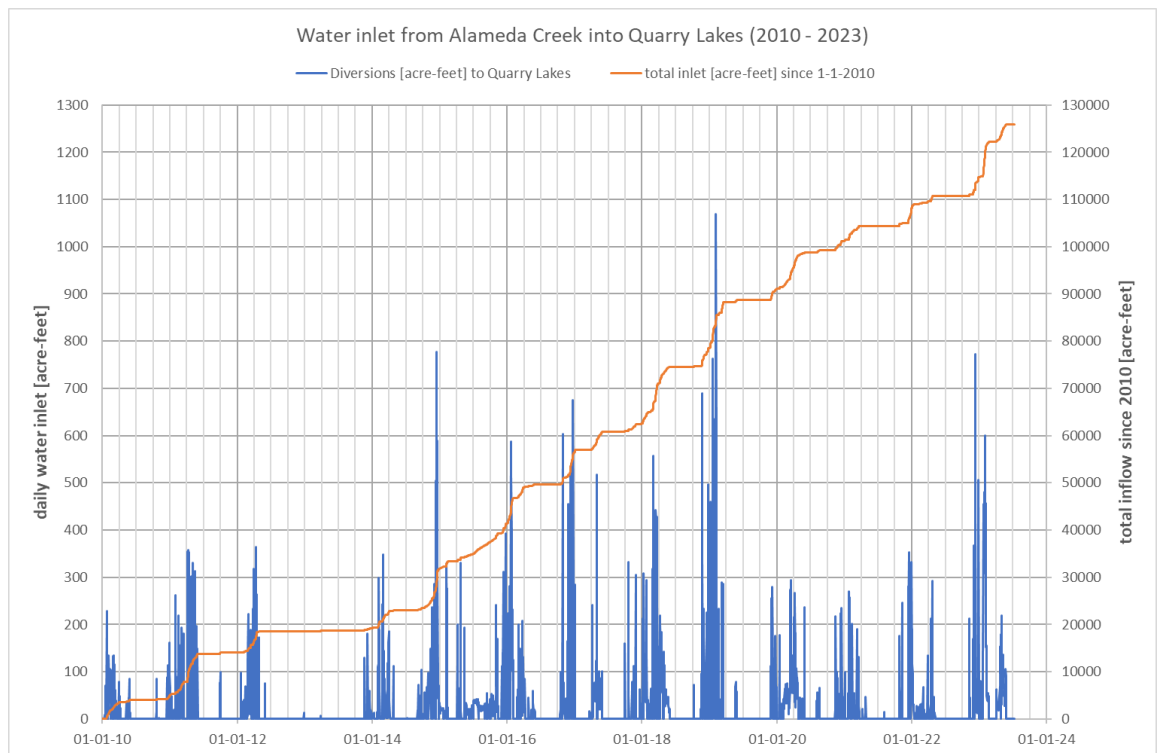


Figure 22 Registered daily diversion volumes from Alameda Creek to Quarry Lakes (source: ACWD).

We determined the infiltration rate based on the difference between lake and groundwater levels, with the understanding that higher lake levels typically lead to increased infiltration rates. However, since groundwater level time series are unavailable, we relied on lake water level time series. Applying short-term (6-day) water balances during depletion periods, we derived the following relationship:

$$\text{Infiltration rate [ft/day]} = (\text{water level drop [ft]} + \text{net rainfall [ft]}) / 6 \text{ [days]}.$$

This formula was applied to observed water levels in Horseshoe Lake, with Shinn Pond and Stevenson Pond showing similar patterns (Figure 26). Over a 20-year period, this method was used for 683 six-day depletion periods, linking infiltration rates to corresponding lake water levels. The results, represented by orange dots, are shown in Figure 23. The red dashed line and the formula in the black rectangle illustrate the trend line and the derived relationship between infiltration rate and lake water level. The blue and green dashed lines mark the boundaries containing 90% of the results.

This method may have limitations in accuracy, but combined with the water balance approach, it provides a reliable order of magnitude for validating the child model's results.

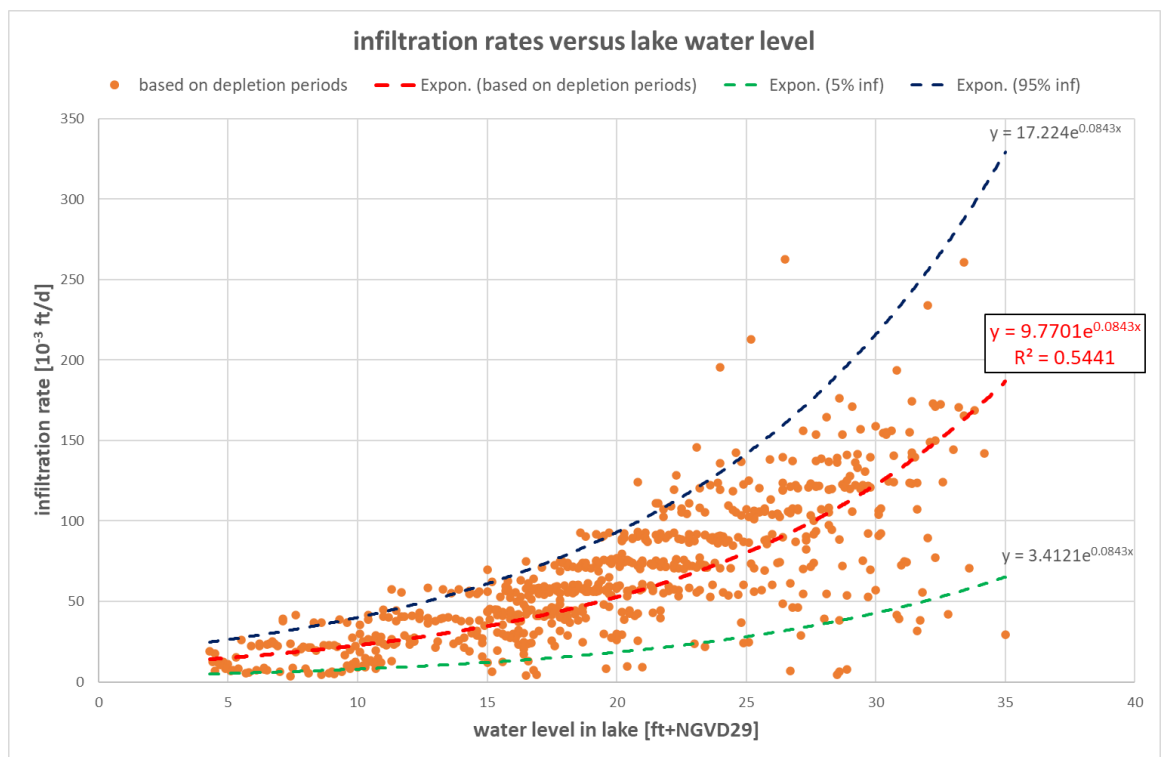


Figure 23 Relation between lake infiltration rate and lake water level, based on observed depletion periods.

3.7 Variations explored

3.7.1 Bed levels

After calibration and validation of our high-resolution local groundwater model in MODFLOW6, three scenarios are explored:

1. **The USACE design:** In this original design the creek has a trapezium shape with a wide horizontal middle section.
2. **The current situation:** In time, the middle section of the bed has changed into the current situation by erosion and by sedimentation due to riverine and tidal influences.
3. **The proposed scenario:** This scenario has a deepened bed relative to the current situation to reduce sedimentation. Therefore, the proposed situation only differs from the current situation in this deepened part of the creek.

For a visual impression of each bed level scenario, one is referred to Appendix B.3.

3.7.2 Water levels

The applied water levels in Alameda Creek are daily averages of the calculated water levels by the Delft3D model. The model was rerun for the different bed level scenarios considered.

3.7.3 Analysis method

In the original design (USACE), the creek has a trapezium shape with a wide horizontal middle section. In time, this middle section of the bed has changed into the current situation by erosion and by sedimentation. Aim of the proposed situation is to reduce sedimentation by deepening part of the current bed between BART weir and the railroad crossing south of Alvarado Blvd (Figure 24, sections 1 to 5). Hence, the proposed situation only differs from the current situation in this deepened part of the creek but differs from the USACE design in the entire middle section of the creek.

Current water management has gradually adapted to the current situation. Therefore, the proposed bed deepening is foreseen to have effect on the current water management. The expected additional upwelling in the creek will have effect on groundwater levels and infiltration rates of the Quarry Lakes. All this may have effect on the water availability for drinking water and may require ACWD to change their water management of both lakes and abstraction wells. Therefore, comparing the proposed situation to the current situation is important. However, since the USACE design is the official standard, the effect of the proposed bed deepening will primarily be compared to the USACE design and secondarily to the current situation.

The proposed bed deepening in Alameda Creek is foreseen to have effect on the surrounding groundwater system. This potential effect will be analyzed with the child model for changes in upwelling of groundwater in the creek (for each section and for the entire part of the creek that lies within the child model), changes in infiltration volumes from the Quarry Lakes and for changes in hydraulic heads in the two aquifers.

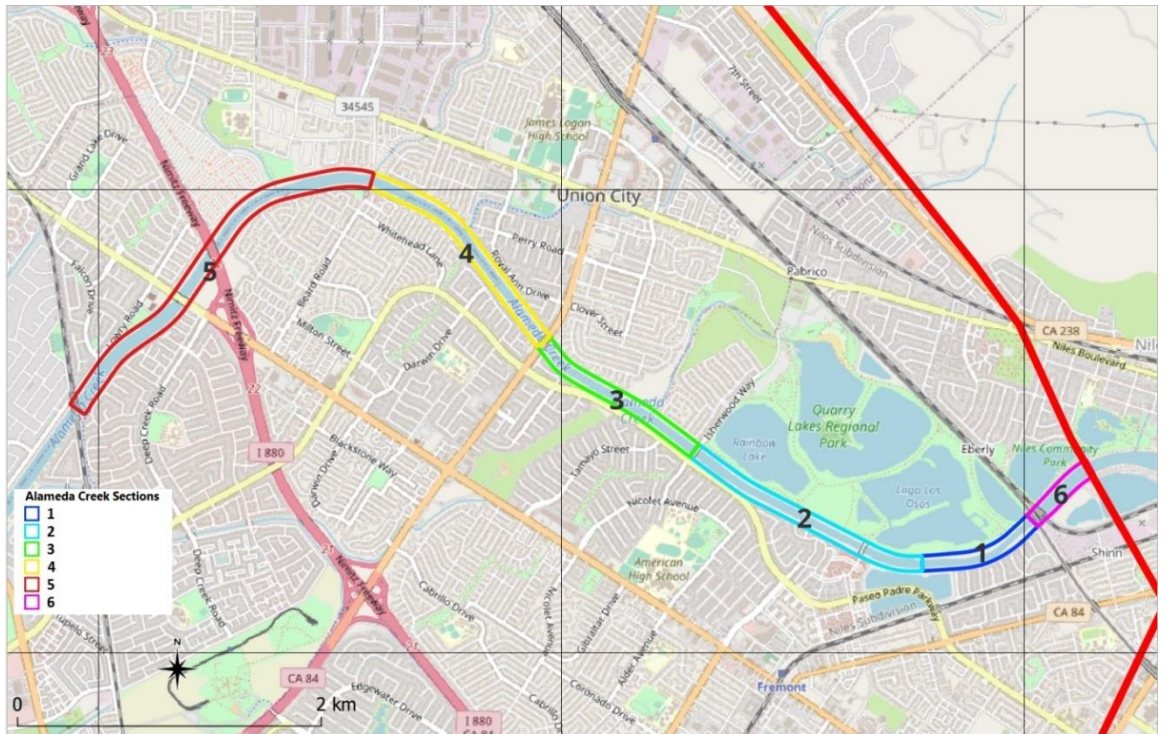


Figure 24 Defined creek sections (1 to 5) for scenario analysis. Section 6, mainly upstream of BART weir, is added.

3.8 Analyzing the effect of Quarry Lakes Water Levels and Rainfall on Hydraulic Heads

Extensive analysis of the observed data shows that changes in recharge by rainfall and evaporation have only a limited effect on the hydraulic heads in the Newark Aquifer, where the water levels in the Quarry Lakes have a large effect. Even at approx. 22,500 ft away of the lakes the hydraulic head in the Newark Aquifer seems still more affected by the water levels in the lakes than by wet or dry periods. Figure 25 compares from 2010 onwards the daily observed water levels in the Horseshoe Lake (blue line, left axis) to observed hydraulic heads in the Newark Aquifer with an observation frequency of 1 month or higher (colored dots, left axis). The figure also contains the rainfall of the previous 365 days as observed in the PT Wellfield (red line, right axis).

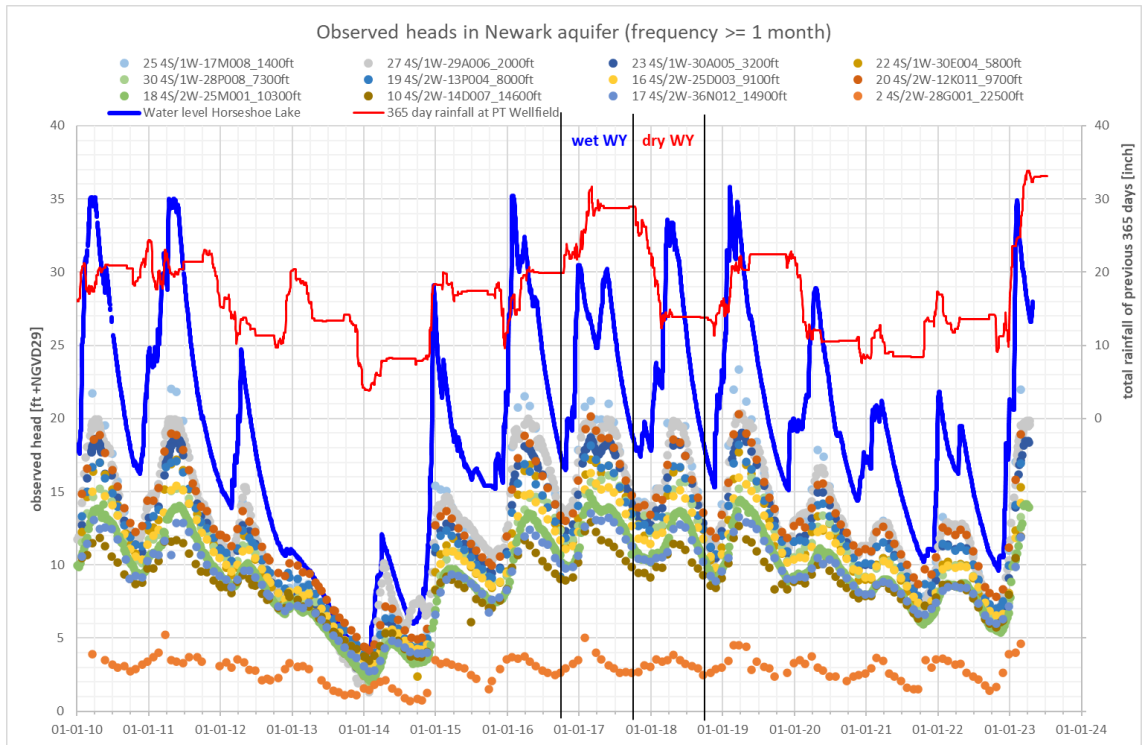


Figure 25 Timeseries of observed groundwater hydraulic heads in the Newark Aquifer (dots). The legend indicates the distance of the observation wells to the Quarry Lakes. The blue line shows the observed water levels in the Horseshoe Lake. The red line indicates the total rainfall of the past 365 days as observed in the PT wellfield. The black vertical lines indicate a wet water year (2017) and a dry water year (2018).

The Water Year 2017 (WY2017 from Oct. 2016 – Sep. 2017) with 28.9 inches of observed rainfall was more than twice as wet as WY2018 with only 13.8 inches of observed rainfall. The average of all observed heads is in WY2018 almost 0.9 ft lower than in WY2017. The average observed water level in the Horseshoe Lake in WY2018 is almost 0.8 ft lower than in WY2017. Figure 26 shows the observation in both water years into more detail. Here it is clearly shown that the heads in the Newark Aquifer are influenced much more by the lake water levels than by the rainfall.

These observations indicate a considerable hydraulic resistance in the top layer and an almost negligible recharge of the aquifer due to rainfall. This supports the decision to simulate the top layer as a singular layer with low vertical hydraulic conductivity. In other words, the detailed differentiation within the top layer might be less critical to simulate groundwater flow in this area than previously thought.

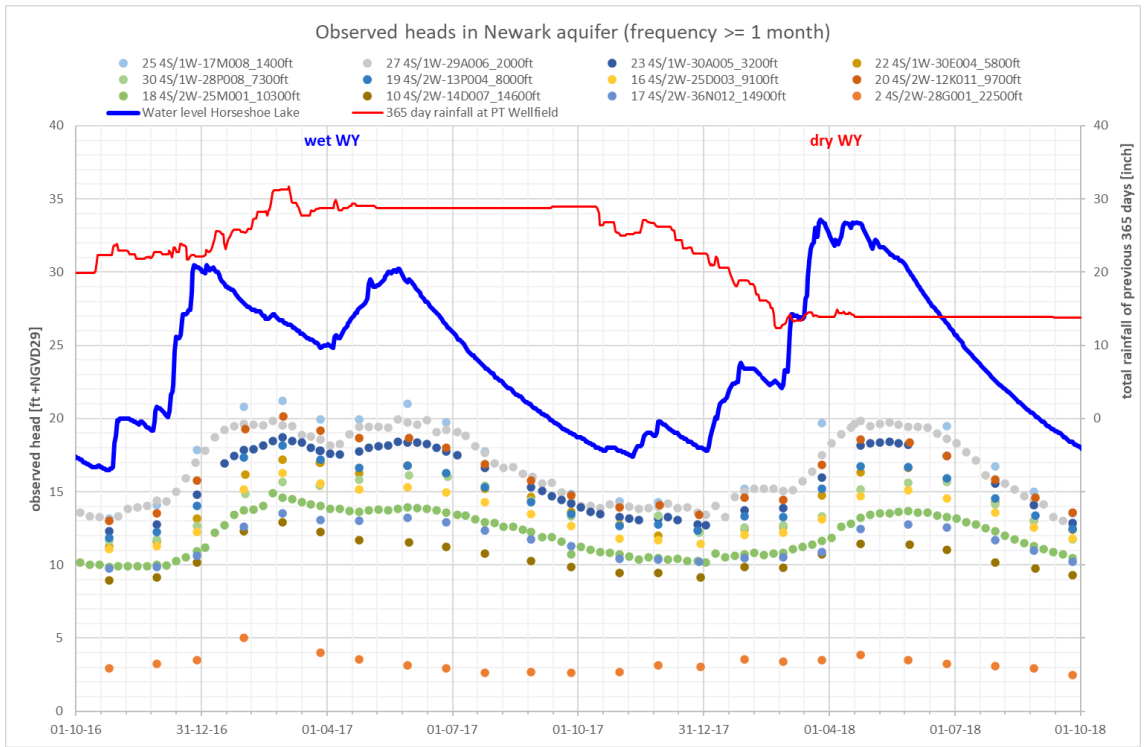


Figure 26 Timeseries of observed groundwater hydraulic heads in the Newark Aquifer (dots) for a wet water year (2017) and a dry water year (2018). The legend indicates the distance of the observation wells to the Quarry Lakes. The blue line shows the observed water levels in the Horseshoe Lake. The red line indicates the total rainfall of the past 365 days as observed in the PT wellfield.

4 Model Calibration and Validation

4.1 Introduction

This report begins with a detailed calibration of the model, initiated through a comprehensive sensitivity analysis of key parameters. The insights gained from this sensitivity analysis were instrumental in selecting the most appropriate grid for the model calculation. In particular, the 16-ft grid provided comparable results to the 8-ft grids and was therefore selected for further use. Moreover, the model underwent a rigorous calibration process for the current scenario by calibrating several most sensitive parameters. The calibration covered a model warmup period from February 15, 2018, to February 14, 2019, and an actual calibration period from February 15, 2019, to February 14, 2020. It was then validated over a longer duration, from January 1, 2010, to January 4, 2023, to ensure its accuracy and reliability. The sensitivity testing can be found in Appendix A2

4.2 Calibration

During calibration the values of several model parameters have been adapted and several remained unchanged. According to previous model calibration efforts (NEBIM) the horizontal hydraulic conductivity of the Newark and Centerville-Fremont aquifers show large spatial variations (Figure 62 and Figure 63 in Appendix B.2). During calibration we applied a factor over the entire area to change these parameter values. Best results were obtained by applying a factor 1 for both aquifers, implying that the parameter values of NEBIM remain unchanged. Parameters that have been adapted during calibration are horizontal hydraulic conductivities of layers 1 and 3 (the aquitards), vertical hydraulic conductivities of all 4 layers (vertical anisotropy factors) and storage coefficients.

Figure 12 in Section 3.4.2 already showed the resulting horizontal transmissivities of the aquifers and the differences between child model and NEBIM of the resulting vertical hydraulic resistances of the aquitards. NEBIM applies two different vertical anisotropy factors per aquifer, one for the above lying aquitard and one for the aquifer itself. The anisotropy factors for the aquitards are already incorporated in the vertical hydraulic resistances that are compared in Figure 12. The vertical anisotropy factors of the aquifers in NEBIM are on average approx. 3 times higher than the factor 5 that we applied in the child model. We envision this will not influence the model results much, but in aquifers with such high hydraulic conductivities an anisotropy factor of 5 is more likely than the average factors 17.4 and 14.2 that are applied in NEBIM for the child model area for the Newark Aquifer and the Centerville-Fremont Aquifer respectively.

Regarding storage coefficients MODFLOW6 uses a specific yield (SY) per model layer, when the groundwater level is below the top of the layer (unconfined), and a specific storage (SS) when the groundwater level is above the top of the layer (confined). Basically, every layer can be confined or unconfined, but in the child model the base of the top layer (layer 1), i.e. the top of layer 2, is always below the groundwater level. Since the phreatic groundwater level is always in layer 1 the SY is only relevant for this layer. Based on literature values for clay and silt layers we applied an SY of 5%, whereas NEBIM applied an average value of 11% for the child model area. For reasons that MODFLOW6 also needs an SY for the other layers, we applied the same SY value for all four layers.

In MODFLOW6 the SS is per thickness unit, so in this model per ft. That means that in a 150 - 200 ft thick layer, like the Newark aquifer, a specific storage of 0.00001/ft will result in a total elastic storage coefficient of 0.003 - 0.005. In NEBIM this works similar. Calibration resulted in a value of 0.00001 for SS in all layers, where NEBIM applied average values of 0.02 for the Newark Aquifer and 0.0005 for the Centerville-Fremont Aquifer. We tried these factors during calibration, but they resulted in much too slow changes in calculated hydraulic heads in the aquifers, especially in the Centerville-Fremont Aquifer. We and therefore deviated from the NEBIM more on this parameter choice.

The sensitivity analysis (Appendix A) showed that the groundwater levels in observation wells are very sensitive for changes in lakebed resistances and hardly sensitive for changes in creek bed resistances. Upwelling of groundwater in the creek is very sensitive for the changes in creek bed resistances and only moderately sensitive for changes in lakebed resistances. Lake infiltration is moderately sensitive for changes in creek bed resistances and, as could be expected, extremely sensitive for changes in lakebed resistances. Based on this calibration resulted in a lakebed resistance of 100 days, with a relatively high reliability. We also applied a value of 100 days for the creek bed resistance, but this has a much lower reliability. In the child model a model cell area is either completely water (lake or creek) or completely not. In NEBIM, streambed parameters required include the hydraulic conductivity and thickness of the streambed. During the calculation of the stream-aquifer interaction, NEBIM internally computes a streambed conductance that is proportional to the conductivity and inversely proportional to the streambed thickness. The NEBIM report contains only a figure on streambed conductivity. Therefore, it is not possible to compare the actual applied bed resistances of the two models.

Table 1 provides an overview of the parameters resulting from calibration of the child model.

Table 1 Resulting calibration parameters.

Layer	Formation	k_H [ft/d]	Factor	k_H high area	k_v	SY	SS
1	Aquitard 1	0.5	-	$k_{H,layer2} / 50$	$k_{H,layer1} / 10$	0.05	1E-05
2	Aquifer 1	NEBIM values	1	-	$k_{H,layer2} / 5$	0.05	1E-05
3	Aquitard 2	0.05	-	-	0.005	0.05	1E-06
4	Aquifer 2	NEBIM values	1	-	$k_{H,layer4} / 5$	0.05	1E-06
Bed resistance of lakes [d]			100				
Bed resistance of Alameda Creek [d]			100				

As mentioned before in both aquifers two observation wells have a weekly monitoring frequency, wells 4S/2W-25M001 and 4S/1W-29A006 in the Newark Aquifer and wells 4S/1W-19L002 and 4S/1W-30A004 in the Centerville-Fremont Aquifer. For these wells the timeseries of the observations and the model results are respectively shown in Figure 27, Figure 28, Figure 29 and Figure 30. The left part of these figures is the warmup period of the model that starts from a steady state calculated average situation.

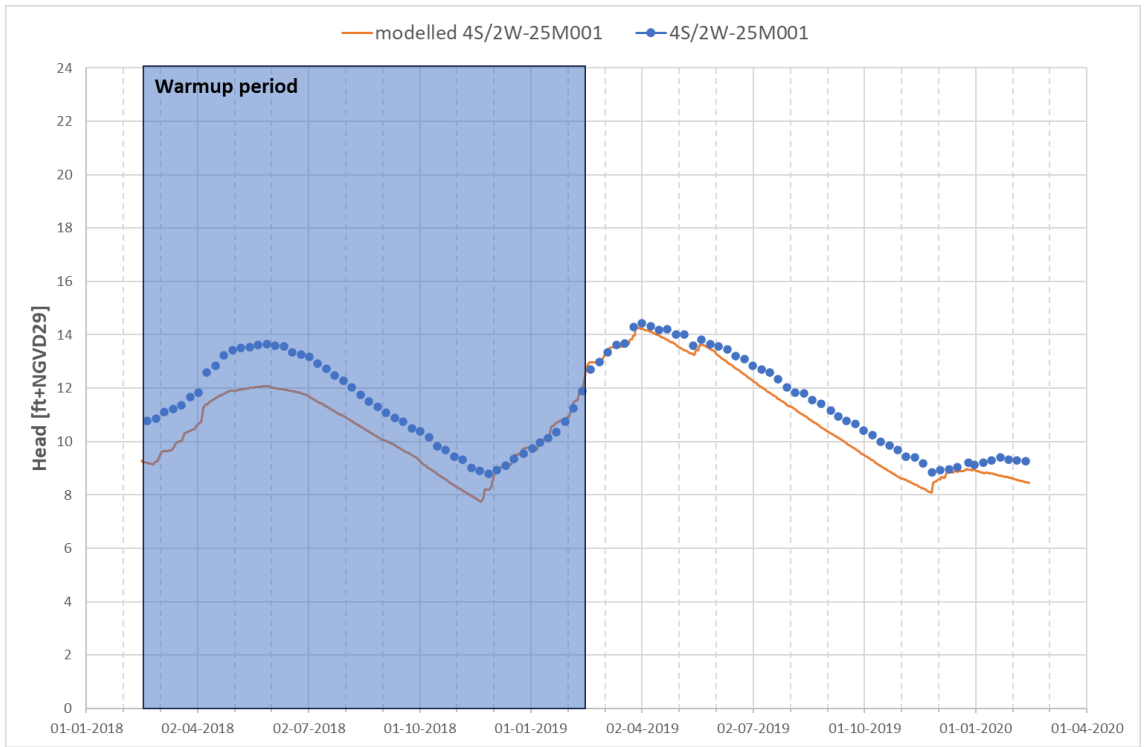


Figure 27 Calibration result for observation well 4S/2W-25M001 in the Newark Aquifer with weekly observations. The blue left part is the warmup period.

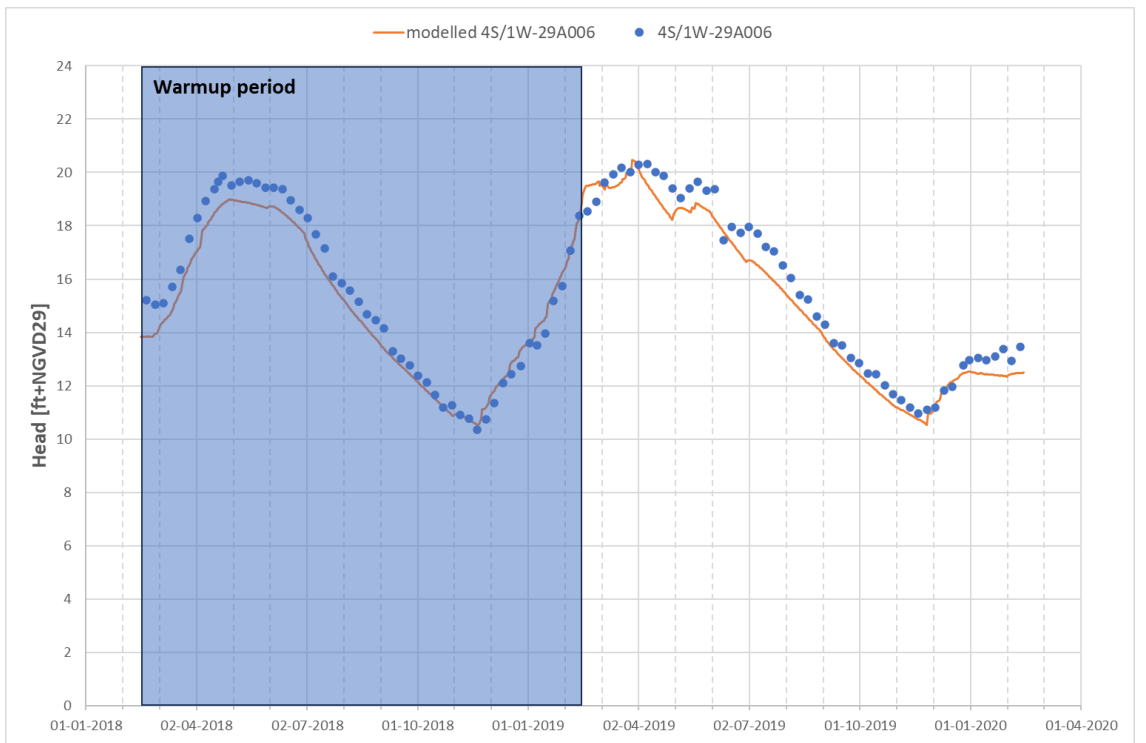


Figure 28 Calibration result for observation well 4S/1W-29A006 in the Newark Aquifer with weekly observations. The blue left part is the warmup period.

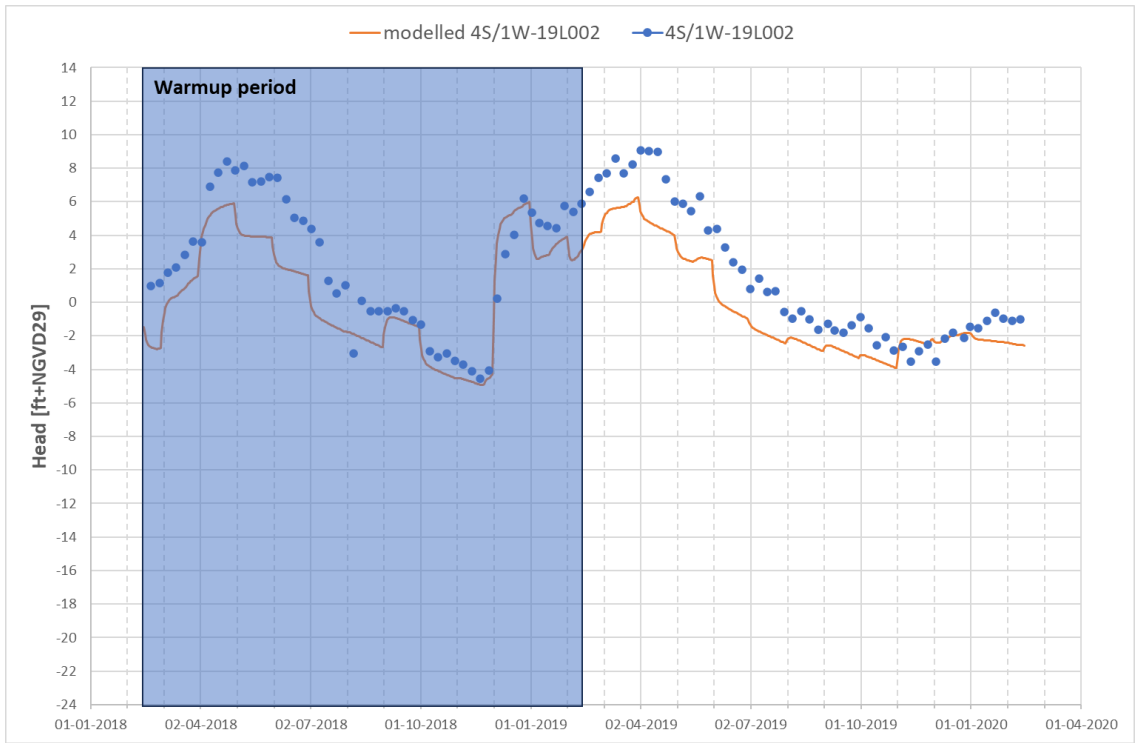


Figure 29 Calibration result for observation well 4S/1W-19L002 in the Centerville-Fremont Aquifer with weekly observations. The blue left part is the warmup period.

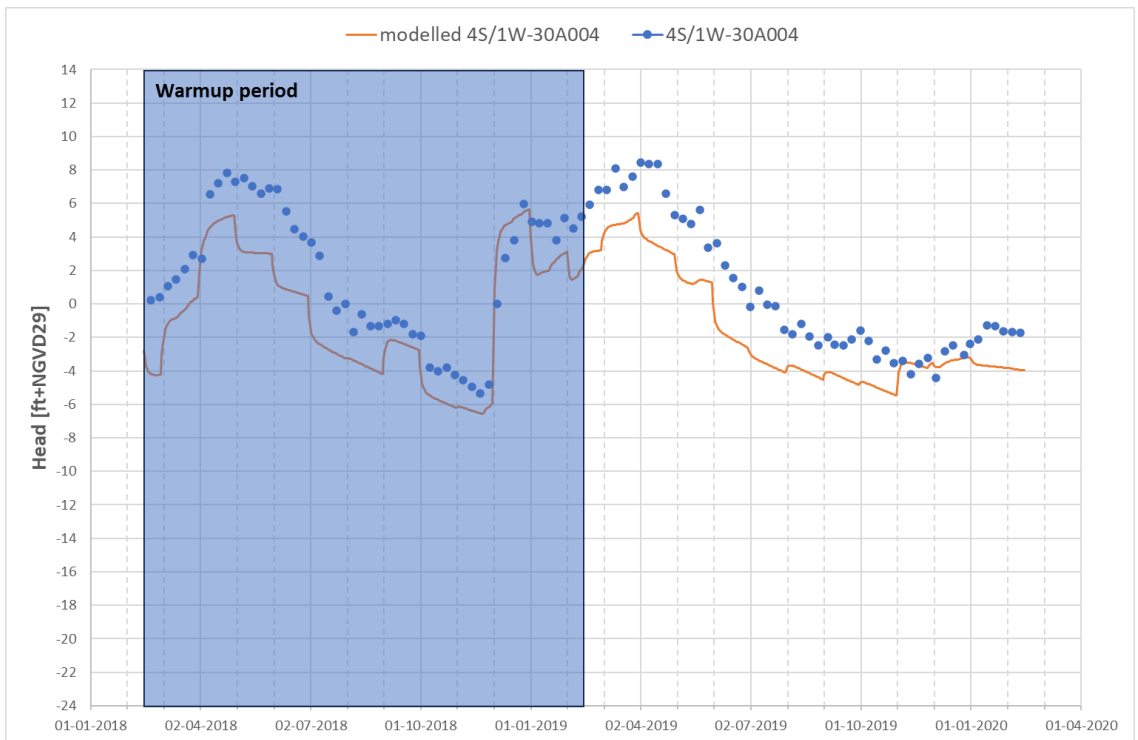


Figure 30 Calibration result for observation well 4S/1W-30A004 in the Centerville-Fremont Aquifer with weekly observations. The blue left part is the warmup period.

The model results at two observation wells in the Newark Aquifer show a very good fit with the observed groundwater heads. For all 52 observations in the calibration period the average absolute deviation is 0.55 (Figure 27), respectively 0.60 ft (Figure 28). The deviations at the two observation wells in the Centerville-Fremont Aquifer are larger, 1.93 (Figure 29) and 2.48 ft (Figure 30). This is partly caused by the applied monthly averages of the rates of the abstraction wells that are visible in the head jumps in the model results. The heads in the Newark Aquifer are dominated by the water levels in the Quarry Lakes over the abstraction wells. In addition, groundwater abstraction rates in the Newark Aquifer are approx. 4 times lower than in the Centerville-Fremont Aquifer (Figure 17). The groundwater heads in the Centerville-Fremont Aquifer are (approx. 50%) less influenced by the lake water levels. This is caused by the damping effect of the aquitard above. In the Centerville-Fremont Aquifer the abstraction rates have a large effect on the groundwater heads. The model results show a similar variation as the observations. The calculated heads in the Centerville-Fremont Aquifer are general 1 to 2 ft lower than the observed heads. In the Newark Aquifer this deviation is less. Considering the purpose of the child model these small deviations from observations are acceptable.

The rest of the applied observation wells (see Figure 18 and Figure 19) are summarized in Table 2 for the Newark Aquifer and in Table 3 for the Centerville-Fremont Aquifer. In both tables the results are presented for observation wells with a monthly (or higher) monitoring frequency and for all applied observation wells.

Table 2 Calibration result for Newark Aquifer.

Newark aquifer number of wells	Monthly or more observations: 11			All observations: 25		
Year 2	average	min	max	average	min	max
Number of observations	20	11	52	10	1	52
Average deviation [ft]	-1.08	-2.25	-0.45	-0.63	-2.74	2.39
Average absolute deviation [ft]	1.10	0.52	2.25	1.15	0.27	2.74
Minimum deviation [ft]	-1.92	-3.55	-0.95	-1.18	-3.55	0.96
Maximum deviation [ft]	-0.24	-1.64	0.94	-0.07	-2.20	4.12

Table 3 Calibration result for Centerville-Fremont Aquifer.

CF aquifer number of wells	Monthly or more observations: 15			All observations: 29		
Year 2	average	min	max	average	min	max
Number of observations	17	11	52	10	2	52
Average deviation [ft]	-0.20	-4.34	2.29	-1.64	-6.56	2.29
Average absolute deviation [ft]	1.87	1.11	4.34	2.54	0.68	6.56
Minimum deviation [ft]	-2.53	-6.88	-0.14	-3.08	-6.93	-0.14
Maximum deviation [ft]	2.13	-0.93	4.12	-0.20	-6.19	4.12

Table 2 shows that the average absolute deviations in the Newark Aquifer of all observation wells (1.15 ft) are slightly higher than for observation wells with a monitoring frequency of once a month of higher (1.10 ft). Table 3 shows larger differences in this for the Centerville-Fremont Aquifer (2.54 ft versus 1.87 ft). On average the calculated groundwater heads in the Newark Aquifer are 0.63 ft lower than the observations. In the Centerville-Fremont Aquifer this difference is a foot larger.

These results give confidence that the calibrated child model can calculate effects of changes in the bed level of Alameda Creek on the surrounding groundwater with sufficient accuracy.

4.3 Validation

4.3.1 Introduction

The calibrated child model primarily focuses on a two-year span, incorporating an initial 'warm-up' year to stabilize the system. However, its validation encompasses a much more extended period, from January 1, 2010, to January 4, 2023. This validation phase is crucial, as it accounts for significant variations in environmental conditions, including notably lower lake and groundwater levels, and higher and more intense rainfall patterns, as indicated previously in Figure 25.

Extending the model's application further back in time raises certain challenges. System changes post-2010 are not incorporated in the model, potentially leading to discrepancies between the calculated and observed groundwater heads. During the validation period, actual rainfall and evaporation data, lake water levels, and monthly averaged rates from groundwater abstraction wells are used. However, potential temporary changes in the infiltration resistances of lake beds, possibly due to cleaning, re-clogging, or weathering during prolonged periods of low water levels, are not accounted for.

The validation figures (Figure 31 to Figure 37) that are discussed in the sections below are presented in Section 4.3.5.

4.3.2 Comparison to Observed Hydraulic Heads

Our validation process includes a detailed analysis of hydraulic heads at several observation wells within both the Newark and Centerville-Fremont Aquifers. Figure 31 through Figure 34 illustrate the validation results for wells that are monitored weekly.

In all these wells, the variation in model-calculated hydraulic heads closely mirrors the magnitude of the observed heads. A notable discrepancy is observed in the model's slower recovery from periods of extremely low groundwater levels, driven by similarly low lake water levels as indicated previously in Figure 25. While observations suggest a recovery period of approximately two years starting in early 2014, the local groundwater model indicates a recovery span of around four years. This difference likely stems from a temporary reduction in the lake beds' infiltration resistance, gradually returning to its original state. It is important to note that the child model assumes constant infiltration resistance throughout the validation period, which does not account for these temporary changes.

Table 4 provides an overview of the validation result in the observation wells in the Newark Aquifer. Table 5 does the same for the Centerville-Fremont Aquifer.

Table 4 Validation result for Newark Aquifer.

Number of wells 01-01-2010 / 04-01-2023	Monthly or more observations: 11			All observations: 31		
	average	minimum	maximum	average	minimum	maximum
Number of observations	271	140	766	111	1	766
Average deviation [ft]	-2.46	-3.56	-1.30	-2.05	-3.58	0.45
Average absolute deviation [ft]	2.47	1.30	3.56	2.18	0.88	3.58
Minimum deviation [ft]	-6.60	-9.06	-3.42	-5.10	-9.06	-1.04
Maximum deviation [ft]	-0.28	-0.83	2.02	0.03	-3.10	4.03

Table 5 Validation result for Centerville-Fremont Aquifer.

Number of wells 01-01-2010 / 04-01-2023	Monthly or more observations: 15			All observations: 30		
	average	minimum	maximum	average	minimum	maximum
Number of observations	223	147	683	123	6	683
Average deviation [ft]	-1.07	-5.17	1.27	-2.47	-8.17	1.27
Average absolute deviation [ft]	2.60	1.84	5.27	3.51	1.68	8.17
Minimum deviation [ft]	-6.65	-10.84	-3.98	-7.66	-13.11	-3.62
Maximum deviation [ft]	5.35	1.73	6.72	3.45	-3.05	7.14

The average absolute deviations between calculated and observed values for the more frequently observed wells in both aquifers are 1.37 ft (Newark Aquifer) and 0.73 ft (Centerville-Fremont Aquifer) larger than for the calibration period. For all observation wells these increases are 1.03 ft and 0.97 ft respectively. Considering the potential system changes mentioned in Section 4.3.1 this is still an acceptable result.

4.3.3 Comparison with NEBIM Model Results

Figure 35 and Figure 36 offer a side-by-side comparison of the outcomes from the local high-resolution groundwater model and the NEBIM model, providing a unique perspective on their respective performances. With the orange lines representing the child model results and the green lines depicting those from NEBIM, these figures encapsulate data spanning from 2010 to 2020. This comparative approach allows for a deeper understanding of how each model behaves under similar conditions and highlights their respective strengths and limitations.

A key observation from these figures is the similarity in recovery velocity discrepancies between both models and the actual observed data. This trend underscores a common challenge in modeling groundwater systems, particularly in accurately capturing the dynamics of recovery periods. Furthermore, the child model's performance in the Newark Aquifer, as shown in Figure 35, aligns more closely with observed data compared to the NEBIM model. This suggests a more refined calibration or a better representation of local conditions in the child model.

In contrast, Figure 36 illustrates that the performance of both models in the Centerville-Fremont Aquifer is more closely matched. This parity indicates that for this particular aquifer, both models are similarly effective in simulating the observed conditions, possibly due to similar underlying assumptions or data inputs.

This comparative analysis not only highlights the relative strengths of the child model but also provides valuable insights into areas where both models exhibit common challenges, guiding future refinements and enhancements in groundwater modeling.

4.3.4 Comparison with Lake Infiltration

In the realm of groundwater modeling, accurately estimating lake infiltration rates is a complex yet vital component. Figure 37 presents an insightful validation of our model's lake infiltration calculations, contrasting them against two independent estimation methods. These methods include lake infiltration rates derived from a comprehensive water balance of the lakes and those obtained through a specifically formulated infiltration equation.

As previously discussed and illustrated in Figure 23, the flow volumes obtained from these derived methods are not exact but rather provide a general scale of magnitude. This approach acknowledges the inherent uncertainties and complexities in accurately quantifying lake infiltration rates.

Crucially, the comparison demonstrates that the total calculated lake infiltration in the model since 2010 aligns well within this estimated order of magnitude. This agreement underscores the model's effectiveness in simulating lake infiltration processes and reinforces the validity of the modeling approach adopted. Such alignment between modeled results and independently derived estimates is a strong indicator of the model's reliability in capturing the essential dynamics of lake-groundwater interactions.

4.3.5 Validation figures

This sections contains the validation figures (Figure 31 to Figure 37) that are discussed above in sections 4.3.2, 4.3.3 and 4.3.4.

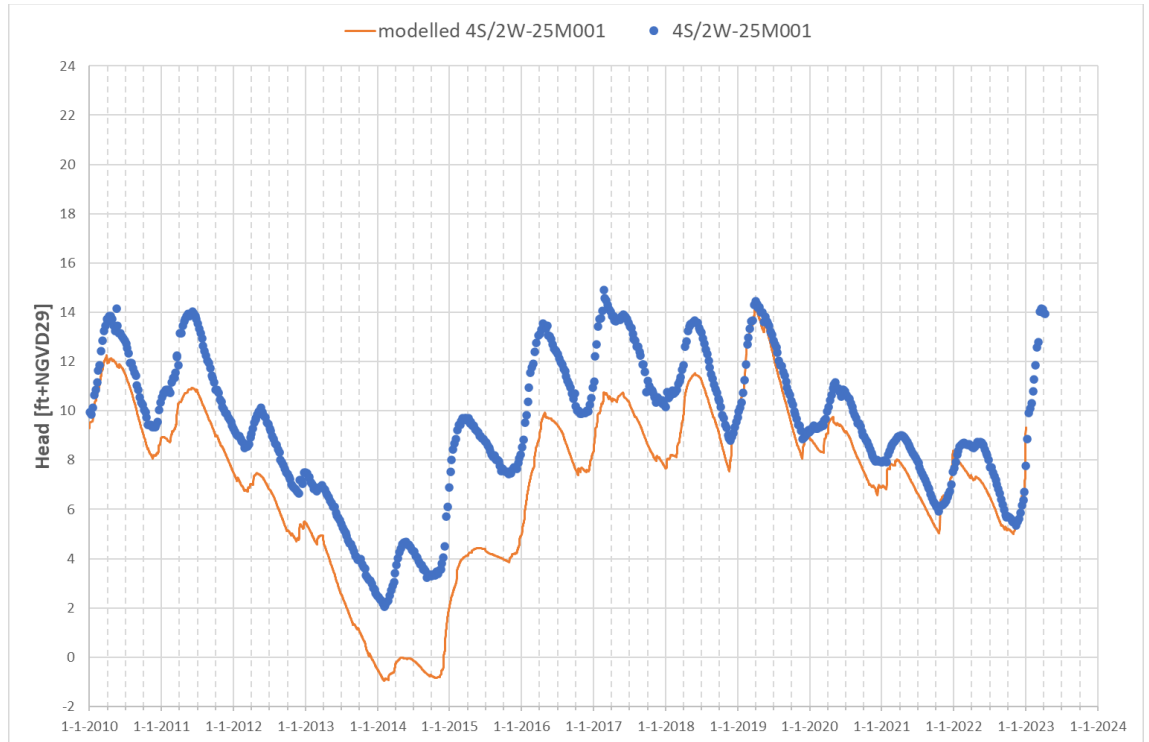


Figure 31 Validation result for observation well 4S/2W-25M001 in the Newark Aquifer with weekly observations.

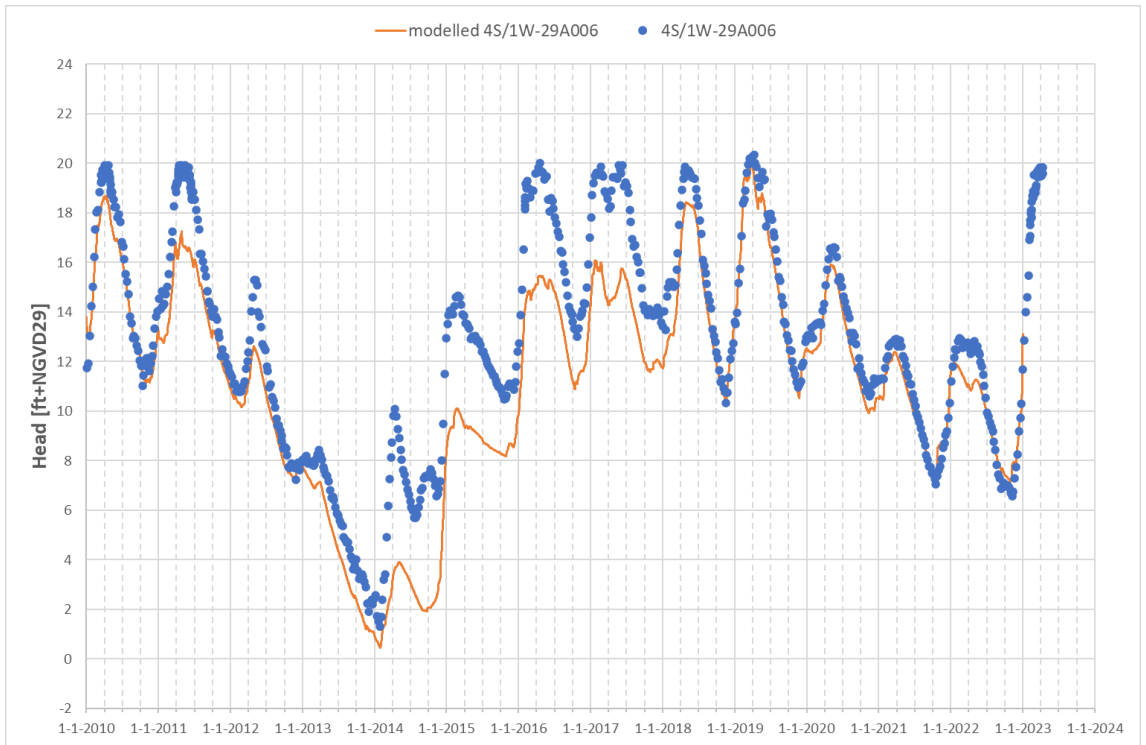


Figure 32 Validation result for observation well 4S/1W-29A001 in the Newark Aquifer with weekly observations.

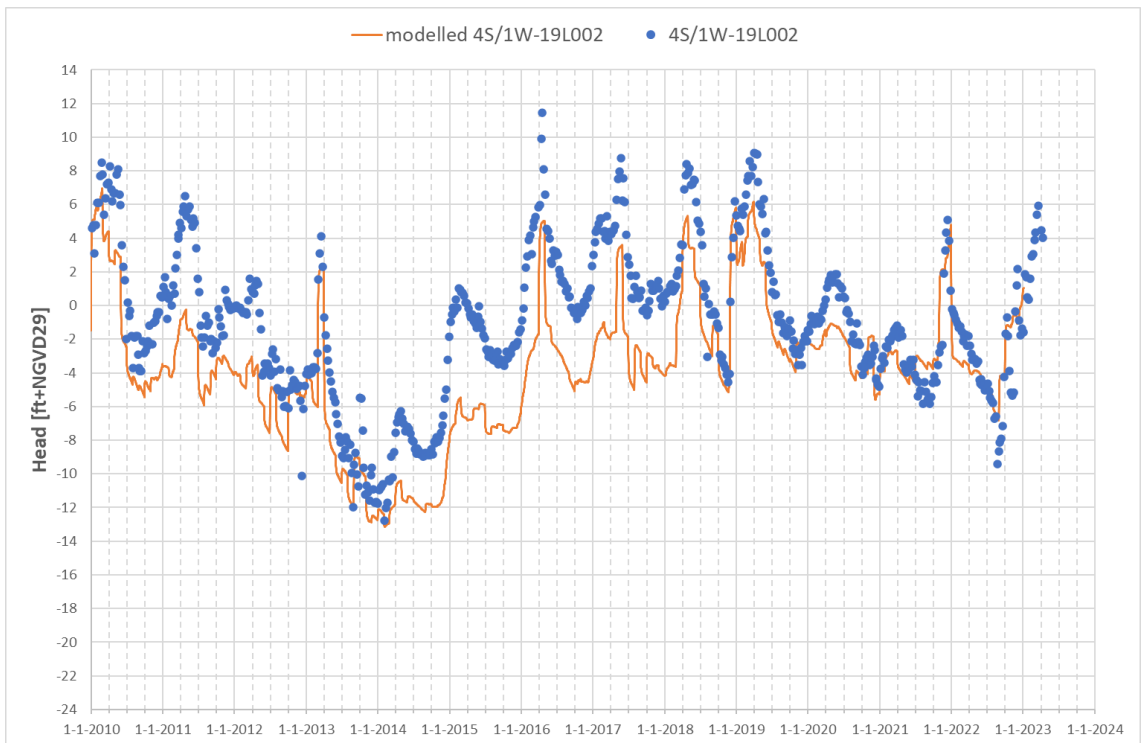


Figure 33 Validation result for observation well 4S/1W-19L002 in the Centerville-Fremont Aquifer with weekly observations.

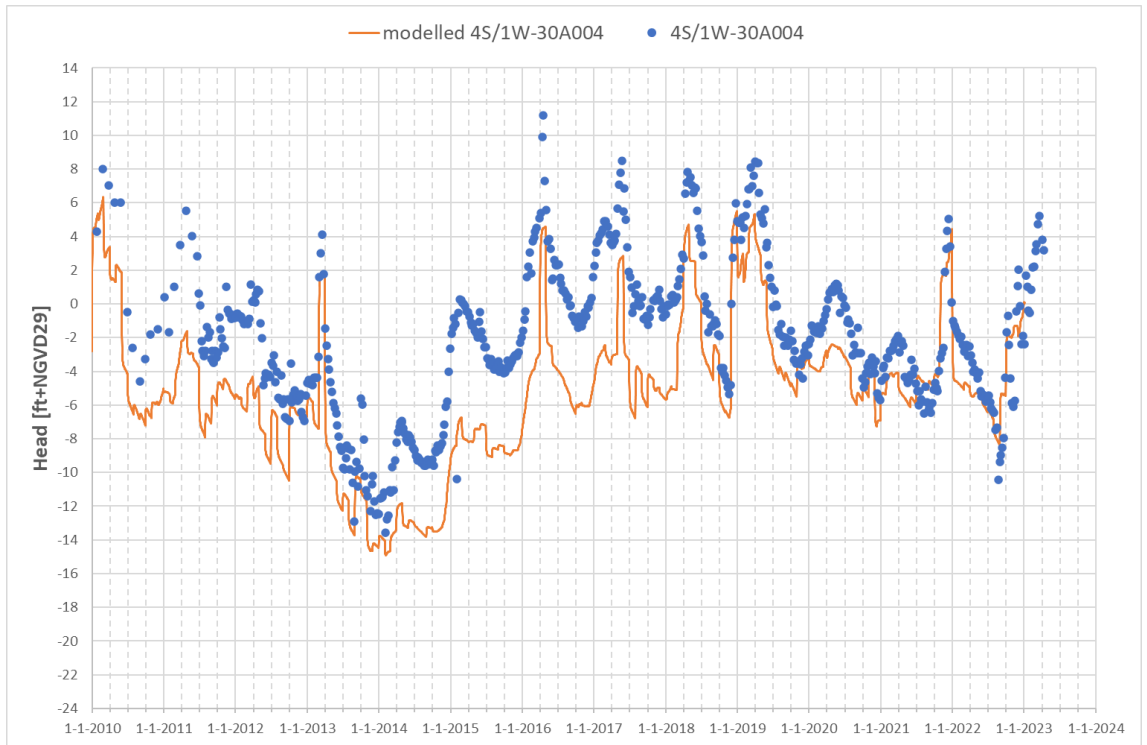


Figure 34 Validation result for observation well 4S/1W-30A004 in the Centerville-Fremont Aquifer with weekly observations.

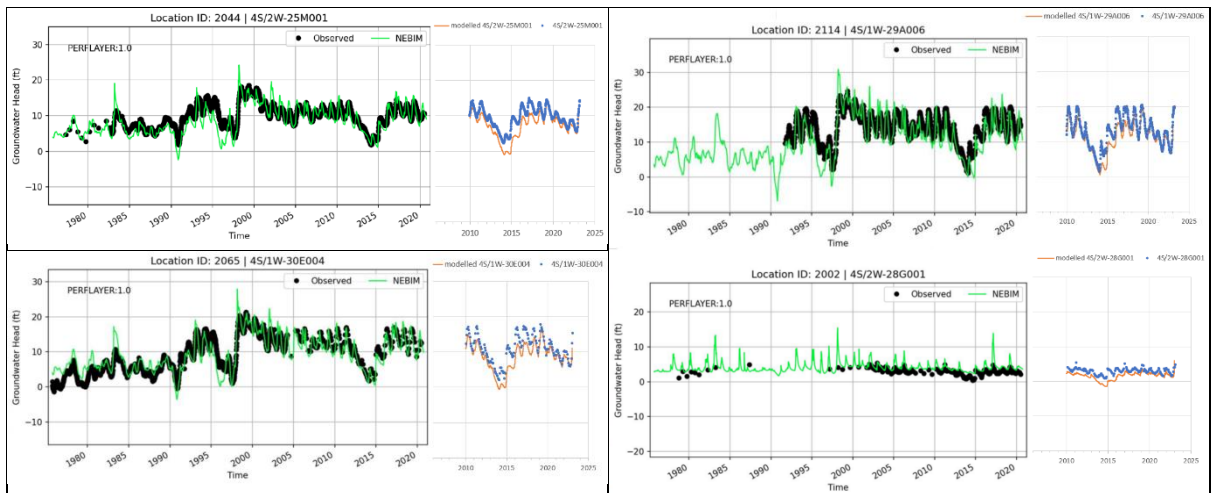


Figure 35 Validation result for 4 observation wells in the Newark Aquifer (orange lines) and comparison with NEBIM results (green lines).

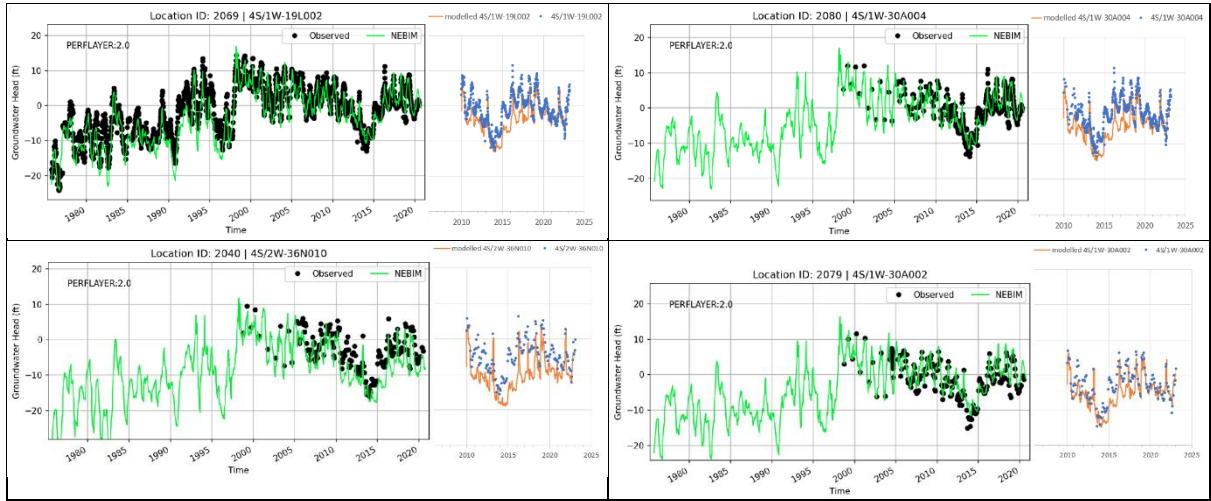


Figure 36 Validation result for 4 observation wells in the Centerville-Fremont Aquifer (orange lines) and comparison with NEBIM results (green lines).

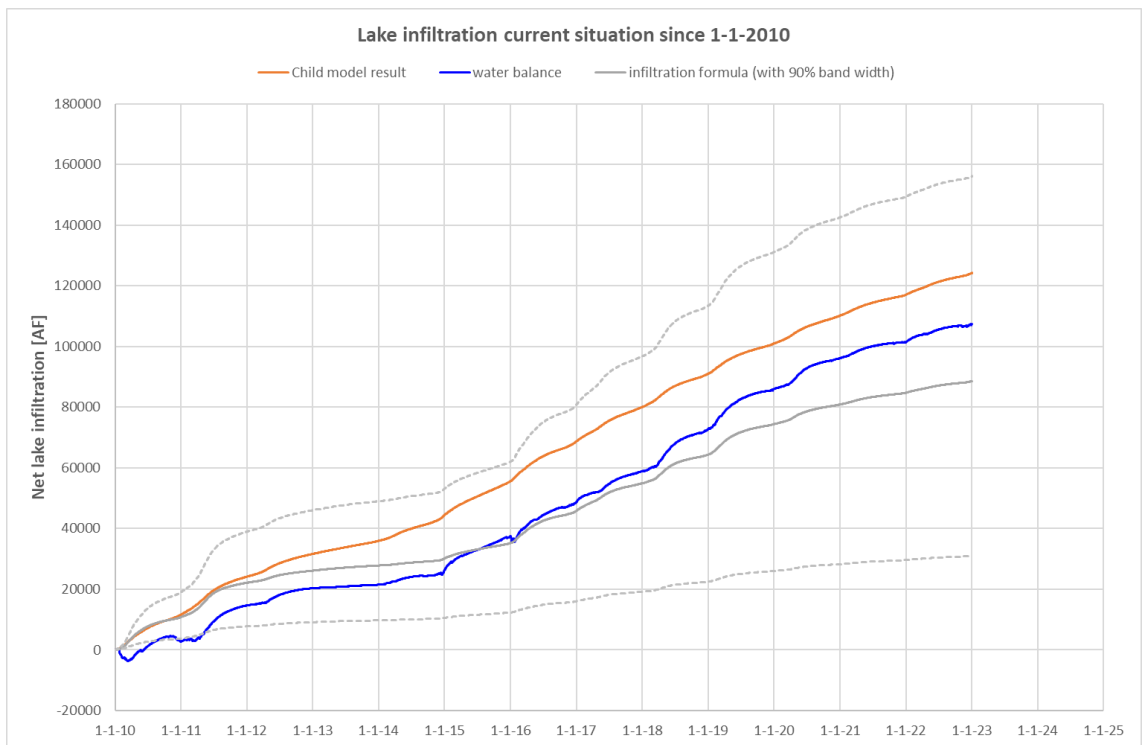


Figure 37 Validation result of total lake infiltration since 2010 (orange line) compared to lake infiltrations, derived from water balance (blue line) and derived from infiltration formula (grey lines).

5 Model Application and Scenario Analysis

5.1 Introduction

This section delves into the methodological approach for assessing the effect of creek bed deepening on the water exchange between the creek and the groundwater. Such changes inevitably influence groundwater levels and, consequently, the infiltration volumes of the nearby lakes. The variations in these effects over time are expected to correlate with the fluctuating groundwater heads and creek water levels, which are significantly driven by the lake water levels and creek discharges.

Key aspects of this validation include evaluating creek-groundwater exchange across specified creek sections, changes in lake infiltration volumes, and shifts in the hydraulic heads within the Newark Aquifer under varying groundwater conditions. Additionally, potential alterations in groundwater volume and the risk of increased saline intrusion are also considered.

The subsequent subsections provide a detailed analysis of these effects, supported by figures and tables that present the comparative results of the three scenarios. These include changes in creek-groundwater exchange, lake infiltration volumes, and hydraulic heads in the Newark Aquifer. The analysis extends to assessing the broader implications, such as the effect on phreatic groundwater levels and the potential for saline intrusion. The comprehensive approach taken in this validation process ensures a robust and thorough understanding of the model's predictive capabilities and the implications of the proposed creek bed changes.

5.2 Effect on Alameda Creek and Groundwater Exchange

Figure 38 to Figure 43 offer a detailed comparison of gross infiltration and seepage across six distinct sections of Alameda Creek, as delineated in Figure 24. This comparison contrasts the proposed modifications with the original USACE design, providing valuable insights into the hydrological effects of the proposed bed level changes.

The analysis is based on a two-year period, presenting daily averages for each section. It accounts for both positive flow volumes, indicative of infiltration into the groundwater, and negative flow volumes, representing seepage into the creek. In scenarios where both infiltration and seepage occur simultaneously within a creek section, the analysis captures this complex interaction.

Key findings from Figure 38 to Figure 43 include:

- A noticeable decrease in infiltration and an increase in seepage in the downstream direction.
- The effect of the proposed bed level changes intensifies as one moves downstream. In Section 1 (between BART and the former RD2), and similarly in Section 6 (upstream of BART where diversions to the Quarry Lakes are made), only infiltration is observed.
- In the proposed scenario (depicted by blue lines), the infiltration is slightly lower compared to the USACE design (grey lines).
- Seepage starts to occur in Section 2 (between the former RD2 and Isherwood bridge), progressively increasing in the downstream sections, and is a constant feature in Section 5 (between Dry Creek and the railroad bridge at Navarro Drive).
- Compared to the USACE design, there is a clear increase in seepage in the proposed scenario. However, these changes remain minor when compared to the minimum guaranteed baseflow of 5 ft³/sec (= 3622 AF/year).

- Table 6 complements this analysis by providing the total net flow volumes from the creek to the groundwater for Sections 1 to 5 across the three scenarios, along with the differences between the proposed/current situations and the USACE design. It is observed that the differences in net flow volumes between the scenarios amount to only a few percent of the baseflow, indicating modest changes in the creek's hydrodynamics under the proposed modifications.

Table 6 shows the total net flow volumes from creek to groundwater for sections 1 to 5 for the three scenarios, and the differences of the proposed and the current situation to the USACE design. The differences between the three scenarios are only a few percent of the baseflow.

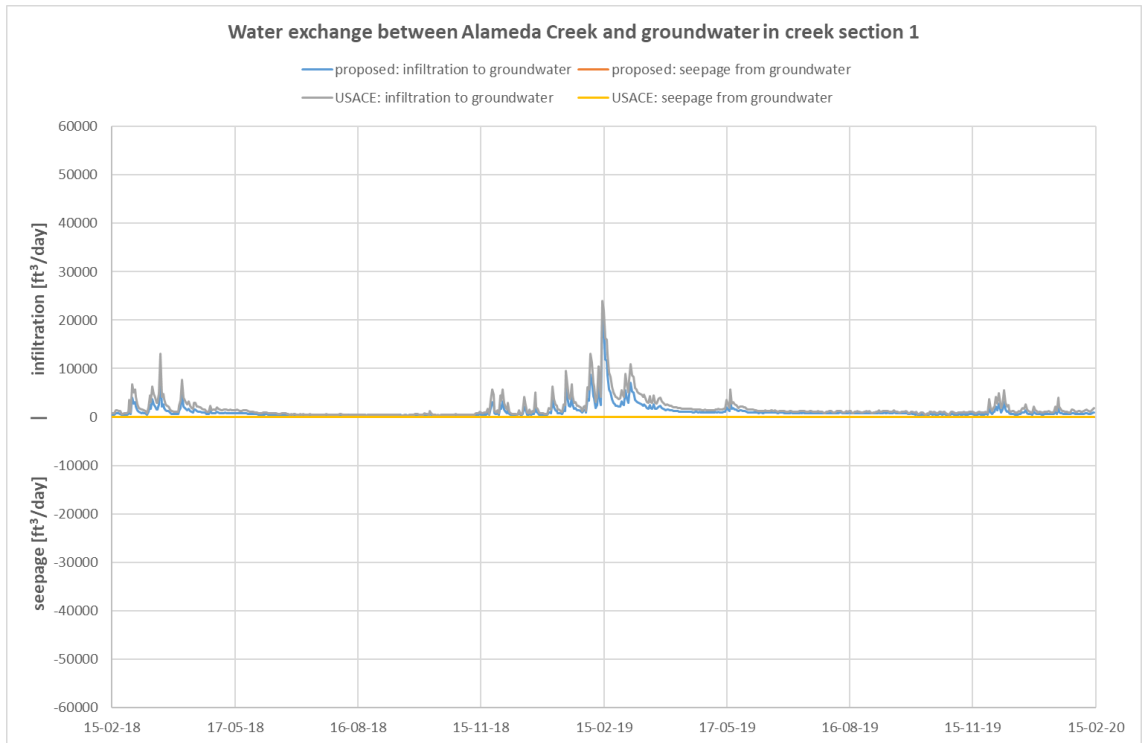


Figure 38 Calculated time series of gross infiltration and seepage volumes for creek section 1, between BART and the former RD2.

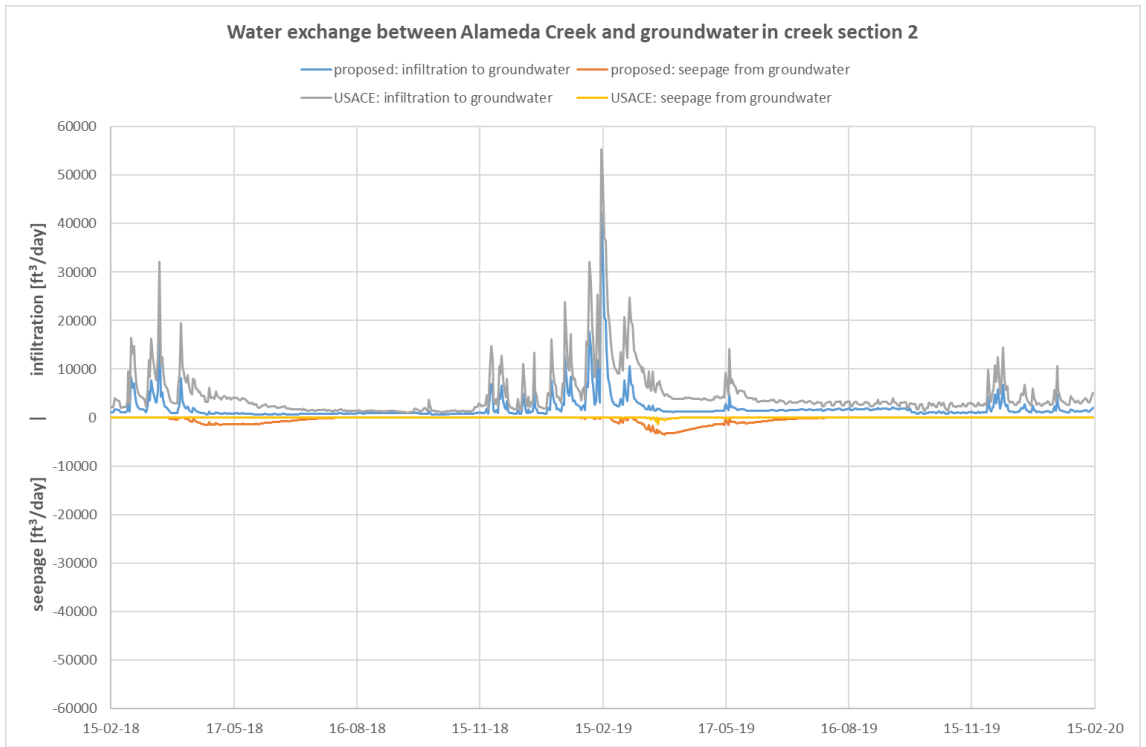


Figure 39 Calculated time series of gross infiltration and seepage volumes for creek section 2, between the former RD2 and Isherwood bridge.

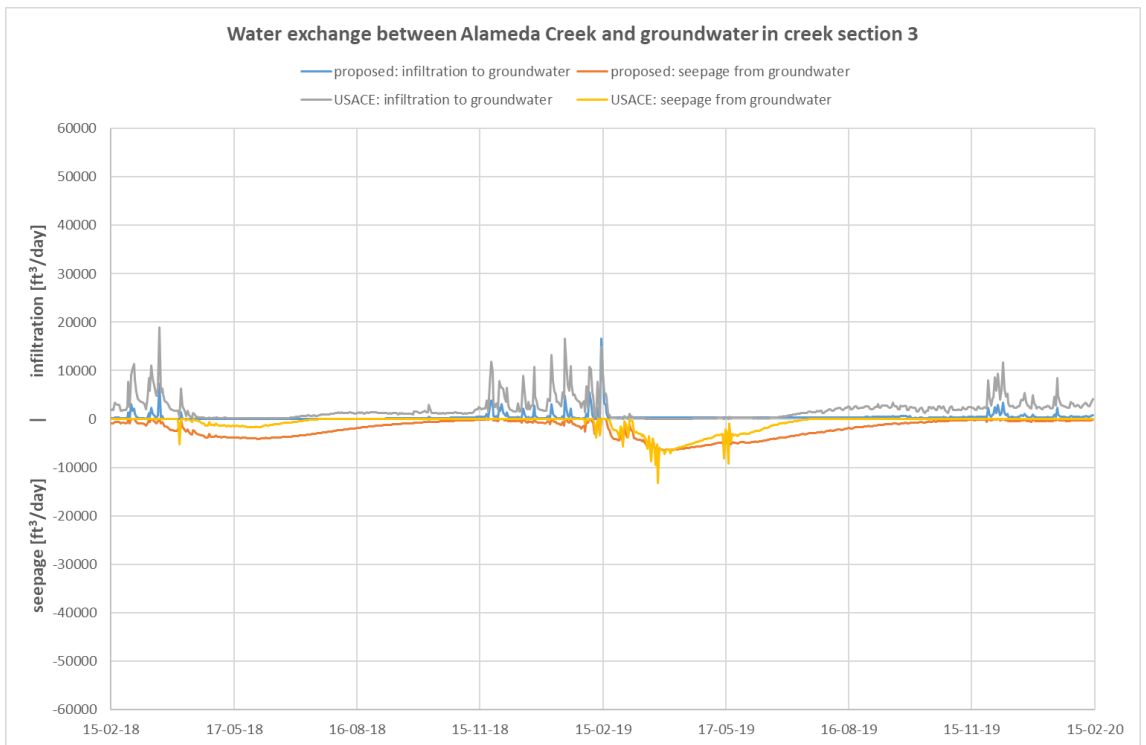


Figure 40 Calculated time series of gross infiltration and seepage volumes for creek section 3, between Isherwood bridge and Decoto Road.

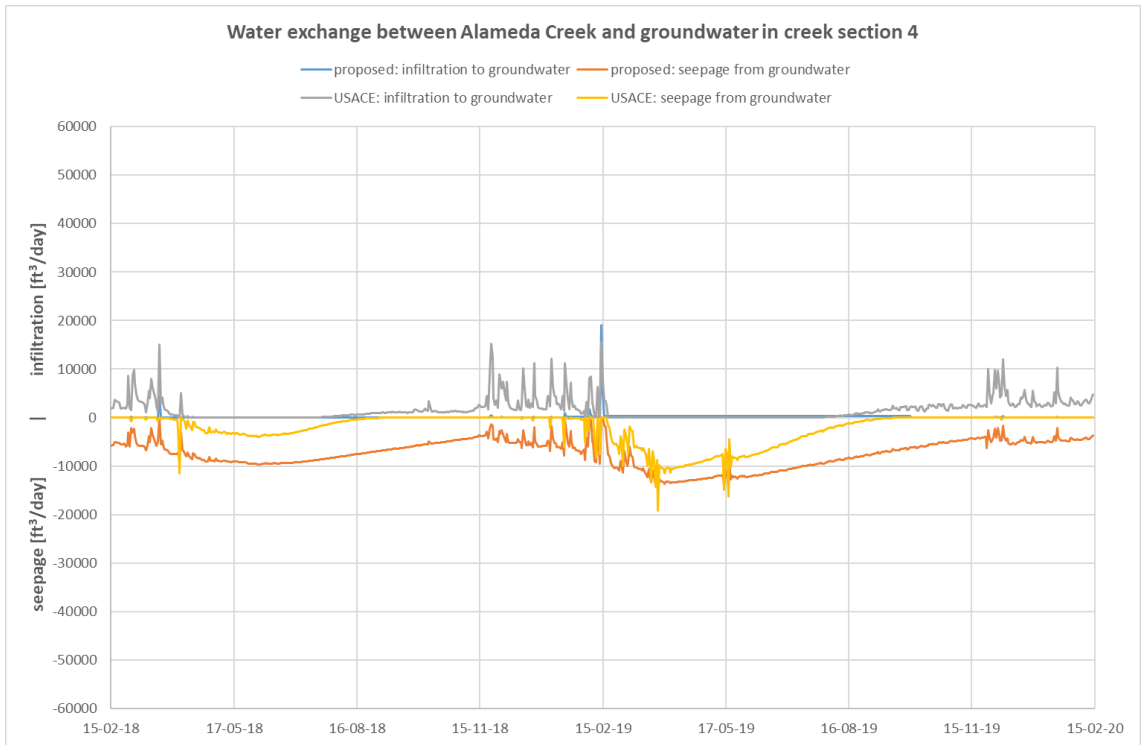


Figure 41 Calculated time series of gross infiltration and seepage volumes for creek section 4, between Decoto Road and Dry Creek.

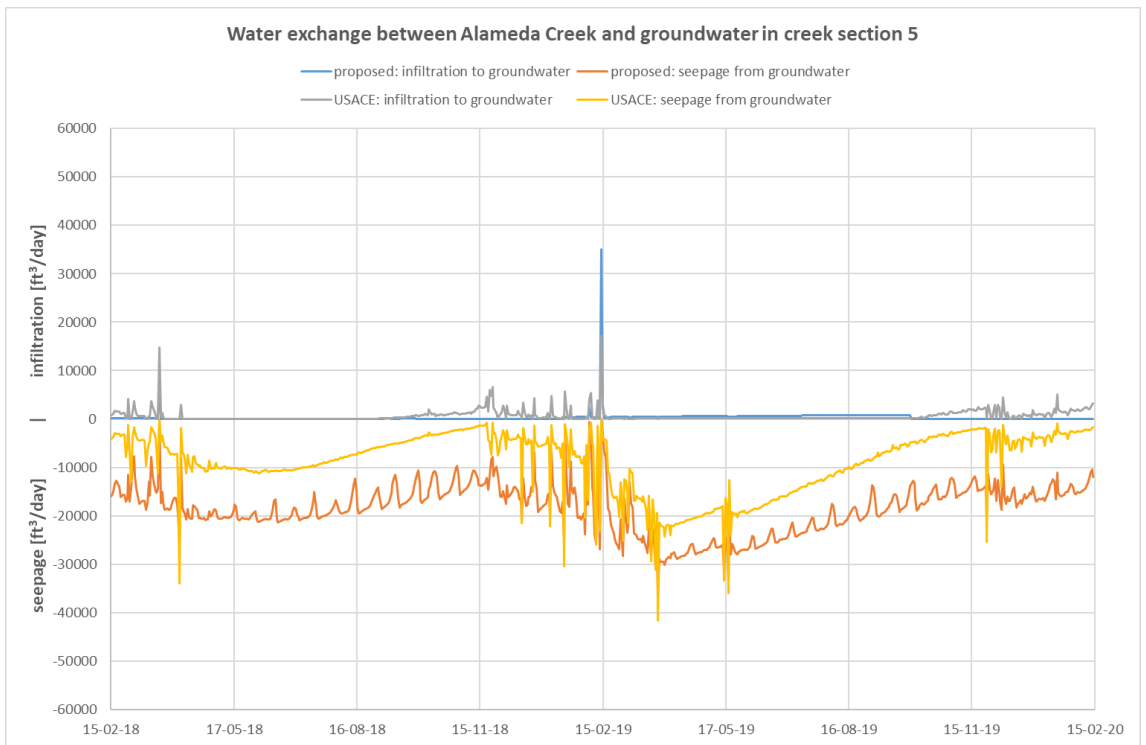


Figure 42 Calculated time series of gross infiltration and seepage volumes for creek section 5, between Dry Creek and the railroad bridge at Navarro Drive.

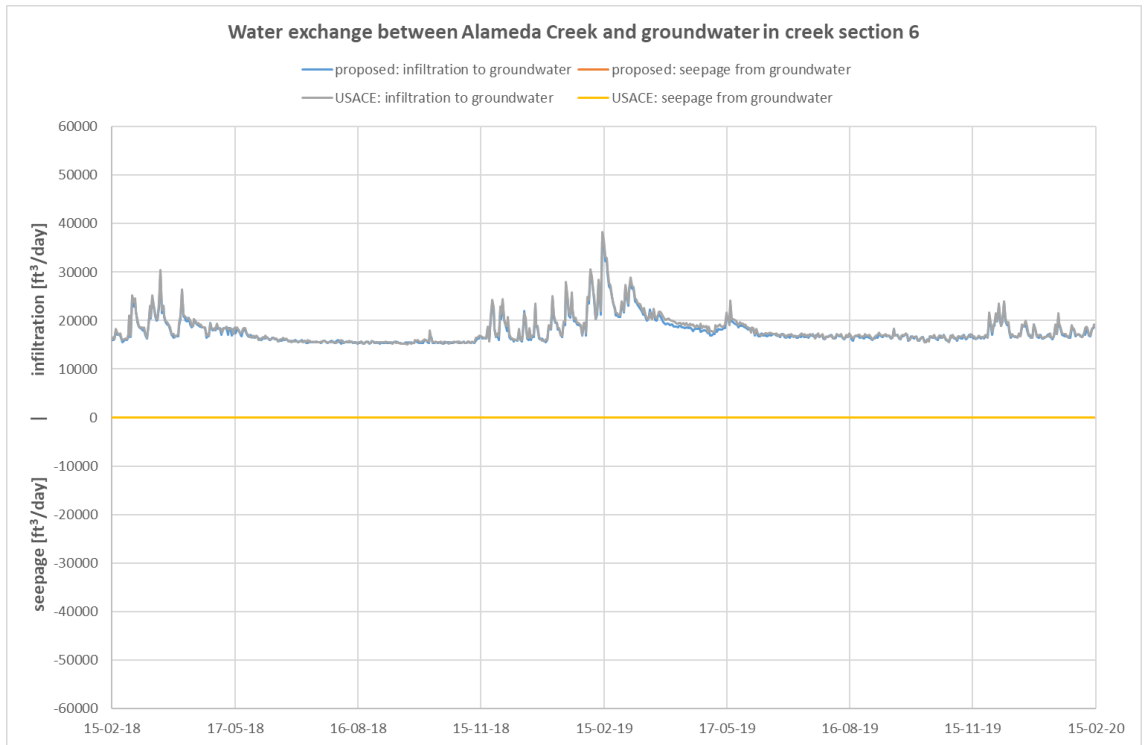


Figure 43 Calculated time series of gross infiltration and seepage volumes for creek section 6, upstream of BART.

Table 6 Average net flow volumes from creek to groundwater for creek sections 1 to 5.

Scenario	Net flow volume		Difference to USACE	
	[ft³/sec]	[AF/year]	[ft³/sec]	[AF/year]
USACE design	-0.01	-10		
Current situation	0.07	51	+0.08	+61
Proposed situation	-0.28	-205	-0.27	-195

5.3 Effect on Lake Infiltration

Figure 44 provides a clear visualization of the variations in lake infiltration across three different scenarios: the current situation, the USACE design, and the proposed modifications. This figure reveals that the differences in lake infiltration among these scenarios are relatively minor. Notably, the lake infiltration in the current scenario is marginally lower than that in the USACE design, while the proposed modifications are expected to result in a slight increase in lake infiltration. Table 7 complements this visual data by presenting the average lake infiltration volumes for each scenario. It highlights that the anticipated increase in lake infiltration for the proposed situation is about 1%. This change, while modest, is significant in the context of overall lake and groundwater interactions. Interestingly, the variations in lake infiltration are approx. half the magnitude of the differences observed in net creek flow volumes, as detailed in Table 6.

This comparative analysis is crucial for understanding the hydrological effects of the proposed bed modifications. It underscores the nuanced interplay between lake infiltration and creek flow dynamics, providing essential insights for effective water resource management and planning in the Alameda Creek area.

Table 7 Average Lake infiltration volumes.

Scenario	Net flow volume		Difference to USACE	
	[ft ³ /sec]	AF/year	[ft ³ /sec]	AF/year
USACE design	14.01	10147		
Current situation	13.97	10119	-0.04	-27
Proposed situation	14.15	10248	+0.14	+101

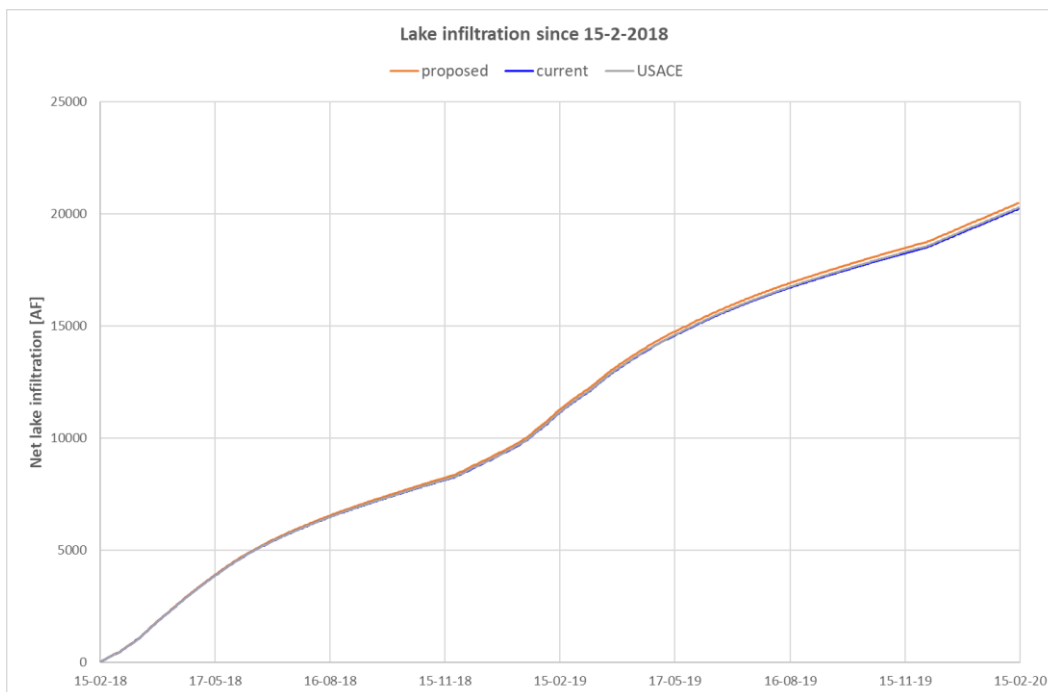


Figure 44 Calculated total lake infiltration [AF] since 15-2-2018 for the proposed situation (orange line), current situation (blue line) and the USACE design (grey line).

5.4 Effect on Hydraulic Heads in the Newark Aquifer

In the evaluation of the Newark Aquifer's hydraulic heads, changes smaller than 2 inches are considered negligible. Such minor fluctuations are challenging to attribute directly to interventions in the groundwater system based on observational data. Consequently, the results presented exclude changes below this threshold, although they are factored into the overall change in groundwater volume.

Figure 45 illustrates that the effects of the proposed creek bed alterations on the average hydraulic heads in the Newark Aquifer are minimal. When compared with the original USACE design, no changes exceeding 4 inches are observed. This indicates that the proposed bed modifications are unlikely to significantly disrupt the existing hydraulic balance in the aquifer.

Further detail is provided in Figure 46, which is divided into two parts. The top section of the figure compares differences in hydraulic heads at specific timesteps corresponding to the lowest and highest head levels. These variations are found to be similar in magnitude, though they occur in slightly different areas within the aquifer. The bottom section of Figure 46 contrasts these differences with the current scenario, revealing marginally larger discrepancies. However, the effect of the proposed bed changes remains relatively consistent across periods of both low and high groundwater levels, aligning with the patterns observed in average hydraulic heads.

This analysis underscores that the projected modifications to the creek bed are expected to have a limited effect on the hydraulic behavior of the Newark Aquifer, maintaining a stable hydrological environment despite the proposed changes.

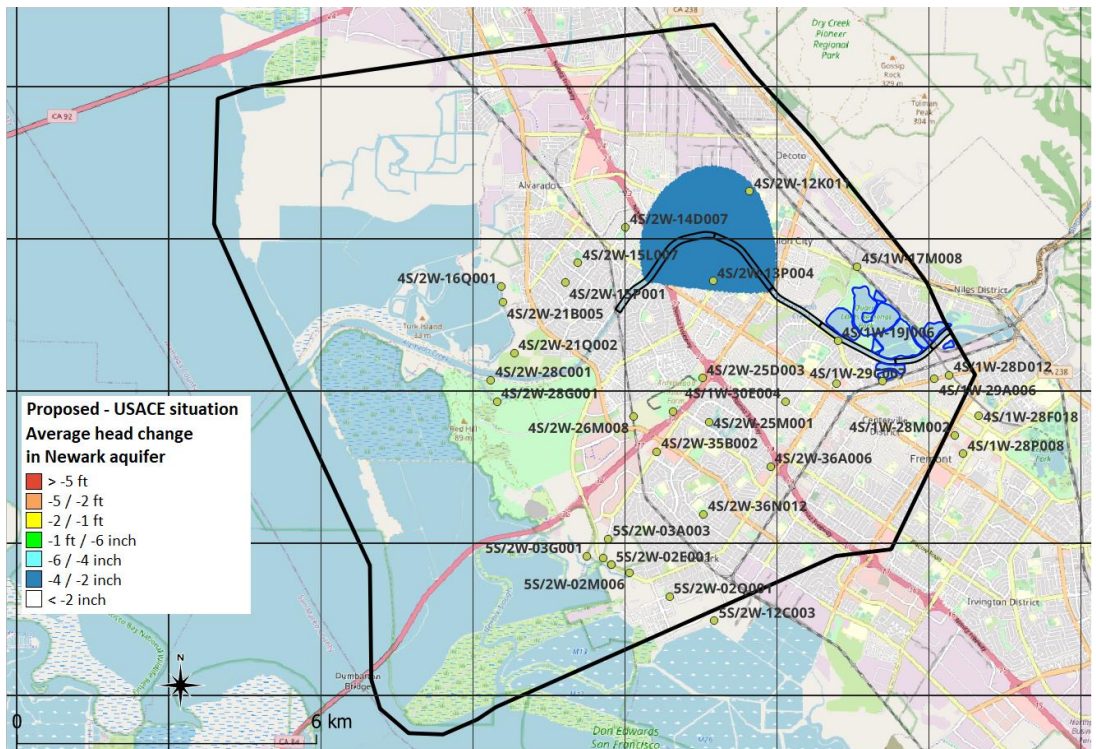


Figure 45 Calculated change in average hydraulic head in the Newark aquifer, proposed situation compared to USACE design.

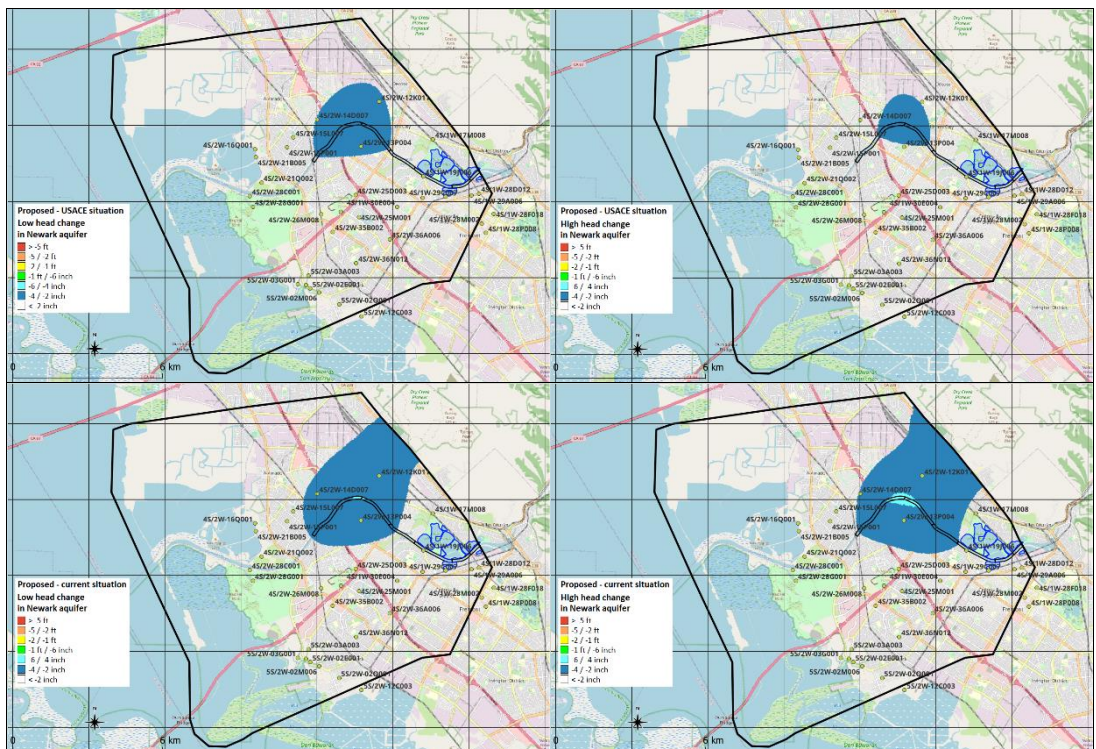


Figure 46 Calculated change in low and high hydraulic head in the Newark aquifer. Top: proposed situation compared to USACE design. Bottom: proposed situation compared to current situation.

5.5 Effects on Phreatic Groundwater Level

Situated beneath an aquitard, the Newark Aquifer's phreatic groundwater level is a critical aspect to consider, especially when evaluating proposed creek bed modifications. Figure 47 presents a comparative analysis of the average phreatic groundwater level changes, contrasting the proposed bed changes with both the USACE design and the current scenario. The variations observed are broadly similar to those noted in the Newark Aquifer. Notably, within the banks of Alameda Creek, there are significantly larger differences, primarily driven by variations in creek water levels. The maximum deviations within the creek banks are 3.5 feet when compared to the USACE design, and 4.6 feet against the current situation.

Table 8 quantifies the overall changes in groundwater volume, considering average, low, and high groundwater levels. The calculations incorporate a phreatic storage capacity of 5%, defined as 5% of the product of the groundwater level difference and the cell area.

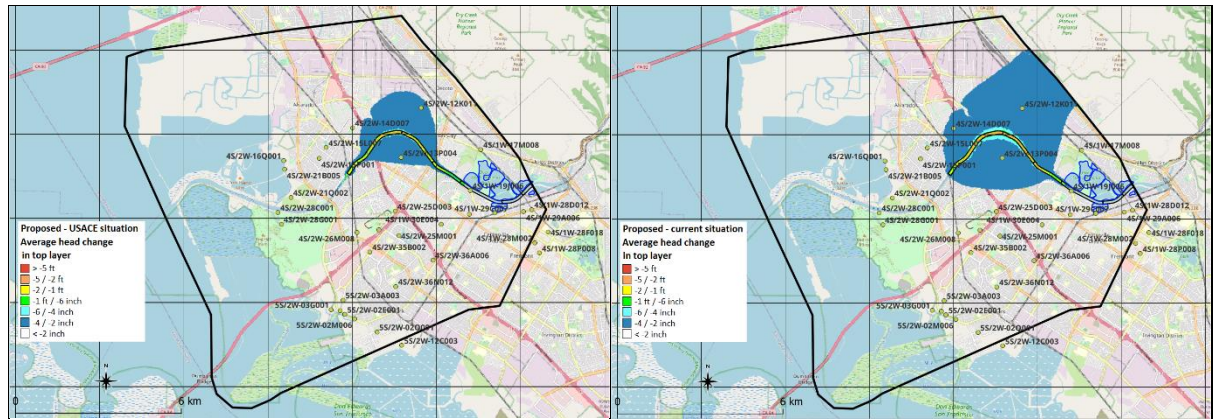


Figure 47 Calculated change in average groundwater level. Left: proposed situation compared to USACE design. Right: proposed situation compared to current situation.

Table 8 Differences in groundwater volume for different groundwater levels.

Proposed situation compared to:	Average [AF]	Low [AF]	High [AF]
USACE design	-105	-117	-93
Current situation	-139	-145	-128

5.6 Saline Intrusion

Another aspect of concern is the risk of saline intrusion. Fortunately, the hydraulic heads generally remain high across all scenarios and act as a safeguard against saline intrusion via groundwater from the Bay. However, the creek's dynamics present a different challenge. Delft3D model calculations suggest that tidal effects, and consequently saline Bay water, may extend further upstream in Alameda Creek due to the proposed bed deepening. The extent of this upstream intrusion was not part of this study.

Figure 48 shows that the proposed bed changes will likely lead to increased seepage from the groundwater into the creek. This implies that even if saline Bay water intrudes as far upstream as Section 5 of the creek, it is unlikely to significantly affect the groundwater.

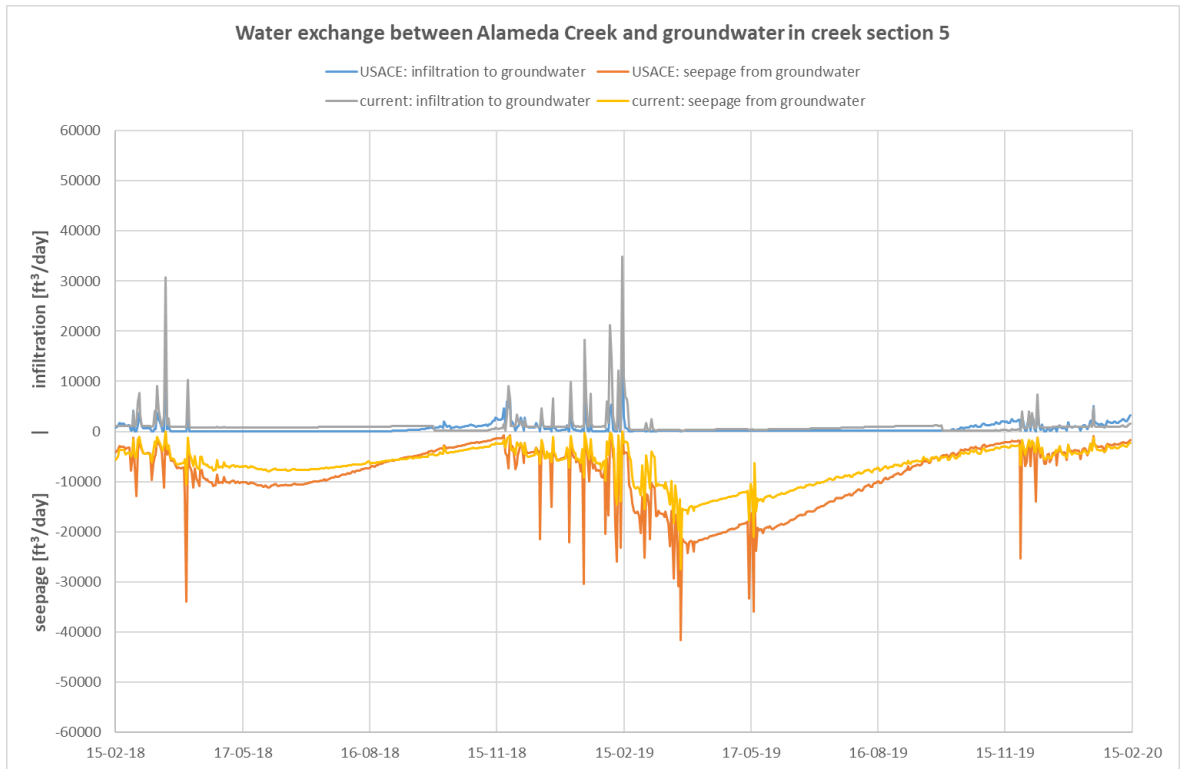


Figure 48 Calculated time series of gross infiltration and seepage volumes for the most downstream creek section. Grey lines: infiltration for current situation. Blue lines: infiltration for proposed situation. Yellow-orange lines: seepage for current situation. Red-orange lines: seepage for proposed situation.

This is primarily because any potential gravity-driven flow of denser saline water at the creek bottom is counteracted by the creek's continuous outflow towards the Bay and regular high discharge events that typically occur several times a year. A measure for these situations was derived by Wooding (Zimmermann et al, 2006). The so-called Wooding number describes the ratio between buoyancy driven forces and the stabilizing forces caused by the vertical upward flow, and is defined by:

$$R_{\delta} = \frac{(\rho_m - \rho_a) \cdot K_z \cdot n_e}{\rho_a \cdot ET}$$

Where $(\rho_m - \rho_a) / \rho_a$ in this case is the maximum relative density contrast between the saline water at the bottom of the creek (ρ_m) and the fresh groundwater, K_z is the vertical hydraulic conductivity, n_e is the effective porosity and ET is the upward seepage flux.

Vertical density driven flow can only be expected above a critical Wooding number of $R_{\delta} = 7$. For values of $(\rho_m - \rho_a) / \rho_a = 0.025$, $K_z = 0.05$ ft/day and $n_e = 0.25$ this can occur when upward seepage is less than 4.5×10^{-5} ft/day. For an area of approx. 500000 ft² this implies a total flow volume of 22 ft³/day. Figure 48 shows that such low flow volumes basically never occur, and if so, only for a very short time.

6 Conclusions and Recommendations

6.1 Conclusions

A comprehensive and detailed model is crucial for accurately assessing the effect of proposed changes in the bed level of Alameda Creek on the surrounding groundwater system. The high-resolution local groundwater model used in this study has undergone effective calibration and validation, providing confidence in its capability to accurately simulate the effects of these changes on the groundwater. This dual approach of meticulous modeling and rigorous testing ensures a reliable understanding of the creek's bed alterations and their hydrological consequences.

The analyses conducted in this study reveal that the primary factor influencing groundwater levels in the area is the water levels in the lakes, overshadowing the effect of rainfall and evaporation. This finding underscores the significant role that lake water levels play in dictating the dynamics of the surrounding groundwater system, with other meteorological factors such as precipitation and evaporation having a comparatively minor effect.

The proposed modifications to deepen Alameda Creek's bed are projected to have a minimal effect on the surrounding groundwater system. This effect is relatively minor, particularly when compared to the original USACE design, and only slightly more significant when compared to the current conditions. The analysis shows that groundwater levels are generally affected by less than 6 inches, except within the creek banks where changes are more pronounced. Additionally, the deepening is expected to lead to a 1% increase in lake infiltration (approx. 100 AF/year), with a potential doubling of upwelling into Alameda Creek. This upwelling, or the movement of groundwater into the creek, is estimated to increase the upward flow volume by about 5% of the creek's baseflow of 5 cfs (3622 AF/year), amounting to about a 0.27 cfs (195 AF/year) increase in flow.

Notably, there is an observable increase in creek upwelling in the downstream direction. This trend suggests that the effects of the creek bed alterations become more significant further downstream the creek's away from the Quarry Lakes. The risk of saline intrusion into the groundwater system from the Bay is not anticipated to increase. The bed deepening might lead to an increased intrusion of saline Bay water into the creek itself, but this is unlikely to significantly affect the groundwater. This is due to several mitigating factors: the enhanced upwelling of fresh groundwater into the creek, the creek's consistent baseflow towards the Bay, and the regular flushing of the creek system caused by heavy rainfall events. These factors collectively help maintain the balance and quality of the groundwater, despite the alterations in the creek's bed.

6.2 Evaluation and recommendations

Based on the results and the conclusions of this project we see no relevant objections for implementing the proposed bed deepening. The positive effects of smaller sedimentation issues and other possible positive effects (e.g. for fishes) need to be weighed to the calculated small negative effects on the surrounding groundwater system and other possible negative effects (e.g. increased energy consumption for groundwater abstraction).

The effects presented in this report are calculated by computer simulation models (Delft3D and MODEFLOW6). However, simulation models are never perfect. Therefore, we recommend to closely monitor the effects of implementation on both creek water levels, lake water levels and groundwater levels and on salinity at the downstream part of the creek. For this, “continuous” monitoring (by Diver water loggers) will provide the most insight. Monitoring should start long before implementation of the creek bed deepening and continue for several years after implementation has been completed.

Some ongoing activities, like determining the hydraulic conductivities of the top layer based on a detailed structure model by W&C, may result in a better description of the local hydrogeological system. Additional research to determine the groundwater recharge more accurately, more detailed boundary conditions and a more detailed model description of the water system at the top, like the salt ponds and urban drainage systems will most likely also result in a better child model. However, all this will not result in a totally different outcome regarding the effect of deepening the bed of Alameda Creek.

These potential model improvements will only become relevant in case the child model will be applied for other purposes, like determining potential groundwater nuisance and measures to mitigate this in urban areas between the Quarry Lakes and the San Francisco Bay.

References

ACWD (2022). Alameda Creek Flood Control Channel Planned Low Flow Channel Modeling: Station 200+00 to 254+00. Powerpoint presentation at meeting on November 16, 2022.

Deltares (2023). Alameda Creek Restoration: Impacts to Local Groundwater Supply. Final report, May 8, 2023.

Deltares (2024). Hydrodynamic & Morphodynamic Modeling of Alameda Creek's Sediment Transport to Evaluate Restoration Alternatives. Final report, February 2, 2024

Hughes, J. D., Russcher, M. J., Langevin, C. D., Morway, E. D., & McDonald, R. R. (2022). The MODFLOW Application Programming Interface for simulation control and software interoperability. *Environmental Modelling & Software*, 148, 105257. <https://doi.org/10.1016/j.envsoft.2021.105257>

Linacre, E.T. 1993. Data-sparse estimation of lake evaporation using a simplified Penman equation. *Agric. & Forestry Meteor.*, 64, 237-56.

Woodard & Curran (2021). Niles East Bay Integrated Model (NEBIM). Model Development and Calibration. Draft Report | October 2021.

Zimmermann, S., Bauer, P., Held, R., Kinzelbach, W., & Walther, J. H. (2006). Salt transport on islands in the Okavango Delta: Numerical investigations. *Advances in Water Resources*, 29(1), 11–29. <https://doi.org/10.1016/j.advwatres.2005.04.013>.

A Sensitivity Analysis

A.1 Analysis of Bed Level Changes

The initial step in assessing the effectiveness of our grid models involves comparing the bed level changes between the current and proposed scenarios across both the 8ft-grid and the 16ft-grid. Figure 49 demonstrates that these changes are remarkably consistent in both grids. The most significant difference observed is a mere 0.02 ft increase in bed level change in the 8ft-grid compared to the 16ft-grid, which is a trivial discrepancy.

Consequently, our preliminary conclusion suggests that the 16ft-grid is likely to provide sufficiently accurate results for our calculations. However, it is recommended to perform a follow-up sensitivity analysis before finalizing the choice of calculation grid. This analysis will compare the results obtained from both grids, ensuring the chosen grid offers the desired accuracy for our study."

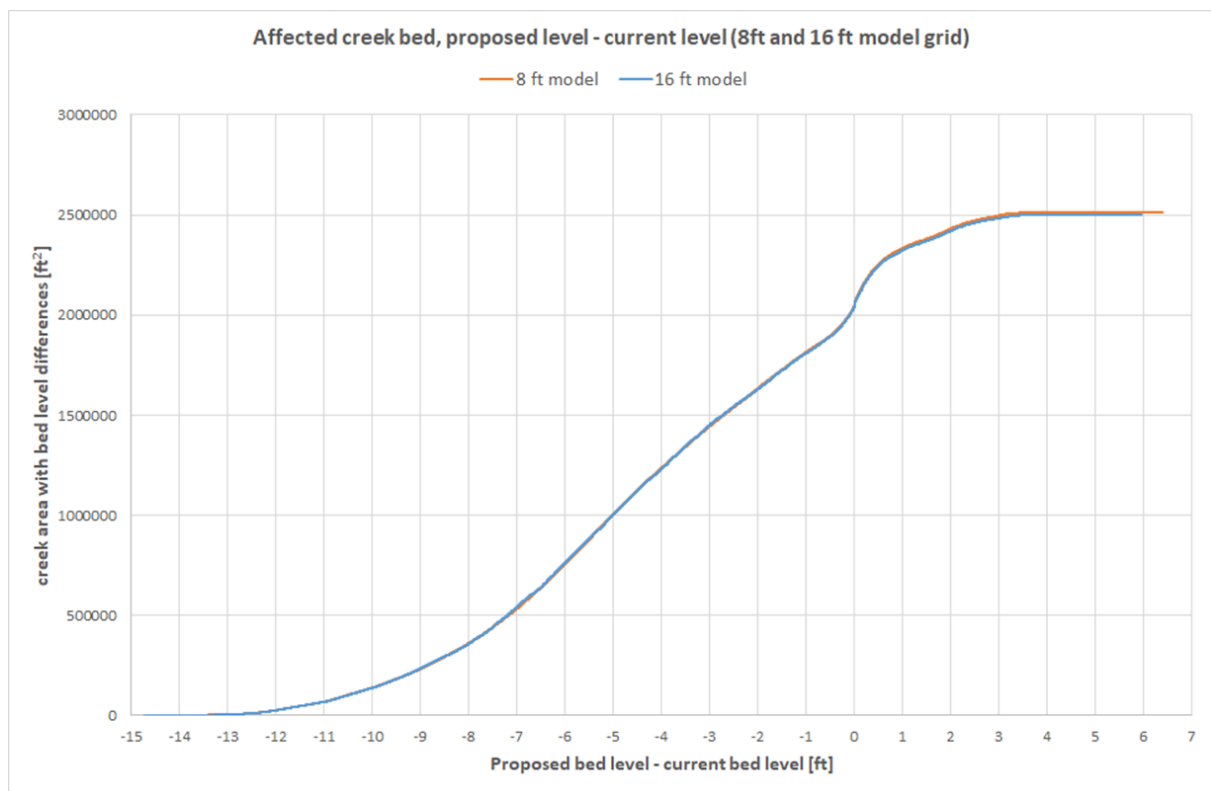


Figure 49 Applied bed level changes between the proposed situation and the current situation for the 8ft-grid (orange line) and for the 16ft-grid (blue line).

A.2 Analysis of Hydraulic Heads and Flow Volumes in Aquifer

The analysis of sensitivity was carried out using a steady-state model across three different creek bed scenarios. Initially, this model was adjusted to reflect the long-term average conditions observed over a 13-year span from 2010 to 2022. This included average data from the Quarry lakes, the abstraction rates from wells, and water levels in Alameda Creek at current bed elevations.

While the model underwent validation, it was not calibrated. Its validation involved comparing whether the hydraulic heads in the Newark and Centerville-Fremont aquifers within the creek and lakes area roughly aligned with recorded observations. The sensitivity analysis entailed comparing several elements:

During the sensitivity analysis, the following results have been compared:

- **Hydraulic heads in Newark aquifer:**
 - At observation wells: average, minimum, and maximum level.
 - In the entire model: average, minimum, and maximum level.
- **In- and outflow volumes:**
 - For the five creek sections.
 - For the Quarry lakes.
- **Grid results:**
 - 8ft-grid.
 - 16ft-grid.

The parameters that have been tested on their sensitivity are presented in Table 9.

Table 9. Parameters varied in the sensitivity testing

Parameter	Value or multiplier 1	Value or multiplier 2
Lake water level	35 ft (normal maximum)	15 ft (normal minimum)
Recharge	Multiplied by 0	Multiplied by 2
Lake bed resistance	Multiplied by 0.1	Multiplied by 10
Creek bed resistance	Multiplied by 0.1	Multiplied by 10
k-vertical layer 1	Multiplied by 0.1	Multiplied by 10
k-horizontal layer 2	Multiplied by 0.1	Multiplied by 10
k-vertical layer 3	Multiplied by 0.1	Multiplied by 10

Figure 50 illustrates the basic results for the three scenarios and both grid sizes, indicating minor differences in hydraulic heads and flow volumes between the two grids. The subsequent figures display the results of the sensitivity analysis for each parameter. These figures show calculated heads and flow volumes, with cell colors indicating sensitivity levels.

Sensitivity run	scenario - grid	OBswells Newark aquifer average	OBswells Newark aquifer minimum	OBswells Newark aquifer maximum	OBswells CF aquifer average	OBswells CF aquifer minimum	OBswells CF aquifer maximum	Heads Newark aquifer average	Heads Newark aquifer minimum	Heads Newark aquifer maximum	Heads CF aquifer average	Heads CF aquifer minimum	Heads CF aquifer maximum
basic run	current - 8 ft	8.9	3.8	14.0	-2.5	-20.0	3.0	11.1	0.6	15.2	0.6	-20.0	5.3
	current - 16 ft	8.9	3.9	14.1	-2.5	-20.0	3.1	10.7	0.6	15.3	0.4	-20.0	5.3
	proposed - 8 ft	8.7	3.7	13.9	-2.7	-20.2	2.8	10.8	0.6	15.1	0.4	-20.2	5.1
	proposed - 16 ft	8.7	3.8	13.9	-2.7	-20.1	2.9	10.5	0.6	15.2	0.3	-20.1	5.2
	USACE - 8 ft	8.8	3.8	14.0	-2.6	-20.0	3.0	11.0	0.6	15.2	0.5	-20.0	5.3
	USACE - 16 ft	8.8	3.8	14.0	-2.6	-20.0	3.0	10.6	0.6	15.3	0.4	-20.0	5.3

Sensitivity run	scenario - grid	Lakes aquifer in	Lakes aquifer out	Creek section 1 aquifer in	Creek section 1 aquifer out	Creek section 2 aquifer in	Creek section 2 aquifer out	Creek section 3 aquifer in	Creek section 3 aquifer out	Creek section 4 aquifer in	Creek section 4 aquifer out	Creek section 5 aquifer in	Creek section 5 aquifer out
basic run	current - 8 ft	1077954	0	2779	0	4672	0	3811	0	3738	0	264	-2528
	current - 16 ft	1078580	0	2783	0	4652	0	3853	0	3706	0	254	-2562
	proposed - 8 ft	1095385	0	1188	0	2365	0	617	-488	0	-4628	0	-14072
	proposed - 16 ft	1095584	0	1188	0	2336	0	604	-505	0	-4631	0	-14003
	USACE - 8 ft	1082595	0	2160	0	5762	0	4705	0	3798	0	98	-7690
	USACE - 16 ft	1083190	0	2184	0	5878	0	4731	0	3748	0	81	-7841

Figure 50 Basic runs for the sensitivity analysis for the 8ft-grid and the 16ft-grid. The top part shows the heads; the bottom part shows the flow volumes.

Highlights from these figures include:

- **Figure 51** shows that the lake water levels, which normally vary between 15 and 35 ft (+NGVD29), clearly affect the hydraulic heads in both the Newark and the Centerville-Fremont aquifer in almost the entire model. Only the minimum heads along the coast are hardly affected. The lake water levels also determine the lake infiltration and high lake levels affect the creek upwelling and infiltration significantly, except for creek section 1, where groundwater levels are generally below creek water level. Lake water levels lower than average affect the exchange between creek water and groundwater much less. When the groundwater level is below the creek bed level, which occurs at large parts of the creek during low lake water levels, the creek infiltration only depends on the creek water level, and upwelling from groundwater is zero. (45)
- **Figure 52** shows a moderate sensitivity of the hydraulic heads for recharge and a higher sensitivity for flow volumes. Especially lake infiltration and the downstream sections of Alameda Creek are sensitive to changes in recharge. This is mainly caused by the changes in groundwater level that affect the driving forces of lake infiltration and exchange between creek water and groundwater. (46)
- **Figure 53** shows a high sensitivity of the hydraulic heads for lakebed resistance, especially for the higher heads in the Newark aquifer. That is caused by the fact that these higher levels occur in the vicinity of the lakes. The flow volumes in the lakes and lower creek sections are also highly sensitive to changes in lakebed resistance. Increasing the lakebed resistance affects the water levels more than decreasing it with a similar factor. Decreasing the lakebed resistance may result in such high groundwater levels that parts of the lakes start draining groundwater instead of feeding it. (47)
- **Figure 54** shows that the hydraulic heads are barely to moderately sensitive to changes in creek bed resistance. The same goes for the flow volumes of the lakes. Flow volumes from the creek, on the contrary, are much more sensitive. This indicates that relatively large changes in flow volumes between creek and groundwater most likely result in moderate groundwater affection. (48)
- **Figure 55** shows that the lower hydraulic heads in the Newark aquifer are more sensitive to changes in the vertical conductivity of the top layer than the higher hydraulic heads. That is most likely caused by the fact that this top layer is much thicker at the low-lying bay side of the model than at the higher east side of the model. The same goes for the flow volumes that are more affected at the downstream sections of the creek. (49)
- **Figure 56** shows that the hydraulic heads in the Newark aquifer are highly sensitive to large changes in horizontal conductivity of this aquifer. That also strongly affects the flow volumes in the lakes and the downstream creek sections. (50)
- **Figure 57** shows that the hydraulic heads in the Centerville-Fremont aquifer are highly sensitive to changes in the vertical conductivity of the aquitard between this aquifer and the Newark aquifer. The hydraulic heads in the Newark aquifer are barely sensitive to these changes. The flow volumes show bare to moderately sensitivity that is increasing somewhat to the downstream part of the creek. (51)

Sensitivity run	scenario - grid	OBSwells		Newark aquifer		OBSwells CF		OBSwells CF		Heads Newark		Heads Newark		Heads Newark		Heads CF		deviation from basic run
		average	minimum	average	maximum	average	maximum	average	maximum	average	maximum	average	maximum	average	maximum	average	maximum	
lake water level: 35ft	current - 8 ft	15.1	7.2	23.5	4.7	-12.7	10.0	18.4	0.9	24.9	7.3	-12	-10 / -5 ft					
	current - 16 ft	15.1	7.2	23.5	4.7	-12.7	10.0	17.7	0.9	24.9	7.0	-12	-5 / -2 ft					
	proposed - 8 ft	14.9	7.2	23.3	4.5	-12.9	9.9	18.2	0.9	24.8	7.2	-12	-2 / -1 ft					
	proposed - 16 ft	14.9	7.2	23.3	4.5	-12.9	9.9	17.6	0.9	24.8	6.8	-12	-1 / +1 ft					
	USACE - 8 ft	14.7	7.0	23.2	4.3	-13.1	9.7	17.9	0.9	24.6	7.0	-13	+1 / +2 ft					
	USACE - 16 ft	14.7	7.0	23.2	4.3	-13.1	9.7	17.3	0.9	24.7	6.6	-13	+2 / +5 ft					
lake water level: 15ft	current - 8 ft	5.0	1.6	8.5	-6.9	-24.4	-0.9	6.6	-0.2	9.3	-3.5	-24	+5 / +10 ft					
	current - 16 ft	5.1	1.6	8.5	-6.9	-24.4	-0.9	6.4	-0.1	9.4	-3.5	-24	> +10 ft					
	proposed - 8 ft	4.9	1.5	8.3	-7.1	-24.6	-1.1	6.4	-0.2	9.2	-3.6	-24						
	proposed - 16 ft	4.9	1.5	8.4	-7.0	-24.5	-1.0	6.2	-0.2	9.3	-3.7	-24						
	USACE - 8 ft	5.1	1.6	8.5	-6.9	-24.4	-0.9	6.6	-0.1	9.3	-3.5	-24						
	USACE - 16 ft	5.1	1.6	8.5	-6.8	-24.4	-0.9	6.4	-0.1	9.4	-3.5	-24						

Figure 51 Sensitivity to the water level in the Quarry Lakes. The top part shows the heads; the bottom part shows the flow volumes.

Sensitivity run	scenario - grid	OBSwells		Newark aquifer		OBSwells CF		OBSwells CF		Heads Newark		Heads Newark		Heads Newark		Heads CF		deviation from basic run
		average	minimum	average	maximum	average	maximum	average	maximum	average	maximum	average	maximum	average	maximum	average	maximum	
Recharge: 0x	current - 8 ft	5.6	0.8	11.5	-5.8	-23.2	-0.5	7.8	-1.3	12.9	-2.7	-23	-10 / -5 ft					
	current - 16 ft	5.6	0.8	11.5	-5.8	-23.2	-0.5	7.5	-1.3	12.9	-2.8	-23	-5 / -2 ft					
	proposed - 8 ft	5.5	0.7	11.3	-6.0	-23.4	-0.7	7.6	-1.4	12.7	-2.9	-23	-2 / -1 ft					
	proposed - 16 ft	5.5	0.7	11.4	-5.9	-23.3	-0.6	7.3	-1.3	12.8	-3.0	-23	-1 / +1 ft					
	USACE - 8 ft	5.6	0.8	11.5	-5.8	-23.2	-0.5	7.9	-1.3	12.9	-2.7	-23	+1 / +2 ft					
	USACE - 16 ft	5.7	0.9	11.5	-5.7	-23.1	-0.4	7.5	-1.3	13.0	-2.8	-23	+2 / +5 ft					
Recharge: 2x	current - 8 ft	11.9	6.7	16.6	0.5	-17.0	6.3	14.0	1.1	17.4	3.7	-17	+5 / +10 ft					
	current - 16 ft	11.9	6.7	16.6	0.6	-17.0	6.3	13.7	1.1	17.5	3.5	-17	> +10 ft					
	proposed - 8 ft	11.8	6.6	16.4	0.4	-17.1	6.1	13.9	1.1	17.3	3.6	-17						
	proposed - 16 ft	11.8	6.6	16.4	0.4	-17.1	6.2	13.5	1.1	17.4	3.4	-17						
	USACE - 8 ft	11.7	6.6	16.4	0.4	-17.2	6.1	13.8	1.1	17.3	3.5	-17						
	USACE - 16 ft	11.7	6.6	16.5	0.4	-17.1	6.1	13.4	1.1	17.4	3.3	-17						

Figure 52 Sensitivity to the recharge (precipitation – evapotranspiration) at the top of the model. The top part shows the heads; the bottom part shows the flow volumes.

Sensitivity run	scenario - grid	OBSwells Newark aquifer average		OBSwells Newark aquifer minimum		OBSwells Newark aquifer maximum		OBSwells CF aquifer average		OBSwells CF aquifer minimum		OBSwells CF aquifer maximum		Heads Newark aquifer average		Heads Newark aquifer minimum		Heads Newark aquifer maximum		Heads CF aquifer average		Heads CF aquifer		deviation from basic run
		OBSwells Newark aquifer average	OBSwells Newark aquifer minimum	OBSwells Newark aquifer maximum	OBSwells CF aquifer average	OBSwells CF aquifer minimum	OBSwells CF aquifer maximum	Heads Newark aquifer average	Heads Newark aquifer minimum	Heads Newark aquifer maximum	Heads CF aquifer average	Heads CF aquifer												
Lake bed resistance: 0.1x	current - 8 ft	13.8	6.6	22.9	3.3	-14.1	8.6	16.8	0.8	26.6	6.0	-14	-10 / -5 ft											
	current - 16 ft	13.8	6.6	23.0	3.3	-14.1	8.6	16.3	0.8	26.7	5.7	-14	-5 / -2 ft											
	proposed - 8 ft	13.8	6.6	22.9	3.2	-14.2	8.5	16.7	0.8	26.6	5.9	-14	-2 / -1 ft											
	proposed - 16 ft	13.8	6.6	22.9	3.2	-14.2	8.5	16.2	0.8	26.7	5.6	-14	-1 / +1 ft											
	USACE - 8 ft	13.7	6.5	22.9	3.1	-14.3	8.4	16.6	0.8	26.6	5.9	-14	+1 / +2 ft											
	USACE - 16 ft	13.7	6.5	22.9	3.2	-14.2	8.5	16.1	0.8	26.7	5.6	-14	+2 / +5 ft											
Lake bed resistance: 10x	current - 8 ft	-10.2	-12.8	-5.3	-23.7	-41.4	-15.5	-10.6	-14.5	0.1	-19.3	-41	+5 / +10 ft											
	current - 16 ft	-10.1	-12.7	-5.2	-23.6	-41.2	-15.4	-10.1	-14.4	0.1	-19.0	-41	> +10 ft											
	proposed - 8 ft	-10.5	-13.2	-5.5	-24.1	-41.7	-15.9	-11.0	-14.5	0.0	-19.7	-41												
	proposed - 16 ft	-10.5	-13.1	-5.5	-24.0	-41.7	-15.8	-10.6	-14.5	0.1	-19.3	-41												
	USACE - 8 ft	-10.2	-12.8	-5.3	-23.7	-41.4	-15.5	-10.6	-14.5	0.1	-19.3	-41												
	USACE - 16 ft	-10.1	-12.7	-5.3	-23.6	-41.2	-15.5	-10.7	-14.4	0.1	-19.0	-41												

Sensitivity run	scenario - grid	Lakes aquifer in		Lakes aquifer out		Creek section 1 aquifer in		Creek section 1 aquifer out		Creek section 2 aquifer in		Creek section 2 aquifer out		Creek section 3 aquifer in		Creek section 3 aquifer out		Creek section 4 aquifer in		Creek section 4 aquifer out		Creek section 5 aquifer		deviation from basic run (lakes)
		Lakes aquifer in	Lakes aquifer out	Creek section 1 aquifer in	Creek section 1 aquifer out	Creek section 2 aquifer in	Creek section 2 aquifer out	Creek section 3 aquifer in	Creek section 3 aquifer out	Creek section 4 aquifer in	Creek section 4 aquifer out	Creek section 5 aquifer												
Lake bed resistance: 0.1x	current - 8 ft	1950323	-527281	2779	0	3870	0	123	-878	0	-4175	0	-11475	0	-11475	0	-11475	0	-11475	0	-11475	0	-11475	-10000 / -10000 ft ³ /d
	current - 16 ft	1963681	-540710	2783	0	3831	0	118	-905	0	-4153	0	-11453	0	-11453	0	-11453	0	-11453	0	-11453	0	-11453	-10000 / -10000 ft ³ /d
	proposed - 8 ft	1964618	-517005	1074	0	246	-2454	0	-5565	0	-11475	0	-11475	0	-11475	0	-11475	0	-11475	0	-11475	0	-11475	+10000 / +10000 ft ³ /d
	proposed - 16 ft	1977335	-530280	1058	0	236	-2446	0	-5569	0	-11407	0	-11407	0	-11407	0	-11407	0	-11407	0	-11407	0	-11407	+25000 / +25000 ft ³ /d
	USACE - 8 ft	1972432	-511316	2160	0	4166	-126	0	-9580	0	-14417	0	-14417	0	-14417	0	-14417	0	-14417	0	-14417	0	-14417	+50000 / +50000 ft ³ /d
	USACE - 16 ft	1985094	-524318	2184	0	4217	-153	0	-9777	0	-14611	0	-14611	0	-14611	0	-14611	0	-14611	0	-14611	0	-14611	> +50000 ft ³ /d
Lake bed resistance: 10x	current - 8 ft	285395	0	2779	0	4672	0	3833	0	5506	0	136	0	136	0	136	0	136	0	136	0	136	0	5000 / -2500 ft ³ /d
	current - 16 ft	285943	0	2783	0	4652	0	3882	0	5483	0	136	0	136	0	136	0	136	0	136	0	136	0	2500 / -1000 ft ³ /d
	proposed - 8 ft	285395	0	1188	0	2387	0	1774	0	2575	0	106	0	106	0	106	0	106	0	106	0	106	0	-100 / -100 ft ³ /d
	proposed - 16 ft	285943	0	1188	0	2364	0	1793	0	2593	0	106	0	106	0	106	0	106	0	106	0	106	0	+100 / +1000 ft ³ /d
	USACE - 8 ft	285395	0	2160	0	5762	0	4705	0	5569	0	102	0	102	0	102	0	102	0	102	0	102	0	+1000 / +2500 ft ³ /d
	USACE - 16 ft	285943	0	2184	0	5878	0	4731	0	5599	0	103	0	103	0	103	0	103	0	103	0	103	0	+2500 / +5000 ft ³ /d

Figure 53 Sensitivity to the bed resistance in the Quarry Lakes. The top part shows the heads; the bottom part shows the flow volumes.

Sensitivity run	scenario - grid	OBSwells Newark aquifer average		OBSwells Newark aquifer minimum		OBSwells Newark aquifer maximum		OBSwells CF aquifer average		OBSwells CF aquifer minimum		OBSwells CF aquifer maximum		Heads Newark aquifer average		Heads Newark aquifer minimum		Heads Newark aquifer maximum		Heads CF aquifer average		Heads CF aquifer		deviation from basic run
		OBSwells Newark aquifer average	OBSwells Newark aquifer minimum	OBSwells Newark aquifer maximum	OBSwells CF aquifer average	OBSwells CF aquifer minimum	OBSwells CF aquifer maximum	Heads Newark aquifer average	Heads Newark aquifer minimum	Heads Newark aquifer maximum	Heads CF aquifer average	Heads CF aquifer												
Creek bed resistance: 0.1x	current - 8 ft	9.7	4.3	15.6	-1.5	-18.9	4.0	12.1	0.6	17.0	1.6	-18	-10 / -5 ft											
	current - 16 ft	9.8	4.4	15.8	-1.4	-18.9	4.1	11.7	0.7	17.2	1.4	-18	-5 / -2 ft											
	proposed - 8 ft	9.3	4.1	15.1	-2.0	-19.4	3.5	11.5	0.6	16.5	1.1	-19	-2 / -1 ft											
	proposed - 16 ft	9.4	4.1	15.3	-1.9	-19.3	3.6	11.2	0.6	16.7	1.0	-19	-1 / +1 ft											
	USACE - 8 ft	9.7	4.3	15.6	-1.5	-19.0	4.0	12.0	0.6	17.0	1.5	-19	+1 / +2 ft											
	USACE - 16 ft	9.8	4.4	15.8	-1.4	-18.9	4.0	11.7	0.7	17.2	1.4	-18	+2 / +5 ft											
Creek bed resistance: 10x	current - 8 ft	8.8	3.8	13.9	-2.6	-20.1	3.0	11.0	0.6	15.1	0.6	-20	+5 / +10 ft											
	current - 16 ft	8.9	3.8	14.0	-2.5	-20.0	3.0	10.6	0.6	15.1	0.4	-20	> +10 ft											
	proposed - 8 ft	8.8	3.8	13.9	-2.6	-20.1	2.9	11.0	0.6	15.1	0.5	-20												
	proposed - 16 ft	8.8	3.8	13.9	-2.6	-20.0	3.0	10.6	0.6	15.1	0.4	-20												
	USACE - 8 ft	8.8	3.8	13.9	-2.6	-20.1	2.9	11.0	0.6	15.1	0.5	-20												
	USACE - 16 ft	8.8	3.8	13.9	-2.6	-20.0	3.0	10.6	0.6	15.1	0.4	-20												

Sensitivity run	scenario - grid	Lakes aquifer in		Lakes aquifer out		Creek section 1 aquifer in		Creek section 1 aquifer out		Creek section 2 aquifer in		Creek section 2 aquifer out		Creek section 3 aquifer in		Creek section 3 aquifer out		Creek section 4 aquifer in		Creek section 4 aquifer out		Creek section 5 aquifer		deviation from basic run (lakes)
		Lakes aquifer in	Lakes aquifer out	Creek section 1 aquifer in	Creek section 1 aquifer out	Creek section 2 aquifer in	Creek section 2 aquifer out	Creek section 3 aquifer in	Creek section 3 aquifer out	Creek section 4 aquifer in	Creek section 4 aquifer out	Creek section 5 aquifer												
Creek bed resistance: 0.1x	current - 8 ft	917959	0	2779	0	4064	0	12129	0	5986	-7	4	0	4	0	4	0	4	0	4	0	4	0	+10000 / +10000 ft ³ /d
	current - 16 ft	908917	0	27826	0	40286	0	11851	0	5711	-7	3	0	3	0	3	0	3	0	3	0	3	0	+10000 / +25000 ft ³ /d
	proposed - 8 ft	975862	0	11878	0	20697	0	1123	-2089	0	-12157	0	-12157	0	-12157	0	-12157	0	-12157	0	-12157	0	-12157	+25000 / +50000 ft ³ /d
	proposed - 16 ft	966398	0	11880	0	20195	0	958	-2187	0	-12196	0	-12196	0	-12196	0	-12196	0	-12196	0	-12196	0	-12196	> +50000 ft ³ /d
	USACE - 8 ft	916250	0	21598	0	56873	0	15655	0	1916	-722	0	-722	0	-722	0	-722	0	-722	0	-722	0	-722	+5000 / -5000 ft ³ /d
	USACE - 16 ft	906738	0	21838	0	57851	0	15031	0	1650	-889	0	-889	0	-889	0	-889	0	-889	0	-889	0	-889	2500 / -1000 ft ³ /d
Creek bed resistance: 10x	current - 8 ft	1092309	0	278	0	467	0	383	0	476	0	0	0	0	0	0	0	0	0	0	0	0	0	5000 / -2500 ft ³ /d
	current - 16 ft	1093588	0	278	0	467	0	388	0	472	0	0	0	0	0	0	0	0	0	0	0	0	0	2500 / -1000 ft ³ /d
	proposed - 8 ft	1094807	0	119	0	238	0	68	-73	0	-723	0	-723	0	-723	0	-723	0	-723	0	-723	0	-723	-100 / +100 ft ³ /d
	proposed - 16 ft	1095987	0	119	0	235	0	67	-76	0	-726	0	-726	0	-726	0	-726	0	-726	0	-726	0	-726	+100 / +1000 ft ³ /d
	USACE - 8 ft	1094219	0	216	0	578	0	471	0	522	0	0	0	0	0	0	0	0	0	0	0	0	0	+1000 / +2500 ft ³ /d
	USACE - 16 ft	1095418	0	218	0	588	0	473	0	520	0	0	0	0	0	0	0	0	0	0	0	0	0	+2500 / +5000 ft ³ /d

Figure 54 Sensitivity to the bed resistance in Alameda Creek. The top part shows the heads; the bottom part shows the flow volumes.

Sensitivity run	scenario - grid	OBSwells		Newark aquifer		OBSwells CF		OBSwells CF		Heads Newark		Heads Newark		Heads CF		deviation from basic run
		Newark aquifer average	OBSwells	Newark aquifer minimum	Newark aquifer maximum	OBSwells CF average	OBSwells CF minimum	OBSwells CF maximum	Heads Newark average	Heads Newark minimum	Heads Newark maximum	Heads CF average	Heads CF minimum	Heads CF maximum		
Kv layer 1: 0.1x	current - 8 ft	11.8	8.8	15.2	-0.2	-17.7	5.7	13.2	6.2	16.3	3.2	-1.7	-1.7	-1.7	-1.7	< -10 ft
	current - 16 ft	11.8	8.9	15.2	-0.2	-17.7	5.7	13.0	6.2	16.4	3.1	-1.7	-1.7	-1.7	-10 / -5 ft	
	proposed - 8 ft	11.6	8.8	15.1	-0.4	-17.9	5.5	13.1	6.1	16.2	3.0	-1.7	-1.7	-1.7	-5 / -2 ft	
	proposed - 16 ft	11.7	8.8	15.1	-0.3	-17.8	5.6	12.9	6.1	16.3	3.0	-1.7	-1.7	-1.7	-2 / -1 ft	
	USACE - 8 ft	11.7	8.8	15.1	-0.3	-17.8	5.6	13.1	6.1	16.3	3.1	-1.7	-1.7	-1.7	-1 / +1 ft	
	USACE - 16 ft	11.8	8.8	15.2	-0.2	-17.7	5.6	13.0	6.2	16.3	3.1	-1.7	-1.7	-1.7	+1 / +2 ft	
Kv layer 1: 10x	current - 8 ft	7.3	0.5	13.7	-3.6	-21.1	1.9	10.1	-2.9	14.9	-0.6	-2.1	-2.1	-2.1	+2 / +5 ft	
	current - 16 ft	7.3	0.6	13.8	-3.6	-21.0	1.9	9.6	-2.9	15.0	-0.8	-2.1	-2.1	-2.1	+5 / +10 ft	
	proposed - 8 ft	7.2	0.5	13.6	-3.8	-21.2	1.7	9.8	-2.9	14.8	-0.7	-2.1	-2.1	-2.1	> +10 ft	
	proposed - 16 ft	7.2	0.5	13.6	-3.7	-21.2	1.8	9.4	-2.9	14.8	-0.9	-2.1	-2.1	-2.1	> +10 ft	
	USACE - 8 ft	7.2	0.5	13.7	-3.6	-21.1	1.9	10.0	-2.9	14.9	-0.6	-2.1	-2.1	-2.1	> +10 ft	
	USACE - 16 ft	7.3	0.5	13.7	-3.6	-21.1	1.9	9.6	-2.9	14.9	-0.8	-2.1	-2.1	-2.1	> +10 ft	

Sensitivity run	scenario - grid	Lakes		Creek		Creek		Creek		Creek		Creek		Creek		deviation from basic run (lakes)
		Lakes aquifer in	Lakes aquifer out	section 1 aquifer in	section 1 aquifer out	section 2 aquifer in	section 2 aquifer out	section 3 aquifer in	section 3 aquifer out	section 4 aquifer in	section 4 aquifer out	section 5 aquifer in	section 5 aquifer out			
Kv layer 1: 0.1x	current - 8 ft	898001	0	2779	0	4334	0	1572	0	196	-308	0	0	0	< -500000 ft3/d	
	current - 16 ft	897859	0	2783	0	4313	0	1554	0	186	-323	0	0	0	500000 / -250000 ft3/d	
	proposed - 8 ft	909329	0	1188	0	2046	0	35	-836	0	-3916	0	0	0	250000 / -100000 ft3/d	
	proposed - 16 ft	909298	0	1188	0	2005	0	30	-848	0	-3921	0	0	0	-10000 / -10000 ft3/d	
	USACE - 8 ft	901352	0	2160	0	5733	0	1234	-28	0	-1671	0	0	0	-10000 / +10000 ft3/d	
	USACE - 16 ft	900998	0	2184	0	5835	0	1203	-35	0	-1719	0	0	0	+10000 / +10000 ft3/d	
Kv layer 1: 10x	current - 8 ft	1207405	0	2779	0	4672	0	3833	0	5074	0	29	29	29	< -5000 ft3/d	
	current - 16 ft	1207749	0	2783	0	4652	0	3882	0	5041	0	29	29	29	5000 / -2500 ft3/d	
	proposed - 8 ft	1225778	0	1188	0	2385	0	844	-367	0	-5243	0	0	0	2500 / -1000 ft3/d	
	proposed - 16 ft	1226117	0	1188	0	2360	0	835	-384	0	-5253	0	0	0	-1000 / -100 ft3/d	
	USACE - 8 ft	1211714	0	2160	0	5762	0	4705	0	5569	0	46	46	46	+1000 / +1000 ft3/d	
	USACE - 16 ft	1212057	0	2184	0	5878	0	4731	0	5599	0	46	46	46	+1000 / +2500 ft3/d	

Figure 55 Sensitivity to the vertical conductivity in layer 1, aquitard above Newark aquifer. The top part shows the heads; the bottom part shows the flow volumes.

Sensitivity run	scenario - grid	OBSwells		Newark aquifer		OBSwells CF		OBSwells CF		Heads Newark		Heads Newark		Heads CF		deviation from basic run
		Newark aquifer average	OBSwells	Newark aquifer minimum	Newark aquifer maximum	OBSwells CF average	OBSwells CF minimum	OBSwells CF maximum	Heads Newark average	Heads Newark minimum	Heads Newark maximum	Heads CF average	Heads CF minimum	Heads CF maximum		
Kh layer 2: 0.1x	current - 8 ft	3.9	-3.8	14.8	-6.2	-24.5	0.0	8.9	-16.2	21.6	-2.6	-2.4	-2.4	-2.4	< -10 ft	
	current - 16 ft	3.9	-3.8	14.8	-6.2	-24.5	0.0	8.5	-16.2	21.8	-2.7	-2.4	-2.4	-2.4	-10 / -5 ft	
	proposed - 8 ft	3.6	-3.9	14.6	-6.5	-24.8	-0.4	8.4	-16.5	21.5	-2.9	-2.4	-2.4	-2.4	-5 / -2 ft	
	proposed - 16 ft	3.6	-3.9	14.6	-6.5	-24.8	-0.3	8.1	-16.5	21.7	-3.0	-2.4	-2.4	-2.4	-2 / -1 ft	
	USACE - 8 ft	4.0	-3.7	14.9	-6.1	-24.4	0.1	9.1	-16.1	21.6	-2.5	-2.4	-2.4	-2.4	-1 / +1 ft	
	USACE - 16 ft	4.0	-3.7	14.9	-6.1	-24.4	0.1	8.7	-16.1	21.8	-2.6	-2.4	-2.4	-2.4	+1 / +2 ft	
Kh layer 2: 10x	current - 8 ft	7.4	5.8	8.8	-5.3	-22.6	0.8	8.0	2.9	9.0	-1.8	-2.2	-2.2	-2.2	+2 / +5 ft	
	current - 16 ft	7.5	5.8	8.8	-5.2	-22.6	0.8	7.9	2.9	9.0	-1.8	-2.2	-2.2	-2.2	+5 / +10 ft	
	proposed - 8 ft	7.4	5.7	8.7	-5.4	-22.7	0.7	7.9	2.9	8.9	-1.9	-2.2	-2.2	-2.2	> +10 ft	
	proposed - 16 ft	7.4	5.8	8.7	-5.3	-22.7	0.8	7.8	2.9	8.9	-1.9	-2.2	-2.2	-2.2	> +10 ft	
	USACE - 8 ft	7.5	5.8	8.8	-5.3	-22.6	0.8	8.0	2.9	9.0	-1.8	-2.2	-2.2	-2.2	> +10 ft	
	USACE - 16 ft	7.5	5.8	8.8	-5.2	-22.6	0.9	7.9	2.9	9.0	-1.8	-2.2	-2.2	-2.2	> +10 ft	

Sensitivity run	scenario - grid	Lakes		Creek		Creek		Creek		Creek		Creek		Creek		deviation from basic run (lakes)
		Lakes aquifer in	Lakes aquifer out	section 1 aquifer in	section 1 aquifer out	section 2 aquifer in	section 2 aquifer out	section 3 aquifer in	section 3 aquifer out	section 4 aquifer in	section 4 aquifer out	section 5 aquifer in	section 5 aquifer out			
Kh layer 2: 0.1x	current - 8 ft	692698	0	2779	0	4672	0	3833	0	5091	0	63	63	63	< -500000 ft3/d	
	current - 16 ft	691605	0	2783	0	4652	0	3882	0	5071	0	63	63	63	500000 / -250000 ft3/d	
	proposed - 8 ft	707215	0	1188	0	2354	0	1221	0	65	-939	0	0	0	250000 / -100000 ft3/d	
	proposed - 16 ft	705860	0	1188	0	2325	0	1213	0	61	-943	0	0	0	-10000 / -10000 ft3/d	
	USACE - 8 ft	688550	0	2160	0	5762	0	4705	0	5569	0	93	93	93	-10000 / +10000 ft3/d	
	USACE - 16 ft	687059	0	2184	0	5878	0	4731	0	5599	0	94	94	94	+10000 / +10000 ft3/d	
Kh layer 2: 10x	current - 8 ft	1716491	0	2779	0	4672	0	3833	0	5204	0	32	32	32	< -5000 ft3/d	
	current - 16 ft	1720100	0	2783	0	4652	0	3882	0	5179	0	32	32	32	5000 / -2500 ft3/d	
	proposed - 8 ft	1725507	0	1188	0	2387	0	1694	0	269	-1201	0	0	0	2500 / -1000 ft3/d	
	proposed - 16 ft	1729028	0	1188	0	2364	0	1698	0	259	-1210	0	0	0	-1000 / -100 ft3/d	
	USACE - 8 ft	1715323	0	2160	0	5762	0	4705	0	5569	0	49	49	49	+1000 / +1000 ft3/d	
	USACE - 16 ft	1718578	0	2184	0	5878	0	4731	0	5599	0	49	49	49	+2500 / +5000 ft3/d	

Figure 56 Sensitivity to the horizontal conductivity in layer 2, Newark aquifer. The top part shows the heads; the bottom part shows the flow volumes.

Sensitivity run	scenario - grid	OBSwells Newark aquifer average		OBSwells Newark aquifer minimum		OBSwells Newark aquifer maximum		OBSwells CF aquifer average		OBSwells CF aquifer minimum		OBSwells CF aquifer maximum		Heads Newark aquifer average		Heads Newark aquifer minimum		Heads Newark aquifer maximum		Heads CF aquifer average		Heads CF aquifer minimum		Heads CF aquifer maximum		deviation from basic run
		average	minimum	minimum	maximum	average	minimum	maximum	average	minimum	maximum	average	minimum	maximum	average	minimum	maximum	average	minimum	maximum	average	minimum	maximum			
Kv layer 3: 0.1x	current - 8 ft	9.4	3.9	15.2	-83.1	-101.7	-72.4	11.7	0.2	16.4	-77.4	-101	-101	< -10 ft												
	current - 16 ft	9.5	3.9	15.3	-83.1	-101.7	-72.3	11.3	0.2	16.4	-76.7	-101	-101	-10 / -5 ft												
	proposed - 8 ft	9.3	3.8	15.1	-83.2	-101.8	-72.5	11.5	0.2	16.2	-77.5	-101	-101	-5 / -2 ft												
	proposed - 16 ft	9.3	3.8	15.1	-83.2	-101.8	-72.5	11.1	0.2	16.3	-76.8	-101	-101	-2 / -1 ft												
	USACE - 8 ft	9.3	3.8	15.2	-83.2	-101.8	-72.4	11.6	0.2	16.3	-77.4	-101	-101	-1 / +1 ft												
	USACE - 16 ft	9.4	3.8	15.2	-83.1	-101.7	-72.4	11.2	0.2	16.4	-76.7	-101	-101	+1 / +2 ft												
Kv layer 3: 10x	current - 8 ft	8.7	4.0	13.5	8.8	-6.5	12.5	10.8	0.7	14.5	9.9	-6	-6	+2 / +5 ft												
	current - 16 ft	8.7	4.1	13.5	8.8	-6.4	12.6	10.5	0.7	14.6	9.5	-6	-6	+5 / +10 ft												
	proposed - 8 ft	8.5	3.9	13.3	8.6	-6.6	12.4	10.6	0.7	14.4	9.7	-6	-6	> +10 ft												
	proposed - 16 ft	8.6	4.0	13.4	8.7	-6.6	12.4	10.3	0.7	14.4	9.4	-6	-6													
	USACE - 8 ft	8.6	4.0	13.4	8.7	-6.5	12.5	10.7	0.7	14.5	9.8	-6	-6													
	USACE - 16 ft	8.7	4.0	13.5	8.8	-6.5	12.5	10.4	0.7	14.5	9.5	-6	-6													
Sensitivity run	scenario - grid	Lakes aquifer in		Lakes aquifer out		Creek section 1 aquifer in		Creek section 1 aquifer out		Creek section 2 aquifer in		Creek section 2 aquifer out		Creek section 3 aquifer in		Creek section 3 aquifer out		Creek section 4 aquifer in		Creek section 4 aquifer out		Creek section 5		deviation from basic run (lakes)		
		in	out	in	out	in	out	in	out	in	out	in	out	in	out	in	out	in	out	in	out					
Kv layer 3: 0.1x	current - 8 ft	951631	0	2779	0	4672	0	3641	0	2992	0	11	11	< -500000 ft ³ /d												
	current - 16 ft	951969	0	2783	0	4652	0	3671	0	2949	0	1	1	500000 / -250000 ft ³ /d												
	proposed - 8 ft	969034	0	1188	0	2280	0	241	-948	0	-5622	0	0	-250000 / -100000 ft ³ /d												
	proposed - 16 ft	969397	0	1188	0	2243	0	228	-970	0	-5614	0	0	-100000 / -10000 ft ³ /d												
	USACE - 8 ft	958052	0	2160	0	5762	0	4408	0	1656	-159	0	0	+100000 / +100000 ft ³ /d												
	USACE - 16 ft	958021	0	2184	0	5878	0	4387	0	1581	-186	0	0	+250000 / +500000 ft ³ /d												
Kv layer 3: 10x	current - 8 ft	1159708	0	2779	0	4672	0	3831	0	3877	0	2	2	< -5000 ft ³ /d												
	current - 16 ft	1160186	0	2783	0	4652	0	3878	0	3845	0	2	2	5000 / -2500 ft ³ /d												
	proposed - 8 ft	1175182	0	1188	0	2382	0	793	-304	0	-4355	0	0	-2500 / -1000 ft ³ /d												
	proposed - 16 ft	1175324	0	1188	0	2355	0	779	-317	0	-4363	0	0	-100 / +100 ft ³ /d												
	USACE - 8 ft	1163594	0	2160	0	5762	0	4705	0	4170	0	0	0	+1000 / +1000 ft ³ /d												
	USACE - 16 ft	1163903	0	2184	0	5878	0	4731	0	4127	0	0	0	+1000 / +2500 ft ³ /d												

Figure 57 Sensitivity to the vertical conductivity in layer 3, aquitard between Newark aquifer and Centerville-Fremont aquifer. The top part shows the heads; the bottom part shows the flow volumes.

B Additional figures

B.1 Differences in bed level between the proposed design and current situation



Figure 58 Differences between proposed and current bed level in Alameda Creek, part 1.

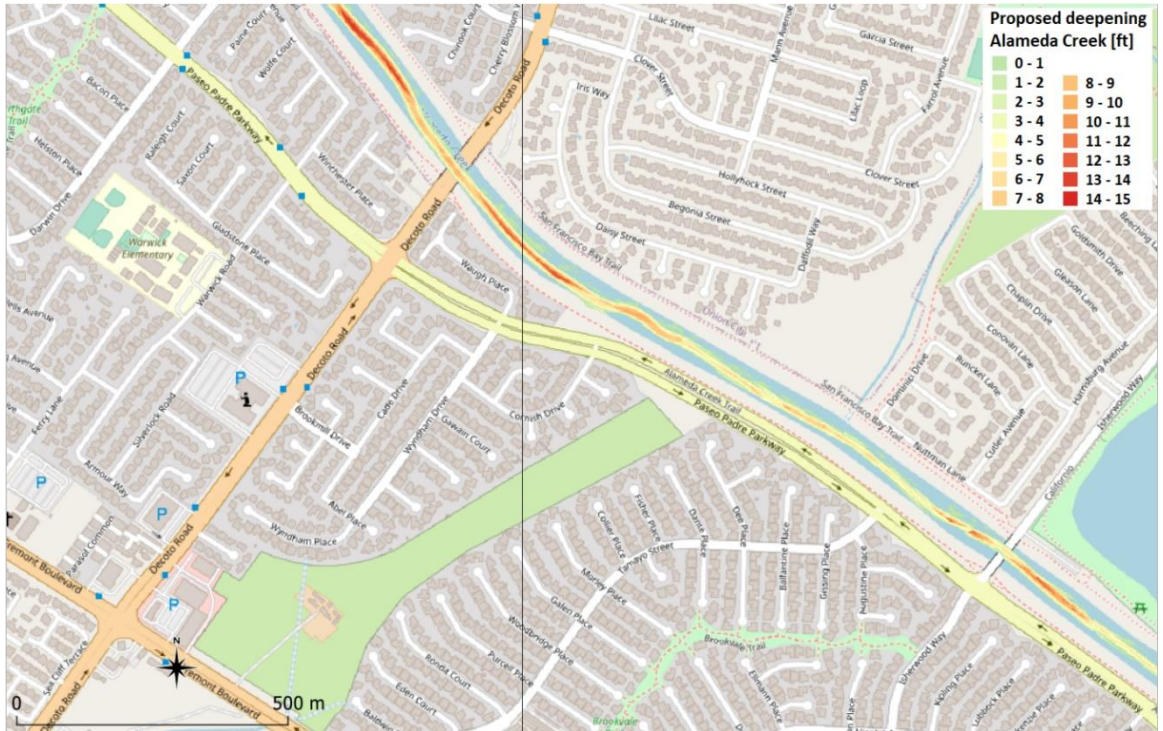


Figure 59 Differences between proposed and current bed level in Alameda Creek, part 2.

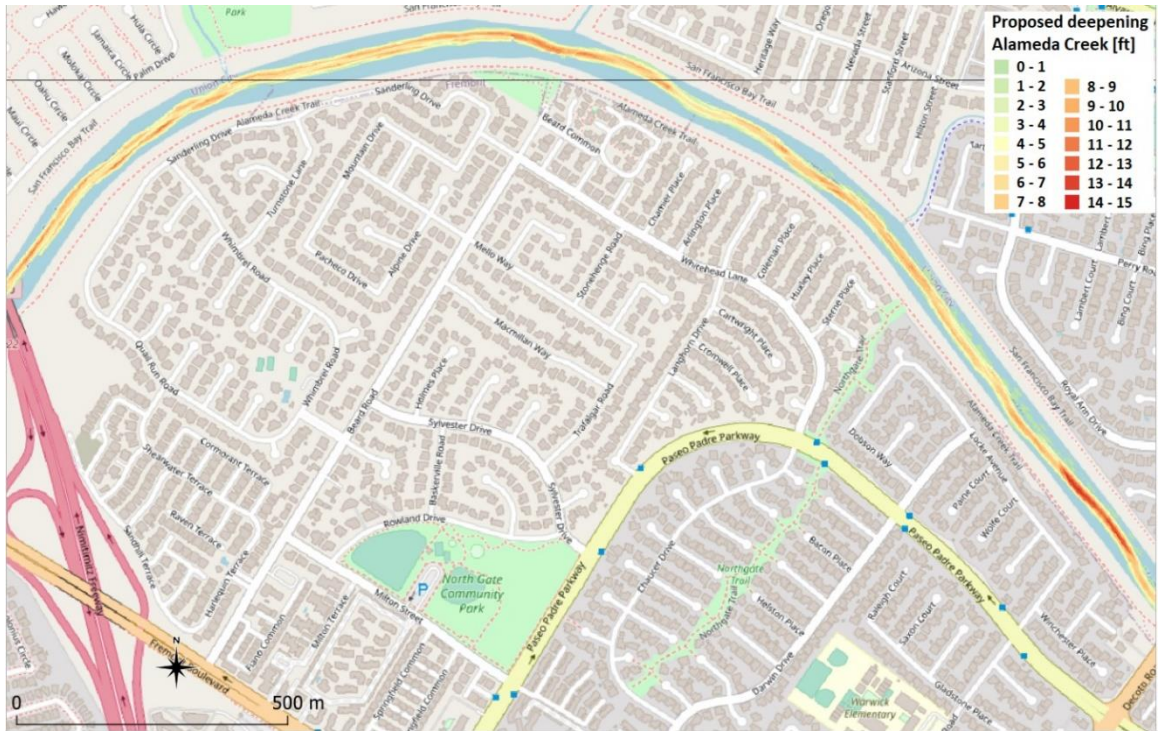


Figure 60 Differences between proposed and current bed level in Alameda Creek, part 3.



Figure 61 Differences between proposed and current bed level in Alameda Creek, part 4.

B.2 Hydraulic conductivity values applied

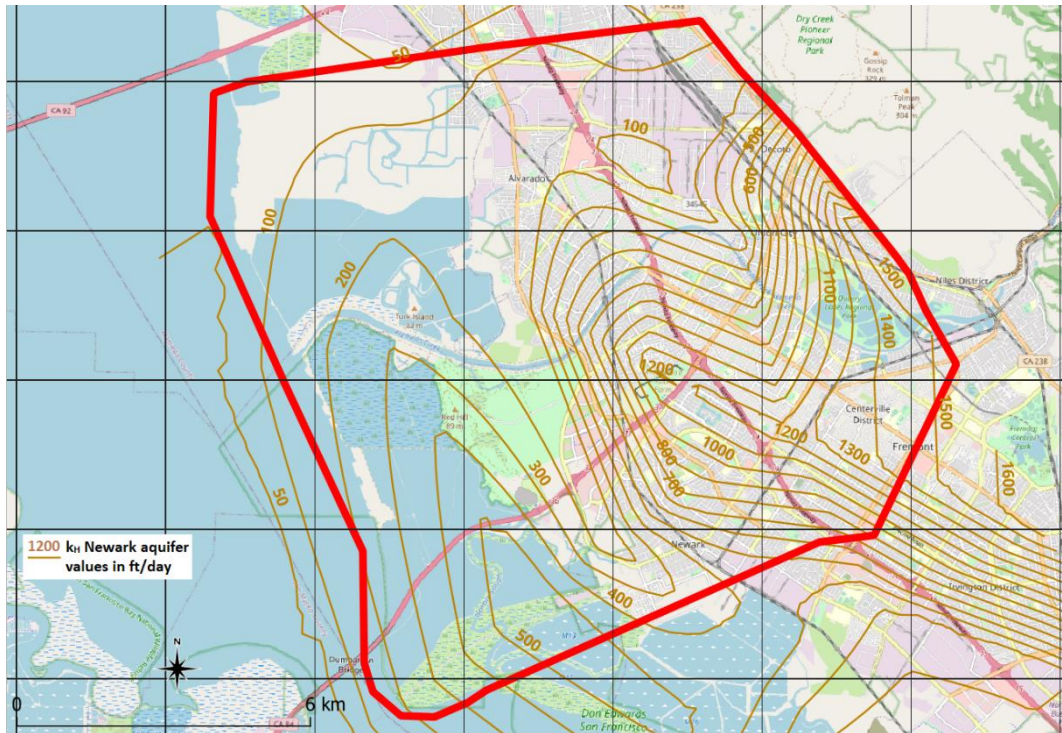


Figure 62 Applied contours of the horizontal hydraulic conductivity of the Newark Aquifer.



Figure 63 Applied contours of the horizontal hydraulic conductivity of the Centerville-Fremont Aquifer.

B.3 Bed levels for variations explored

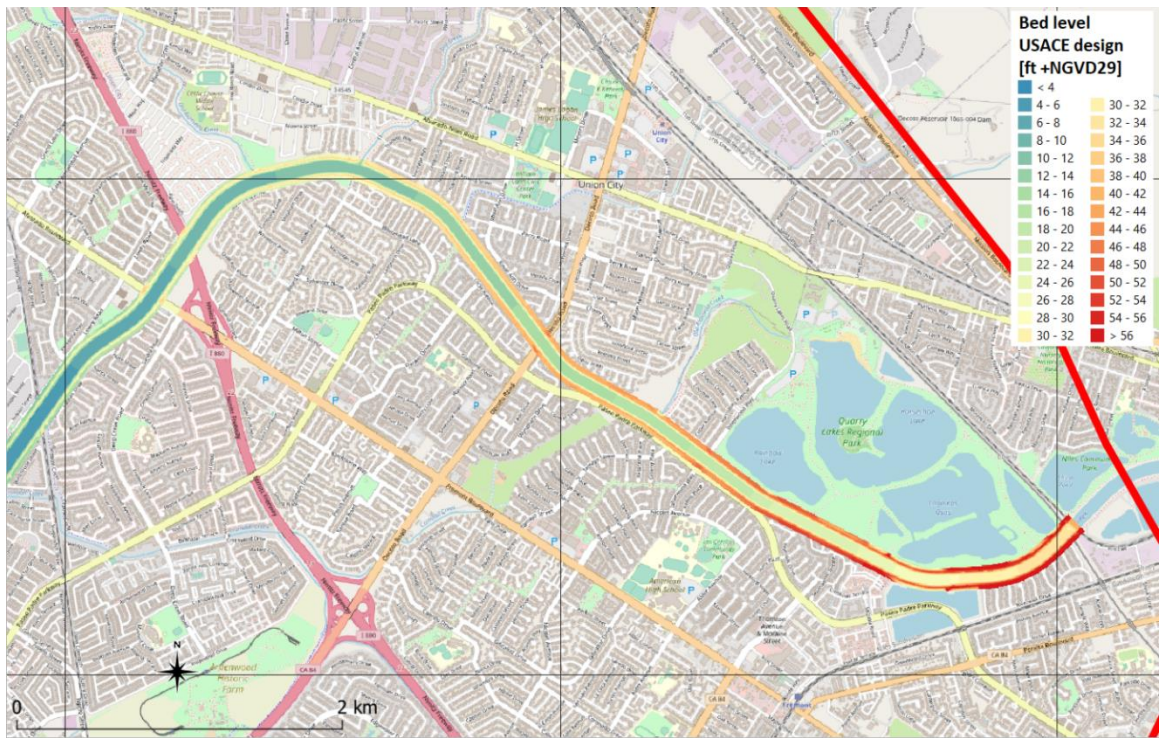


Figure 64 Creek bed levels for the USACE design.

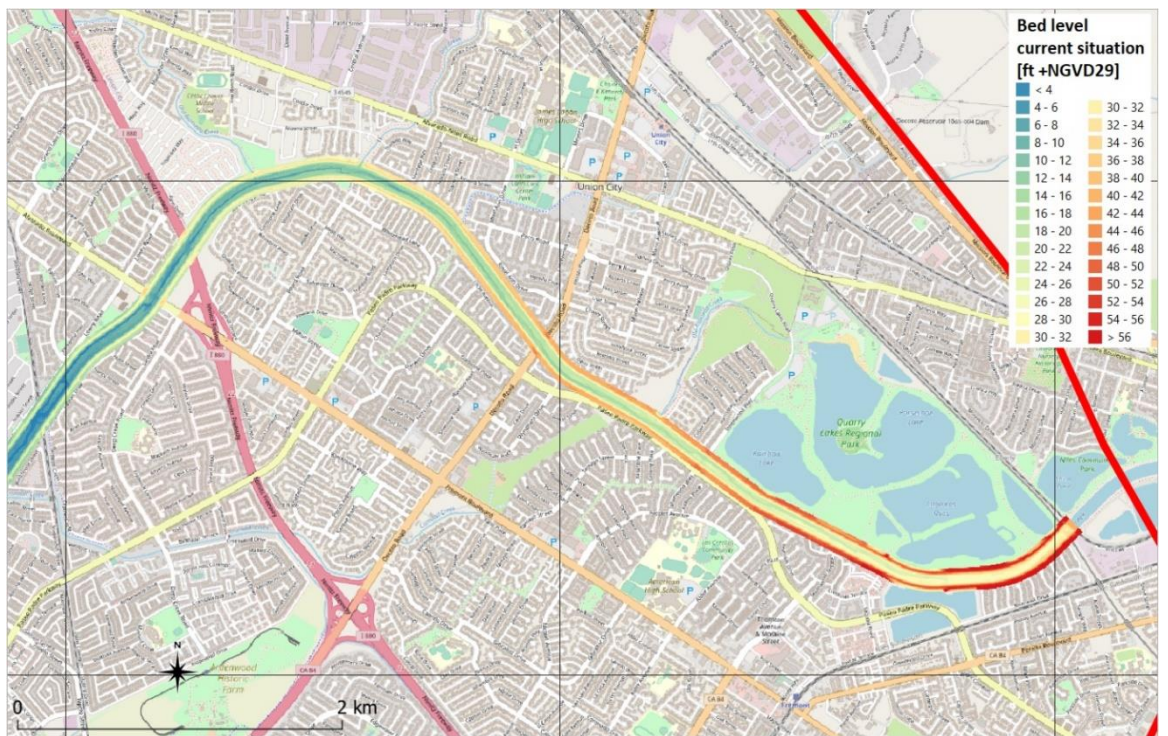


Figure 65 Creek bed levels for the current situation.

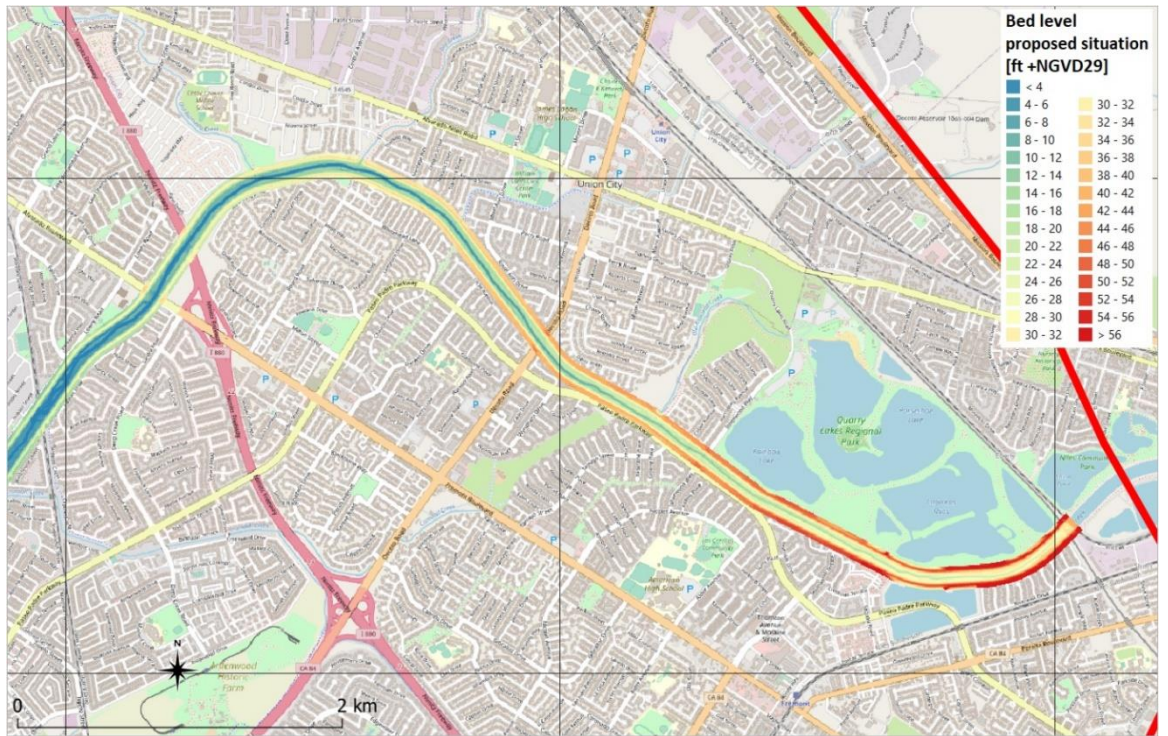


Figure 66 Creek bed levels for the proposed situation.

Deltares is an independent institute for applied research in the field of water and subsurface. Throughout the world, we work on smart solutions for people, environment and society.

Deltares

www.deltares.nl